LENGTHSCALE ISSUES IN THE MECHANICAL BEHAVIOR AND FAILURE OF COMPOSITE STRUCTURES

Final Technical Report
for work conducted
during the period February, 2007 through January, 2011
under Award with the Office of Naval Research

Paul A. Lagacé and Jeffrey T. Chambers
Professor of Graduate Student
Aeronautics & Astronautics
and of Engineering Systems

Technology Laboratory for Advanced Materials and Structures
Department of Aeronautics and Astronautics
Massachusetts Institute of Technology
77 Massachusetts Avenue
Cambridge, Massachusetts 02139

May, 2011

REPORT DOCUMENTATION PAGE

Form Approved
OMB No. 0704-0188

1. REPORT DATE *(DD-MM-YYYY)*	2. REPORT TYPE	3. DATES COVERED *(From - To)*
01/05/2011	Final Technical	Feb 2007 - Jan 2011

4. TITLE AND SUBTITLE
Lengthscale Issues in the Mechanical Behavior and Failure of Composite Structures

5a. CONTRACT NUMBER

5b. GRANT NUMBER
N00014-07-1-0614

5c. PROGRAM ELEMENT NUMBER

6. AUTHOR(S)
Paul A. Lagacé
Jeffrey T. Chambers

5d. PROJECT NUMBER

5e. TASK NUMBER

5f. WORK UNIT NUMBER

7. PERFORMING ORGANIZATION NAME(S) AND ADDRESS(ES)
Massachusetts Institute of Technology
77 Massachusetts Avenue
Cambridge, MA 02139

8. PERFORMING ORGANIZATION REPORT NUMBER
TELAMS 2011-1

9. SPONSORING/MONITORING AGENCY NAME(S) AND ADDRESS(ES)
Office of Naval Research
875 North Randolph Street
Arlington, VA 22203-1995

10. SPONSOR/MONITOR'S ACRONYM(S)
ONR

11. SPONSOR/MONITOR'S REPORT NUMBER(S)

12. DISTRIBUTION/AVAILABILITY STATEMENT
Approved for Public Release; distribution is Unlimited

13. SUPPLEMENTARY NOTES

14. ABSTRACT
This effort, part of a larger four-year NICOP research effort, focused on improving the effectiveness of the prediction of the overall behavior, particularly failure, of composite structures. A key lacking item is the ability to effectively utilize data and observations made at lengthscales associated with laboratory-sized specimens in predicting the actual behavior manifested in full-scale structures. The specific work accomplished in this effort establishes a basic methodology for characterizing the details of damage and failure so that these can be effectively utilized in such an overall approach, thereby dealing with issues of different lengthscales and different levels of structural complexity.

15. SUBJECT TERMS
composite materials, composite structures, failure, damage, damage mechanisms, lengthscales, structural complexity, Building Block Approach

16. SECURITY CLASSIFICATION OF:			17. LIMITATION OF ABSTRACT	18. NUMBER OF PAGES	19a. NAME OF RESPONSIBLE PERSON
a. REPORT	b. ABSTRACT	c. THIS PAGE			Paul A. Lagace
					19b. TELEPHONE NUMBER *(Include area code)*
U	U	U	UU	109	617-253-3628

Foreword

This investigation was conducted in the Technology Laboratory for Advanced Materials and Structures (TELAMS) of the Department of Aeronautics and Astronautics at the Massachusetts Institute of Technology during the period February, 2007 through January, 2011. The work was sponsored by the Navy – Office of Naval Research under Grant Number N00014-07-1-0614.

Table of Contents

Abstract

This effort was part of a larger four-year NICOP research effort with a focus on improving the effectiveness of the prediction of the overall behavior, including failure, of composite structures. This is motivated by the increased use of composite materials in many DoD, as well as commercial, applications. Despite over a quarter century of work on understanding and characterizing the failure of composite materials and their structures, the ability to predict such failure is still quite lacking. There is much to be accomplished in order to be able to properly and fully characterize and predict composite behavior, even at the ply and laminate levels. From the point of understanding at these fundamental levels, much needs to be accomplished to be able to use such an understanding in an ability through to the prediction of the behavior and failure of full-scale structures. A key item that is lacking is the ability to effectively utilize data and observations made at lengthscales associated with laboratory-sized specimens in predicting the actual behavior manifested in full-scale structures. In large part due to this lack of understanding, composite structures currently are designed and certified/validated for safe operating by using a primarily empirically-based methodology known as the "Building Block Approach" along with "knockdown factors." This causes a smaller fraction of the full capability of the basic material to be employed in the final structure. These issues were first addressed in this work primarily via the effort of characterizing the overall behavior at the baseline level. From there, the issues associated with increasing levels of structural complexity and higher orders of structural lengthscale were characterized (e.g., stress field gradients, manifestation of different damage mechanisms) and the results characterized at lower levels are to be used in associated efforts via the Dissipated Energy Density to bring that knowledge to the higher levels of complexity and lengthscale. With such an overall methodology established, the ability to guide the overall design process will be increased, thereby reducing the number of experiments which would substantially reduce cost and overall risk in structural development, as well as lead to fuller utilization of basic material capability. The work accomplished in this effort establishes a basic methodology for characterizing the details of damage and failure so that these can be effectively utilized in such an overall approach.

1. Introduction

This effort was part of a larger four-year NICOP (Naval International Cooperative Opportunities in Science and Technology Program) research effort with a focus on improving the effectiveness of the prediction of the overall behavior, including failure, of composite structures. This is motivated by the increased use of composite materials in many DoD, as well as commercial, applications.

Despite over a quarter century of work on understanding and characterizing the failure of composite materials and their structures, the ability to predict such failure is still quite lacking. The results from the recent World-Wide Failure Exercise for composites, organized and coordinated by Mike Hinton (and colleagues) [1], show just how far the overall composites community and industry are from being able to predict general failure behavior of relatively simple composite configurations – coupon

specimens under various loading conditions. In particular, they note that even in predicting the initial strength (i.e. at onset of first failure/damage) of multidirectional laminates that: "the level of agreement between theoretical predictions and the available experimental results was generally not very good." Furthermore, it is noted that in progressing to the prediction of final strength (i.e. ultimate failure), that: "the 'exercise' has shown that the current theories are not sufficiently robust." [1]. There is, therefore, much to be accomplished in order to be able to properly and fully characterize and predict composite behavior, even at the ply and laminate levels.

From the point of understanding at these fundamental levels, much needs to be accomplished to be able to use such an understanding in an ability to predict the behavior and failure through the levels up to full-scale structures. A key item that is lacking is the ability to effectively utilize data and observations made at lengthscales associated with laboratory-sized specimens in predicting the actual behavior manifested in full-scale structures [2]. As one moves through various levels, greater complexity is added due to the variety of structural details and the geometry of the basic structural configuration, structural response and phenomena with different lengthscales, and the occurrence of damage and the lengthscales associated with such. This is further complicated by the interaction of these items and the stress fields associated with that. At a recent conference organized by Peter Beaumont on, "Advances in Multi-Scale Modelling of Composite Material Systems of Components" [3], the invited participants, in their individual presentations and in discussion sessions, all made the point and agreed that there is much to be accomplished in order to work fully across the multiple lengthscales in the mechanical behavior of composite structures, particularly with regard to failure, when considering a real-life operative environment including the presence of damage. This, furthermore, has yet to progress to fully addressing long-term behavior including damage propagation.

In large part due to this lack of understanding, composite structures currently are designed and certified/validated for safe operating by using a primarily empirically-based methodology known as the "Building Block Approach" along with "knockdown factors." This approach, illustrated in Figure 1, is fundamentally based on demonstrating behavior via experiments and preforming assessment using probabilistic approaches, often as a simple determination of "performance values" via assumed statistical models for a large database of behavior characterization. Such behavior is first documented at the most basic operative level of composites -- the material ply. Greater structural complexity is then progressively addressed as experiments are conducted on specimens of larger lengthscales -- subelements, elements, subcomponents, components, and full-scale structures. While structural complexity and the various lengthscales involved increase at each step along the building block, the number of tests conducted at each step decrease. Nevertheless, the approach relies heavily on experimentation and therefore is very costly. There are also points along the approach where it can be necessary to return to a previous step as what was manifested at a lower level of the building block was not seen in a specimen of greater complexity. The lack of understanding also results in use of "knockdown factors." This causes a smaller fraction of the full capability of the basic material to be employed in the final structure.

These issues were addressed in this work primarily via the effort of characterizing the overall behavior at the baseline level. From there, the issues associated with increasing levels of structural complexity and higher orders of structural lengthscale were characterized (e.g., stress field gradients, manifestation of different damage mechanisms) and the results characterized at lower levels are to be used in associated effort via appropriate failure models/parameters, such as the Dissipated Energy Density, to bring that knowledge to the higher levels of complexity and lengthscale. With such an overall methodology established, the ability to guide the overall design process would be increased, thereby reducing the number of experiments needed, which would substantially reduce cost and overall risk in structural development, as well as lead to fuller utilization of basic material capability. The work accomplished in this effort establishes a basic methodology for characterizing the details of damage and failure so that these can be effectively utilized in such an overall approach.

2. Objectives and Overall Approach

This work was part of a larger four-year NICOP (Naval International Cooperative Opportunities in Science and Technology Program) research effort entitled "Methodology for Determination of Mechanical Behavior and Failure in Composite Structures" with the overall goal to develop an efficient, validated methodology for the determination of mechanical behavior leading up to and including failure in complex fiber-reinforced plastic composite structures. The three primary research locations where the work took place are: M.I.T. (Massachusetts Institute of Technology), NRL (Naval Research Laboratory), and CRC-ACS (Cooperative Research Centre for Advanced Composite Structures). The following objectives were included in the overall effort:

- Build upon and extend the NRL data driven constitutive material characterization approach to develop a methodology for the determination of mechanical behavior in complex composite structures subjected to realistic loading conditions including the ability to address degradation in structural performance and structural failure in as-produced and damaged composite structures.

- Validate the methodology through testing on coupons and subcomponents at ambient conditions with a focus on issues of lengthscales manifested across this range.

- Develop an overall approach to couple the methodology with commercial software for calculating stress state and assessing overall structural behavior.

The particular objectives of this specific work, which supported the goal and objectives of the overall effort, were to develop an understanding of the issues associated with bridging the lengthscales involved in the behavior and failure of composite structures and to use this understanding in the development of a prediction methodology for the behavior of such structures.

The technical approach of this particular effort was involved with three research tasks defined in the larger four-year NICOP research [4] effort. The first is to assess a number of current failure models for their suitability to be used with the NRL composite material characterization methodology. The second is to develop a methodology for the determination of mechanical behavior leading up to and including failure in fiber reinforced plastic composite structures (as produced and damaged), constructed from the characterized material system. The third is to validate and appropriately adapt the methodology through testing coupons and small substructures at ambient conditions, with a focus on issues of extension through lengthscale range including observation and documentation of issues of damage initiation, damage growth, and final failure.

For this particular effort, the concentration was on the second of these three. A key piece of this, however, was the outcome of the first item in the overall work as that outcome was essential in establishing the approach and evolving methodology to be utilized. In particular, the automated and custom-made NRL mechatronic loading machine was to be used as a system identifier apparatus that generates the required data by exposing the material system to loading sequences that stimulate all strain states by which a material can ever be influenced. There must be a way to "describe" this data so that it can be utilized for more complex configurations at increasing lengthscales. A constitutive and failure model, or coordinated set thereof, thereby serves as a "language" to allow description and utilization of the material characterization at the very basic level as determined via the NRL machine and characterization methodology. It was therefore essential that this specific effort assessed various current failure models for their suitability in use with the NRL composite material characterization methodology. This assessment included, from the perspective of this particular work, ability for use in bridging lengthscales.

Thus, a base piece of the effort was in conducting a literature review in order to document the knowledge that exists surrounding damage, failure, and effect of lengthscales in composites and their structures. This helped to provide background of the topics related to the project and in planning an approach to accomplish the project goals. This included the development of a "question tree" in order to identify the information that is needed, what exists, and what needs to be sought.

From that overall perspective, the central effort in this work was on developing a methodology that allows the characterization at the basic material and laminate level to be employed as greater structural complexity is introduced in considering lengthscales of increasing magnitude (e.g., subelement, element, subcomponent, and component as used in the Building Block Approach. This is discussed in Section 3.3 of the "Literature Review".). This works to provide the needed information involving various behaviors and complexities. One such complexity includes gradients in stress fields due to overall structural configurations and details (e.g. holes) and those gradients due to overall structural response (e.g. buckling). Furthermore, there are stress gradients at various lengthscales due to the presence of damage or various as-produced anomalies. Work then proceeded to coordinate with outcomes from the assessment of current failure models. The technique described in the overall effort resulted in a fundamental

characterization quantity, dissipated energy density, that is, a volume-density quantity. This quantity is basically independent of scale and is thus applicable across all lengthscales. The quantity can be used in a pointwise fashion in considering the issues across the various lengthscales, and thus to "translate" the data through the lengthscales including with damage present. This, however, depended upon the specific failure models chosen, so the details of further effort depended on such outcomes. The effort also included a probabilistic assessment as basic behavior is not deterministic and thus probabilistic/statistical aspects were included at that basic level along with means to incorporate these aspects across the lengthscales included. This must also involve probabilistic aspects associated with production of actual structures as well as loading of actual structures.

A key part of the overall effort, as well as for the specifics of this particular effort, was the testing work that took place at the levels of coupons and small substructures including observations and documentation of damage initiation and growth up through final failure. The planning process for testing and the subsequent data results were essential in assessing the outcome from this specific work. Furthermore, this process was not simply a serial effort as there was an interaction and interdependence of the various objectives and related work. The overall effort required integrated coordination among the researchers at the three primary locations where the work took place.

The work that took place on the development and refinement of procedures to document damage and the subsequent documentation of damage illustrates the relationship between these items and the associated levels of structures, as well as the cooperation among the various research sites. In the work on damage documentation, the approach taken was able to characterize the damage based on its basic characteristics, but also regarded the specifics of the structure and loading associated with such. Considerations included being aware of and capturing the various lengthscales associated with these various factors.

In general, many final details of the work downstream could not be identified until earlier results were available. Thus, there continued to be (re)considerations and updates to overall and specific approaches and their details as the work moved forward. This included the details of the damage documentation.

3. Literature Review

As previously noted, a review of the literature on composite damage/failure and on the current predictive capabilities of the composites community was conducted as part of this work. Damage and failure within composites has been of great interest to composite engineers and designers. Significant research has been done on these topics with the goal of achieving an understanding of the damage/failure processes. While the selected literature spans a variety of topics, from basic damage modes to failure prediction, the primary focus of this review was to identify the underlying lengthscale effects which, although not directly addressed by the authors, were intrinsically affecting the results presented in the works. The review is broken into five sections: basic composite damage/failure modes, mode interaction, design approach, prediction

of damage and failure, and lengthscales in composites. Overall, the literature review was used in an interactive means with the "Question Tree" (described in Section 4). The work of the literature review helped to formulate the question tree as well as to provide answers to some of the basic questions from the tree. Overall, this helped shape the procedure for investigating lengthscale effects during this work.

3.1 *Basic Composite Damage/Failure Modes*

An understanding of the basic damage and failure modes in composites was required before considering more complex damage, such as interacting damage modes. Significant research has been done on these topics by others with the goal of achieving such an understanding. Basic composite damage modes can be categorized into two types: in-plane and out-of-plane. In-plane damage modes involve the constituents and include fiber fracture, matrix cracking, fiber microbuckling, and interfacial debonding (also known as pull-out or push-out) [5-8], while the one out-of-plane damage mode, occurring at the laminate level, is ply delamination [9]. The basic mechanics of each damage mode and the analytical and experimental procedures which historically have been used to study these modes is subsequently presented. In an ensuing section, on "Mode Interaction", the situation where two or more of these basic damage modes interact is discussed.

3.1.1 *Fiber Fracture*

Fiber fracture occurs in composites when loading on the laminate causes a fiber to break perpendicular to its length. Typically, this happens when loading on the composite results in a longitudinal-tensile load in a lamina exceeding the strength of a fiber. Once the loading causes stress in a fiber to exceed the critical strength of the fiber, the fiber fractures and the loading redistributes locally to the regions surrounding the failed fiber [10]. An illustration of a fiber fractured in a unidirectional lamina due to longitudinal tension is shown in Figure 2. Catastrophic failure (all fibers fracturing at once) does not typically occur at the load causing initial fiber fracture due to the variation of individual fiber strength [11, 12]. The variation of fiber strength can be attributed to manufacturing variations (e.g., distribution of flaws within fibers, variation in fiber geometries, or variations in fiber material properties). These variations in fiber strength are often modeled by probabilistic distributions (e.g., Weibull distributions) of fiber strength [8, 13-15]. Continued loading past the initial fiber fracture load causes adjacent fibers to reach their critical strength and fracture, increasing the density of fractured fibers within the ply. The load continues to redistribute until the remaining fibers cannot support the load, and catastrophic failure occurs.

Fiber fracture may also occur under certain conditions when a ply experiences longitudinal compression. Under such loading, the matrix provides support of the fibers and the fibers may microbuckle (discussed in the section "Microbuckling"). If microbuckling occurs, the fibers bend and may eventually fracture due to bending [16]. However, even though this damage results in a fractured fiber, it is not typically

referred to as fiber fracture, but instead is encompassed in the microbuckling damage mode.

Mechanistic models are used to understand and predict fiber fracture in composites. In the strength of materials approach, composite fibers are modeled as simple cylindrical, transversely isotropic solids. The model also assumes the fibers to be loaded longitudinally (along the cylindrical axis) and the geometry to be constant throughout. More complex models incorporate additional parameters, such as flaws within the fiber (to account for defects inherent in the manufacturing process) or transverse loading on the fiber (to account for the interaction with the matrix), to more accurately capture the response of fibers [17].

In addition to studying fiber fracture with models, this damage mode is commonly observed in experimental tests of composite laminates. There is good agreement between the strength of materials model and the experimental mean fiber strengths. In experiments on composite laminates, fiber fracture is observed as the dominant final failure mode in cross-ply laminates and also in laminates with angle plies and a large number of 0° and 90° plies [18, 19]. The effects of fiber diameter on fiber strength have also been studied in experiments. In such studies, the strength of fibers increases as the fiber diameter is decreased. This increase in strength is attributed to the probability of fewer flaws being present in smaller diameter fibers. Researchers found that as the fiber diameter was decreased, the presence of larger flaws (on the order of the fiber diameter) caused the fibers to break during manufacturing. Therefore, the smaller diameter fibers precluded the presence of larger flaws, resulting in inherently stronger fibers [8, 15, 20].

3.1.2 Matrix Cracking

Matrix cracking is a common damage mode observed in composites structures. The mode initiates as microcracks within the matrix. These microcracks typically begin at singularities (e.g., voids, flaws, material discontinuities) within the material [21] but can also begin at points in the matrix where the stress field exceeds the matrix strength. As the microcracks grow, they interconnect, creating a main crack that will typically grow normal to the loading direction. As loading is increased, and if matrix cracking is the only damage mode present in a laminate, a uniform density of matrix cracks form within the damaged laminate layer until the loading exceeds a critical point, causing the cracks to propagate into neighboring layers or initiate other failure modes (e.g., delamination) [9, 22]. An illustration of matrix cracking in a unidirectional lamina is provided in Figure 3.

Mechanistic models are used to understand and predict matrix cracking in composites. These models range from simple strength of materials models to damage-dependent constitutive models. The simple models typically predict the initiation of matrix cracks, while the more complex damage-dependent models capture the effects of matrix cracking on laminate strength [23]. This cracking reduces the strength of the laminate [9]. Another approach to predicting the initiation and growth of matrix cracking uses concepts from linear elastic fracture mechanics [5].

The parameters influencing matrix cracking have been studied by analytical models, such as those previously mentioned, and in experimental tests. Flaggs and Kural [5] observed that the formation and growth of matrix cracks depend strongly on laminae thickness and also on the orientation of adjacent plies. These variables have been found to influence the matrix crack spacing (distance between cracks) within a laminate. In other works, transverse cracking was observed to initiate in the off-axis (90°) plies of laminates (of many different layups) under longitudinal tensile loading (loading along the 0° axis) [5, 24-27]. These transverse cracks would grow through the ply within which they initiated until reaching an adjacent ply. If the cracks met an adjacent ply at the same orientation, the crack would continue to propagate through the adjacent ply. If the crack met an adjacent ply of another angle, the crack would typically arrest (not continue into the adjacent ply) and may act as the initiation point for local (interior) delamination [23, 28].

3.1.3 Microbuckling

Microbuckling is the dominant compressive damage mode observed in composite laminates [29]. Microbuckling has been studied since the 1950's and two different theories on the mode have emerged [30]. The first group of theories assumes the fibers and matrix behave elastically, while the second group assumes a plastic response. For the elastic microbuckling case, compressive loading causes the continuous fibers to locally buckle (i.e., buckling occurring at the fiber level as opposed to structural (Euler) buckling, which involves buckling of the entire composite specimen), resulting in either an extensional or shear mode of fiber buckling [7, 16, 31]. In the extensional mode, the fibers buckle out of phase and create regions of compressive and tensile loading in the matrix between the fibers. In the shear mode, the fibers buckle in phase and create a shear loading in the matrix between the fibers [10, 31]. The two types of elastic microbuckling are illustrated in Figure 4 and Figure 5. If the magnitude of the buckling becomes large enough, the extensional or shear stress (depending on elastic buckling mode) exceeds the matrix strength, causing matrix failure. As mentioned in the section on fiber fracture, the fibers continue to locally buckle until the amplitude of buckling causes fiber fracture due to bending. In both modes of elastic microbuckling, the matrix behaves in a linear elastic manner. For the plastic microbuckling case, which has been found to be more common than elastic microbuckling [30, 32, 33], the compressive loading causes a nonlinear (plastic) response in the matrix. In this type of microbuckling, a localized group of relatively misaligned fibers kink when the compressive load is applied, forming a "kink band" as shown in Figure 6. During plastic microbuckling, the matrix behaves in a nonlinear fashion.

Many models have been proposed to capture the mechanisms of microbuckling [e.g. 7, 16, 30, 33-36]. The various models were developed due to the varying theories of the dominant compressive failure mechanisms. In the 1960's, Rosen [7] was one of the first to model elastic microbuckling. His model assumed elastic bending of the fibers, elastic shear of the matrix, and perfect fiber alignment. The Rosen model has served as the base for many subsequent models developed. In the 1990's, Budiansky and Fleck [33, 35] developed one of the first models for plastic microbuckling. Their model assumed an initial fiber misalignment that, when loaded in compression, lead to nonlinear behavior of the matrix and the formation of a kink band. The predictions from

the Budiansky-Fleck [30] model have good agreement with limited amount of experimental kinking results.

Many experimental investigations on microbuckling can be found in the literature. Jelf and Fleck [30] were able to achieve elastic microbuckling using non-traditional composites (one made of glass fibers and the other of wheat flour/spaghetti fibers, both in a silicone matrix). They found that the matrix must behave in a linear elastic fashion up to high strains in order to observe elastic microbuckling. When the matrix met this requirement, Jelf and Fleck had good agreement with the predictions of the Rosen model. However, they note that the majority of matrices used in commercially available composites do not exhibit this behavior. The more common experimentally observed form of this damage mode is plastic microbuckling. Berg and Salama [37] were among the earliest to observe plastic microbuckling in graphite/epoxy composites followed by more extensive studies by Weaver and Williams [38]. Many experimental studies have followed since and typically find plastic microbuckling to occur in plies aligned with the loading direction when a multidirectional laminate is loaded in compression [16, 29, 30, 34, 37-40]. Experimental observations from these studies have found the kink bands (area of plastic microbuckling) to be nearly parallel and to scale with fiber diameter [29, 34].

3.1.4 *Interfacial Debonding*

Interfacial debonding, or fiber pull-out/push-out, is a damage mode in composite laminates loaded in tension or compression where the embedded fiber debonds from the matrix, allowing the fiber to slide past the matrix. Interfacial debonding has two main steps: the first is the debonding between the fiber and matrix; the second is the extraction (sliding) of the fiber from the matrix [41-43]. These mechanisms are both governed by the interfacial shear stresses. An illustration of interfacial debonding is shown in Figure 7.

Analytical models of interfacial debonding have been proposed [e.g. 41-47]. Many of the models represent the fiber and matrix as a single cylindrical fiber embedded in a cylindrical block of matrix. The fiber is then either pulled or pushed out of the matrix. Each model uses different assumptions about the mechanisms at work during the interfacial debonding process, according to the underlying theory of the model. In shear lag theory, the axial stress in the fiber is assumed to be entirely transferred to the matrix through shear stress at the fiber-matrix interface, the residual radial stress to be uniform, and the debonding to initiate from the top surface. Other theories incorporate friction effects, relax some of the assumptions used in the shear lag theory, and/or use finite element methods to analyze the process [e.g. 42-44]. The advantage to the shear lag theory is that it provides a closed-form solution, allowing the effects of the model parameters to be efficiently analyzed. These parameters include the elastic mismatch between the fiber and matrix, fiber radius, bonded fiber length, and residual stress.

Experiments have been conducted to study the parameters of interfacial debonding. Kelly and Tyson [48] were some of the earliest researchers (1965) to investigate the pull-out phenomenon by testing metal-metal composites. Continued

experimental work by Kelly [41] found direct relationships between the extraction load (required to pull out an embedded wire from a matrix) and the wire's embedded length and the wire's diameter. Another parameter found to be important in the pull-out process is friction. Bowden [49] and Takaku and Arridge [42] studied frictional effects and found that the compressive stress between the matrix and fiber had a significant effect on the friction stress and therefore on the load required to extract fibers. Beaumont and Phillips [50] observed pull-out during their research on the tensile strength of notched composites. In their work, fibers were surface-treated and the mean fiber pull-out lengths were recorded. The mean fiber pull-out lengths ranged from 0.02 mm to 0.24 mm (2 to 30 fiber diameters) for carbon fibers in a polymer matrix with various fiber surface treatments [50]. El-Zein and Reifsnider [51] observed fiber pull-out to be the dominant failure mode in angle-ply tensile specimens with a central hole when the ply angles were small (less than 30°). This finding shows that interlaminar effects influence interfacial debonding. It was also observed that changing the constitutive properties (e.g., changing the fiber or matrix type) affects the stress state and hence the interfacial debonding damage mode [21, 46].

3.1.5 Delamination

Delamination is an out-of-plane damage mode in composite laminates where plies separate from neighboring plies. Delamination initiates due to interlaminar stress gradients (e.g., gradient stress fields due to structural details, flaws, the presence of other damage modes, ply-drops, or free-edge effects) developed from in-plane and/or out-of-plane loading of laminates, resulting in a separation between two laminate layers [6, 9, 28, 52, 53]. This separation causes the internal loads to redistribute around the delamination [54, 55]. Delamination itself does not typically coincide with final failure. Instead, the redistribution of loads due to the delamination results in an in-plane failure mode causing final failure [56]. For in-plane loading, delamination typically initiates at points where large stress gradients are present, such as at ply-drops and free edges. For out-of-plane loading, such as low velocity impact, delamination can typically initiate anywhere within the laminate (through the thickness) near the point of transverse loading [54]. An illustration of an edge and an internal delamination is shown in Figure 8.

Two basic approaches have been used to model delamination in composites. In the mechanics of materials approach, the prediction of interlaminar stresses is used and compared with the interlaminar strength of the composite [56, 57]. This method relies on an accurate prediction of the interlaminar stresses and determination of the interlaminar strength. Various methods, such as the semi-analytical approach, have been suggested to predict the interlaminar stresses [56-60]. After obtaining the interlaminar stresses, the methods predict delamination to initiate once this stress has exceeded the interlaminar strength over a characteristic length. Kim and Soni [57] take this length to be a ply thickness. The other approach to predicting delamination is a fracture mechanics approach. This approach treats the delamination as a crack propagating between two dissimilar layers. The approach typically defines a critical strain energy release rate to determine crack propagation [9, 54, 61, 62]. Limitations of this method include the necessity of defining a crack initiation point and a propagation path before the analysis.

Much work has also been done experimentally to reach a better understanding of the delamination process in composites [e.g. 28, 54, 55, 57, 62]. Many of the studies revealed the thickness of laminates, in particular the relative thickness of plies, to be an important parameter. Pagano and Pipes [6] found the stress required for the onset of delamination to be dependent on the composite material, and that the developed stress fields were dependent on the laminate thickness and stacking sequence. O'Brien [53] studied the effect of the stress-free edge on the growth of local delamination and found the thickness of the laminate to control whether edge delaminations or local delaminations initiated. Salpekar and O'Brien [28] studied the effect of ply thicknesses on delamination in $[\pm 25/90_n]_s$ laminates. They found that edge delaminations formed at the -25/90 interfaces when n is less than 3. However, when n is greater than or equal to 4, local delaminations formed in the 90° plies. These papers all found the ply thickness to be a critical parameter in the stress fields affecting the delamination process. Others also investigated the effect of interlaminar stresses on delamination. As mentioned above, Pagano and Pipes [6] found the stacking sequence of a laminate to affect delamination initiation. They found the angle between neighboring plies to affect the interlaminar stresses. Brewer and Lagacé [56] applied their quadratic delamination criterion to experimental tests and showed the interlaminar stresses and an averaging dimension (defined for each laminate) to be directly proportional to the effective ply thickness. From their criterion, they found the interlaminar strength parameters to be material constants, but their averaging dimension had to be determined experimentally. In further work, Lagacé and Bhat [63] found they were able to suppress delamination by altering the interlaminar stresses in a laminate with the addition of interlayers. These interlayers were found to delay delamination initiation by providing a reduction of interlaminar stresses.

3.2 *Mode Interaction*

A knowledge of the basic damage modes, as discussed in the section "Basic Composite Damage/Failure Modes", is necessary to understand damage and failure of composites. However, in actual test specimens and structures, the damage process usually involves more than one active damage mode. Each damage type present affects the stress distribution in the composite and therefore causes interactions (even if indirect) between the modes. An example of a commonly observed interaction is between matrix cracks and delaminations. Flaggs and Kural [5] observed this interaction, noting that matrix cracking was present in all their tested T300/934 composite specimens (with various stacking sequences) before interlaminar delamination occurred. While research has historically focused on understanding of the individual damage modes, it is essential to also understand how the modes interact.

Studies investigating mode interactions are relatively limited. Of these, the interaction of matrix cracking and delaminations has received the most focus. Some studies have shown the modes to interact in ways to resist further damage. For example, Armanios, Rehfield, and Weinstein [64] conducted experiments and found matrix microcracks to interact with delaminations resulting in a resistance behavior to delamination growth. O'Brien [9] observed another interaction between matrix cracks and delaminations called: "delamination shifting," where a delamination growing

along one interface comes to a transverse matrix crack and the delamination face switches to a new interface. Other research has observed matrix cracking in the wake of interfacial debonding and it has been proposed that the interaction between the modes determines the direction of damage propagation [65]. Similar to O'Brien's observations, O'Brien and Kim observed matrix cracking in all experimental test specimens that exhibited ply delamination [57, 66]. For the case of a $[0_2/\pm\theta_2]_S$ graphite/epoxy laminate under tension-tension fatigue loading, matrix cracking in the -θ plies always preceded the onset of local delamination at the θ/-θ interface [61]. O'Brien [66] also found that the presence of matrix cracks alters the stress state at the free edges which effect the initiation of edge delaminations.

The influence of interlaminar effects on damage modes also contributes to mode interaction. These interlaminar effects include stacking sequence, ply thicknesses, holes and details of components, free edges, ply-drops, and fiber bridging. Pagano and Pipes [6] were among the first to investigate the influence of the stacking sequence on the strength of laminates. They demonstrated that interlaminar stresses (responsible for delamination) could be controlled by changing the stacking sequence of a composite [6, 67]. The stacking sequence has also been found to change the mode of failure within laminates [68, 69]. Jen, Kau, and Hsu [18] found the stacking sequence of the laminate to control the shape of delaminations.

An interlaminar effect that has received much attention in the literature is the effect of specimen size on material characterization and damage. Changing the in-plane (width and length) and out-of-plane (thickness) dimensions resulted in a change of specimen strength and in some cases a change in failure mode [70-72]. Similar work has investigated the effects of scaling specimens. Scaling composites in the thickness direction presented challenges since composites are a layered material. To increase the through-thickness dimension of specimens, two methods are common: ply-level scaling and sublaminate-level scaling [73]. Ply-level scaling increases the thickness of each ply for a given stacking sequence, while sublaminate-level scaling repeats stacking of a basic sublaminate to form thicker laminates. Herakovich [72] found that the strength and toughness of angle-ply laminates increased significantly when using a sublaminate-level scaling compared to using the ply-level method. This increase in strength and toughness is related to the effect of the ply thickness on interlaminar stresses. The effect of grouping plies of the same angle (the ply-level method) can be viewed as equivalent to having an "effective" single ply with a thickness equal to the combined thicknesses of the combined plies [74]. The observations Herakovich found was due to influence of ply orientations (and location through the thickness) on the interlaminar stress in the laminate. Jackson [70] tested scaled rectangular specimens in flexure and found the cross-ply laminates exhibited a transition in failure mode with specimen size. The smaller scale specimens were observed to fail by fiber fracture while the larger scaled specimens failed by delamination. These works show that lengthscales do not simply scale with geometric lengths and that an interaction between the loading (and hence the present strain-fields) and the mechanisms controlling the initiation of damage modes changes as the specimen size changes. An example of this phenomenon is the strength of a laminate. Some researchers claim that the strength is influenced by the material volume without considering the individual dimensions [75]. However, other research has shown that the in-plane dimensions (width and length) have little effect on the

strength of a laminate and that the out-of-plane dimension (thickness) and location of plies through the thickness is directly related to the strength of a laminate [71, 74, 76].

Fiber bridging is another interlaminar effect observed in composites. It occurs when a delamination runs through a ply, resulting in fibers bridging the two surfaces created by the delamination [64]. This damage exposes multiple lengthscales that must be considered, such as the length of bridging fiber and the distance of the delamination opening at the bridge. Fiber bridging causes artificially high values of the critical strain energy release rate, G_{Ith} [77] when using fracture mechanics to describe delamination. Therefore, this bridging affect must be considered when developing and using damage models in order to accurately capture the composite behavior.

Another interlaminar interaction observed experimentally is referred to as "stitch cracking." Stitch cracks are a form of high density matrix microcracks that develop in layers above or below a traditional matrix crack. Some of the earliest researchers to observe this mode were Jamison et al. [78]. The breakthrough for discovering these small matrix cracks was due to the development of higher resolution X-ray technique. Before the high resolution technique, these cracks were not resolved in X-ray images. However, Jamison et al. only noted the observation of small matrix cracks crossing over larger matrix cracks and did not investigate them any further. Further study did not occur until Lavoie and Adolfsson [79] observed these small cracks while investigating matrix cracking using computed microtomography (CμT). Their work utilized the newly available CμT nondestructive evaluation technique to investigate damage of composites in three dimensions. Lavoie and Adolfsson recognized that small cracks were forming in the neighboring layers around traditional matrix cracks. They observed that these cracks appeared to be 'stitching' the traditional matrix crack and referred to this phenomenon as "stitch cracks." An image from Lavoie and Adolfsson's work showing stitch cracks is shown in Figure 9. These stitch cracks formed within the -45° plies, the cracks aligned with the fiber direction, and repeating along the path of the traditional matrix cracks in the 90° plies. Lavoie and Adolfsson found that the difference in angle between neighboring plies determined whether stitch cracking or delamination initiated from these traditional matrix cracks.

3.3 *Design Approach*

The general intent of studies on composite failure is to gain the knowledge necessary to design safe composite structures. The current approach to designing safe (avoiding damage) composite structures is the building block approach (BBA). This approach was first demonstrated by Whitehead and Deo [80] when they discussed the necessity of an approach for certification of composite structures in aircraft. The building block approach defines experimental tests along the levels leading up to the final, full-scale component. As part of this process, Whitehead and Deo emphasize the need for verification tests starting at lower levels (i.e., coupons) and leading up to a full-scale test. The verification tests at lower levels allow designers to reach an understanding of the behavior of structural features individually. As Guyett and Cardrick [81] discuss, reaching the same understanding through full-scale testing is cost prohibitive due to the number of tests required and the expenses in producing and instrumenting the full-scale, more complex components.

The building block methodology has become the accepted approach for certifying composite structures [82-84]. It has been proven to produce successful and safe structures [2, 83]. As described in Composite Materials Handbook 17 [82], the method provides a systematic way of treating composite materials to obtain material "allowables." These allowables are determined through extensive experimental testing at various structural detail levels. The building block approach splits the levels into three main groups [82], as shown in Figure 10, with each group building off the lower one.

The base group of the BBA, group A shown in Figure 10, begins with collecting material data on candidate materials and making a decision on which material(s) will be selected for a given project. Numerous experimental tests are conducted on coupons to gather statistically significant material data for the selected material(s). The next higher level in this group assumes the preliminary material and processing data have been collected. The objective of this level is to study the effects of process variables on the material behavior. The third level in this group establishes "firm" material allowables to be used in the design of composite structures using such a material [82, 84]. These allowables take into account environmental effects (e.g., hygrothermal), lamination effects (e.g., ply orientations, stacking sequence, laminate thickness), and effects of defects and variability during manufacturing. Once the testing of group A is completed, details of the material system are fully established. These details are then passed upward to the next group of testing.

The second group of the BBA, group B, begins introducing structural details that are often project specific. The first level of this group tests structural details that are found within the structure being designed (e.g., joints, bolt or rivet holes, stiffeners). The data collected from these tests are frequently used to support analytical techniques. Testing at this level becomes more time consuming and costly than the base level because of the increased complexity of the specimen (compared to the coupon specimens). Therefore, fewer and fewer tests are run at the higher levels (a trend throughout the entire BBA) [82, 84]. In the second level of group B, data on subcomponents is collected. The subcomponents combine multiple structural details into one specimen to permit assessment of load redistribution due to local damage.

The final group of the BBA, group C, is the final stage of testing. At this point, the material specifics are well-established and damage resulting from structural details has been well studied. The final test required by the BBA is a single test of the designed component [82]. This one test is used to verify model predictions, such as strains and deflections, and is the final stage in the certification process.

While the building block approach has provided a methodology for certifying safe composite structures, the approach has limitations and does not allow full utilization of the advantages and efficiencies offered by composites. After material allowables are determined at a lower level, they are passed to higher levels by using knockdown factors. These knockdown factors decrease the material allowables to account for, often unknown, changes in material response (i.e., strength and/or stress field variabilities) as more structural complexities are included. However, to establish

valid knockdown factors, the damage type present in the lower level test is required to remain the same throughout higher level testing. As an example, if a stiffener buckles at the sub-component level but buckling was not observed at the element level, additional testing would have to be done at the element level to determine the buckling behavior of the stiffener. Any variation in the damage type (e.g., an additional damage mode, not present in the lower level test, initiating during the higher level test) or interaction of damage types nullifies the establishment of a valid knockdown factor. This is a considerable limitation of the building block approach, resulting in a virtually one-way process relying heavily on empirical and semi-empirical approaches. Any new observations made at higher levels indicating the necessity of changes at lower levels result in restarting the process from a previous level, or in some cases restarting from the beginning; otherwise, the designer proceeds with a sub-efficient design [2].

The other key limitation to the building block approach is its inability to allow researchers and designers to investigate lengthscale effects. Without knowledge of how damage mechanisms change across levels, the design process is very inefficient. Preliminary designs of structures are made without knowledge of how damage will affect the performance/strength of the structure. Testing then must be done, following the BBA, to decide if the preliminary designed structure will meet performance criteria. If the preliminary design does not meet the criteria, a redesign is necessary and testing must be repeated from the early stages of the BBA. Even if the preliminary design meets the performance criteria set for the component, there is no guarantee that the most efficient design has been reached, only that the design is adequate. Spearing, Lagacé, and McManus [2] identify these drawbacks and offer a more efficient philosophy for the process that makes greater use of mechanism-based models in the certification process. Using such models allows the mechanisms controlling damage, as well as how these mechanisms change across lengthscales, to be better understood. This enhanced understanding allows a two-way design process to be achieved, permitting information gathered at each level to be shared across levels, resulting in a more efficient design process. However, this process relies on an ability to predict the effects of damage on the structure.

3.4 *Prediction of Damage and Failure*

In order to use composites to their full potential as structural materials, it is important to have the capability to predict the conditions under which the composites fail. Failure criteria use models, often with implicitly associated lengthscales and occasionally with explicitly associated lengthscales, to attempt to capture the behavior of composites. Many of the models were developed before the importance of lengthscale effects were recognized. Therefore, these lengthscale effects were not explicitly worked into these models. The ultimate goal of these criteria is to accurately predict when damage/failure will occur. The numerous criteria proposed can be grouped into two general categories: non-mechanistic and mechanistic. The non-mechanistic-based criteria predict failure in a general sense (without predicting the damage mode(s) responsible for failure), while the mechanistic-based criteria predict the particular damage mode(s) causing damage/failure. The development of failure criteria has been the focus of many researchers around the world [85, 86].

In the 1990's, concerns about the general problems faced when designing with composites led to an 'experts meeting' held in the United Kingdom [85]. Composites experts from around the world were invited to discuss failure and failure criteria. There were two outcomes from the meeting: (1) there was no universal definition of 'failure' in composites, and (2) there was a lack of confidence in the universal applicability of the failure criteria [85]. From these results and the discussions at this meeting, two researchers, Hinton and Soden, began organizing the World Wide Failure Exercise.

The World Wide Failure Exercise (WWFE) was developed to 'test' current failure criteria through a series of round robin studies. The exercise began in 1998 and was concluded in 2004. The goal of the exercise was to provide an unbiased comparison between the various criteria, offer a summary of the strengths and shortcomings of each criterion, and establish the current level of maturity of composite failure prediction. Originally, eleven groups decided to participate, with other groups later joining the exercise [85, 87]. The exercise was broken into two parts. The first part required participants to predict failure for a series of test cases from data made available to all participants. The participants were provided with the test geometry, laminate arrangements, laminate material properties, and loading cases. However, the participants were kept 'blind' by not being provided with the experimental failure data during the first part of the exercise. The 'blind' failure predictions were collected from the participants by the organizers and compared for each of the 14 test cases. The second part of the exercise provided the participants with the detailed experimental procedures and failure results from the test cases. The participants were then asked to compare their original predictions to these results and discuss any refinements made to their predictions after receiving the failure data. The organizers again collected papers from the participants and compared the refined theories [85].

The results from the WWFE showed that the current predictive criteria were unable to fully capture failure in composites [88]. Criteria could typically predict failure for certain load cases (e.g., a specific in-plane biaxial load) reasonably well, but would break down for other loadings (e.g., changing the regime of biaxial loading). The WWFE also showed that many of the criteria are empirically dominated. Empirically based criteria rely on experimental data collected from laminates to set failure envelopes. However, these criteria are unable to adjust for changes in laminates (such as simply changing the order of the layup) without requiring additional experimental data to be collected. Failure predictions were made via the criteria involved in the WWFE given the supplied data for the six laminate layups tested, but a few of the criteria were designed for unique laminates and had limitations allowing them to make predictions only for a subset of the tests. A detailed summary with comparisons between the performance and capabilities of the criteria from the World Wide Failure Exercise is found in references [1, 89, 90].

While literature has traditionally classified failure criteria (such as those to participate in the WWFE) as either based on strength of materials or based on fracture mechanics, it is more useful to understand the lengthscales involved in failure criteria by classifying them as mechanistic- or non-mechanistic-based. Mechanistic-based methods have the advantage that they allow researchers to gain knowledge of the parameters influencing damage and failure in composites. The mechanistic-based

methods [e.g. 91] help identify critical lengthscales and allow the effects of changing laminate properties (e.g., fiber and matrix constituents, laminate layups) to be observed without the need for extensive testing. However, non-mechanistic methods [e.g. 92-95] are based on empirical fitting and do not offer insight on the lengthscales involved in the damage/failure process. In the following sections, some of the current non-mechanistic and mechanistic criteria are presented and discussed.

3.4.1 *Non-Mechanistic-Based Methods*

The majority of failure criteria, to date, are non-mechanistic and rely on empirical data to predict the conditions for failure of composites at the constituent and ply levels. The simplest, and some of the first, criteria offered to predict failure in composites are the maximum-stress and maximum-strain criteria. These criteria descended from metallic failure criteria, with the basic idea that there exists a critical level of stress, or strain, that, once exceeded, will cause failure in the material. One of the earliest researchers to apply a maximum-strain criterion to composites was Waddoups [96, 97]. The maximum-strain criterion considers in-plane strains and is a non-interactive model, requiring five empirically-determined critical values to predict failure. The critical values necessary for the criterion are the maximum strains for a ply. These include the tensile and compressive values along the fiber direction, the tensile and compressive values along the transverse direction, and the shear value. The damage type occurring in the composite is usually inferred by the critical value exceeded. For example, when the critical value along the fiber direction is exceeded, fiber fracture (for tension) or microbuckling (for compression) is assumed. However, the model does not explicitly give the failure mode. Bogetti developed a variation of the maximum-strain criterion which allows nonlinear shear behavior and includes a simple progressive failure method [92, 98]. As with the maximum-strain criterion, the maximum-stress criterion considers only in-plane stresses and is a non-interactive model, requiring five empirically-determined strength values. For the maximum-stress criterion, the strength values determined are critical stress values. Zinoviev developed a maximum-stress criterion which assumes linear-elastic material behavior up to initial failure and includes continuous correction factors for the effects of the change in fiber orientation [93, 99]. Bogetti and Zinoviev both submitted their criteria to the World Wide Failure Exercise (WWFE) and were ranked highly (performed well) compared to the other participating criteria. The implicit lengthscale associated with the maximum-strain and maximum-stress based criteria is on the order of a ply thickness. This is due to the method used in calculating the ply level strains or stresses, which is traditionally done by using the classical laminated plate theory (CLPT).

The Tsai-Wu [94] criterion is another criterion involved in the WWFE and also ranked highly. The criterion includes terms representing a full three-dimensional state stress as well as stress interaction terms, resulting in a quadratic failure surface. The criterion requires empirically-determined material strengths to define critical tensile, compressive, and shear stresses. To determine the interaction terms, combined stress testing (such as biaxial stresses in appropriate planes) is required. While the Tsai-Wu criterion does define different strengths for tensile and compressive loading, it does not differentiate between matrix-controlled and fiber-controlled damage/failure. As with the maximum-stress and maximum-strain criteria, ply level stresses are determined

with CLPT and therefore the implicit lengthscale associated with the Tsai-Wu criterion is on the order of a ply thickness.

The criterion developed by Puck and Schürmann uses a phenomenological model which incorporates nonlinearities due to microdamage, matrix cracking, and changes in fiber angle [95, 100]. The criterion uses two fracture criteria to differentiate between two damage modes: fiber fracture and matrix cracking. The model also identifies uncertainty in damage/failure prediction when different laminates are analyzed by considering stress concentration factors and the effects of stiff neighboring plies on cracks. In their work, Puck and Schürmann used CLPT to determine strains and stresses in each layer, and, like the previous criteria, the implicitly associated lengthscale is the ply thickness. However, unlike the Tsai-Wu criterion, Puck and Schürmann's criterion also have some explicitly associated lengthscales included in their phenomenological model, such as the change in fiber angle within a ply. Puck and Schürmann's criterion and the Cuntze criterion (discussed in the next section, Mechanistic-Based Methods) were the top two ranking criteria to participate in the WWFE [90], although even these criteria only marginally handled all the cases tested in the WWFE.

3.4.2 *Mechanistic-Based Methods*

Very few failure criteria are based on mechanistic principles. The advantage to mechanistic-based methods is that they use physical parameters to model the failure process, allowing the mechanisms involved in damage to be better understood. Thus, mechanistic-based methods offer true (i.e., capturing the actual physical damage process) predictive capabilities. While a purely mechanistic-based method would be desirable, composites are too complex with many parameters that at best can be modeled by probabilistic distributions. However, the move away from criteria that rely on empirical curve-fitting allows researchers to better understand the mechanisms critical to the damage process. Mechanistic-based methods also require fewer experimental tests to obtain necessary variables for failure criteria and therefore can save time and money.

One of the earliest researchers to develop a mechanistic-based criterion for composites was Chamis [91]. His criterion is semi-empirical, using constitutive properties to predict uniaxial strengths of lamina. The model used to predict these strengths considers many parameters of the composite: volume fractions, fiber size and distribution, and elastic and strength properties of the fiber and matrix. Chamis realized that not every variable affecting the properties of composites could be accounted for directly, so he introduced "theory-experimental correlation factors." These factors indirectly account for variables introduced during the fabrication process (e.g., void size, void distribution, fiber misalignment, interfacial bond strength, residual stresses) into the criterion. Chamis used the constitutive properties and the correlation factors to create governing equations for the strengths of the laminate. These strengths are used to define a combined-stress strength criterion based on a distortion energy principle [91]. Because the Chamis criterion uses a mechanistic approach, there are multiple associated lengthscales: fiber diameter, fiber spacing, and the ply thickness. Chamis [101, 102] participated in the WWFE, with his criterion preforming adequately.

As noted by Hinton et al. [1] when comparing the performance of the participating theories, Chamis' criterion had a few significant and fundamental weaknesses, such as a lack of robustness and maturity in the approach taken for post-initial failure modeling.

The criterion developed by Cuntze is another mechanistic-based criterion. It uses nonlinear analysis to predict progressive failure. The criterion considers three-dimensional failure mechanisms and includes interactions between failure modes due to probabilistic effects. The main idea of Cuntze's criterion is the formation of five independent damage models: two for fiber failure and three for matrix failure. These include the fiber fracture, fiber microbuckling, and matrix cracking modes as discussed in the section "Basic Composite Damage/Failure Modes". Delamination and interfacial debonding are not modeled in this criterion. For each of the five damage modes Cuntze considers, a single strength and modulus are used to characterize the damage mode [103]. Unlike Chamis' criterion, Cuntze's criterion relies more heavily on empirical data. However, Cuntze's criterion investigates the mechanisms of damage in greater detail and also includes parameters for mode interaction [104]. The lengthscales associated with the criterion include the ply thickness, the void or nucleation size responsible for the initiation of microcracks, and the fiber diameter. Cuntze's criterion was in the top two ranked criteria to participate in the WWFE [90].

3.5 *Lengthscales in Composites*

Many lengthscales associated with composite materials can be identified throughout the literature, although very few authors actually refer directly to the lengthscales in their manuscripts. One of the earliest papers addressing the role of lengthscales in composites was published in 1998 by Spearing, Lagacé, and McManus [2]. Relatively few papers directly addressing lengthscales in composites have since appeared. However, consideration of the many previous works on composite damage reveals investigations of the damage modes and mechanisms controlling damage at specific lengthscales. For example, the investigations on fiber fracture find the critical lengthscale of that damage mode to be a fiber diameter. While one can look through the literature on composite damage and extract information associated with lengthscales of each of the damage modes, no specific studies investigating the lengthscale effects have been found. Although the community has observed changes in damage characteristics as the scale of testing changes, there has been no explicit recognition or call out of these changes as lengthscale effects. To capture these changes in the composite structure certification process, the community developed multiple levels of testing. Before addressing lengthscale effects explicitly, it is therefore important to understand the levels commonly used for testing composites and how these are tied to manufacturing and assembly of such structures.

The current levels identified in the literature and used in design are the sub-ply, ply, laminate, sub-element, element, sub-component, and component [2, 80, 82]. Examples of the levels used in composite engineering are shown in Figure 11. Beginning at the sub-ply level, the mechanical properties of the composite constituents (matrix and fiber) are individually determined. Moving up a level to the ply level, the constituents are combined into a composite ply. Simple loading cases are typically tested to determine the properties of this ply [82]. Varying the constituents (from the

sub-ply level) results in changed properties at the ply level. Proceeding to the next level, plies are stacked at various angles to form laminates. These laminates are produced by stacking plies and/or fabric layers to form unidirectional, cross-ply, angle-ply, quasi-isotropic, or other laminates. The laminate level is traditionally where most coupon testing is conducted [80, 82-84]. At the next level, that of the sub-element, structural details (e.g., holes, ply-drops, stiffeners) begin to be included. At the sub-element level and higher, structural features and configurations introduce lengthscale effects different from the material effects that dominate the lower levels. Sub-elements and laminates are combined at the element level to comprise structural details (e.g., sandwich structures, stiffened panels) that are repeated within the structure [82]. The sub-component level is again more complex than the lower element level, typically being sections of the full component, such as a wing box. The final level is the designed component. An example could be a composite wing formed of various laminates, stiffeners, holes, and other structural details that are all of smaller lengthscales.

As discussed in the section on "Design Approach," these levels are utilized throughout the Building Block Approach. The lower levels (i.e., sub-ply, ply, and laminate) are based on convenient test sample sizes, related to testing procedures, while the higher levels (i.e., sub-element, element, sub-component, and component) are based on manufacturing and assembly techniques and issues. These specific levels are therefore not based on particular damage behavior observed, but rather on convenient lengths associated with manufacturing and production aspects. In the Building Block Approach, each level builds upon the previous lower level, with structural complexity increasing across the levels.

3.5.1 *Lengthscales of the Basic Composite Damage Modes*

Lengthscales associated with each of the basic composite damage modes (those discussed in the section "Basic Composite Damage/Failure Modes") have been collected from the literature. These lengthscales have been identified by previous researchers as influencing the individual damage modes (although very few authors actually refer directly to the lengthscales). The lengthscales found in the literature associated with fiber fracture are the fiber length, fiber diameter, and inter-fiber spacing [8, 10, 12, 14, 15, 17]. From the analytical and experimental studies in the literature, the key parameter identified for fiber fracture is the fiber diameter. This lengthscale has been shown to affect the fiber strength and the probability of flaws being present in the fiber. Therefore, the fiber diameter is the critical lengthscale for the fiber fracture damage mode.

The lengthscales associated with matrix cracking include the void or nucleation size responsible for the initiation of microcracks, the ply thickness, the spacing between cracks, and the length of the matrix crack [5, 27, 21-24, 28]. It is also noted that the angle between plies plays an important role. However, there is no "length" defined to measure the angle between plies. Therefore a length associated with this measure needs to be defined. From the literature, a single critical lengthscale for the matrix cracking damage mode has not been identified. Rather, multiple lengthscales contribute to the behavior of matrix cracking.

The lengthscales associated with microbuckling include the fiber diameter, buckling wavelength, and fiber misalignment [7, 10, 16, 29-35, 37-40]. The elastic and plastic microbuckling each has its own critical lengthscales since the mechanisms controlling each mode change. For elastic microbuckling, the critical lengthscales are on the order of a fiber diameter or smaller [7]. For plastic microbuckling, the critical lengthscales are on the order of 10-20 fiber diameters [16, 29, 31, 33, 34, 40].

The lengthscales associated with interfacial debonding include the fiber diameter, the bonded fiber length, and the sizing thickness [21, 41-47, 49-51]. Other factors, such as the stress state acting at the interface of the fiber and matrix, affect the mechanisms controlling interfacial debonding. The lengthscales associated with these factors have not been identified in the literature. The critical lengthscale for interfacial debonding, identified in the experimental and analytical studies, is on the order of tens of fiber diameters.

The lengthscales associated with delamination include the ply thickness, the length of the delamination crack, the interply region thickness, and the characteristic length of the interlaminar stress-field [6, 9, 28, 53-63]. The characteristic length has two typical definitions in models of delamination. The first defines the length as the distance over which the stress must exceed the strength of the material. The second defines the length as the distance away from a stress-concentrator that the stress has to exceed a critical value before delamination will initiate. As with matrix cracking, the angle between plies also plays an important role in delamination and a length associated with this measure needs to be defined. The literature has identified the laminate thickness as a critical lengthscale for delamination. The thickness of the laminate was found analytically to dominate the effects of interlaminar stresses and was found experimentally to determine the type of delamination to initiate. The literature also identifies the effect of the stacking sequence on the associated lengthscales.

A summary of the lengthscales associated with each of the basic damage/failure modes is shown in Table 1. These lengthscales were collected over the course of the literature review and have been identified by previous researchers as having influence on the individual damage modes. While these researchers may not have explicitly referred to these lengthscales, upon reexamination of their works, the associated lengthscales were identified. Other lengthscales may exist that influence the individual damage modes, but they were not identifiable from the previous works.

3.5.2 *Lengthscales Associated with Inspection Techniques*

An important consideration when investigating lengthscales in experimental studies of composite specimens and structures is the observable lengthscale of inspection techniques. In order to observe and study damage in composites, the damage must be resolvable with the inspection technique. An example is the observation of stitch cracks (described in the section "Mode Interaction"), which had previously been undetected. Prior to the higher resolution X-ray technique, researchers had not been able to observe this damage type. Since composite inspection methods continue to improve, damage modes previously unknown are being (and may continue

to be) identified. Bossi [105, 106] was one of the first to apply computed tomography to composites in order to preform failure analysis. Since then, others have used the

Table 1 Lengthscales associated with the basic damage modes

Damage Mode	Associated Lengthscales
Fiber Fracture	Fiber diameter, fiber length, inter-fiber spacing
Matrix Cracking	Void/nucleation size, ply thickness, angle between plies*, crack length, crack spacing
Microbuckling	Fiber diameter, buckling wavelength, fiber misalignment
Interfacial Debonding	Fiber diameter, bonded fiber length, sizing thickness
Delamination	Ply thickness, crack length, angle between plies*, interply region thickness, characteristic interfacial stress length

*A length measure associated with the angle between plies needs to be defined.

technique to investigate internal damage of composites. Schilling et al. [107] did further studies on stitch cracking as well as looking at the more general geometry of internal flaws and damage. Wright, Sinclair, and Spearing [108] have pushed the observable lengthscale even smaller using synchrotron X-ray tomography. The synchrotron X-ray tomography offers three-dimensional resolution down to a fraction of a fiber diameter. With an observable lengthscale down to that level, interactions occurring at levels smaller than a fiber diameter can be studied. As inspection techniques continue to improve, lengthscales not yet identified may be discovered. The new inspection techniques also allow the currently identified damage modes and mode interactions to be studied with great resolution.

3.5.3 *Moving Across Lengthscales*

An important component of designing with and utilizing composites as structural materials is the capability to transfer material properties across the multiple levels used. As was discussed in the section "Design Approach," the BBA is the currently used method for passing material allowables up through the levels of testing and design. However, the BBA has considerable limitations that result in partial utilization of the full potential of composites. Using a lengthscale approach will enable scientists and engineers to better their understanding of the mechanisms influencing damage and hence material properties as the structural lengthscales change.

Many studies in the literature on composites can be reanalyzed to show the importance in choice of the appropriate lengthscale(s) for damage modes to have a good understanding of lengthscale effects. Lengthscale effects can then be used to help researchers better understand how damage behavior changes as the level of testing changes, permitting a more efficient procedure for transferring material properties

across the many levels of testing. Lengthscales also permit a new approach to studying damage mode interactions, allowing investigation into how the critical lengthscale for an individual mode changes (if it does) as it interacts with other modes. A lengthscale approach also allows the interactions of stress-field gradients on damage modes to be investigated in a new way.

3.6 *Summary of Literature Review*

Identifying the lengthscales involved in composites is an important step to advancing the understanding of damage and failure of composites. A review of the literature has extracted many composite lengthscales from physical, experimental, and analytical studies. While the majority of studies did not specifically address lengthscales, through their investigations to understand composite behavior, associated lengthscales have been determined. Each basic composite damage mode is presented in the section on "Basic Composite Damage/Failure Modes" and mechanisms influencing these damage modes are identified. Interactions between damage modes are then discussed in the section on "Mode Interaction," bringing up questions on how the lengthscales from the basic damage modes are affected or changed by interactions with other modes (and hence, other lengthscales). The review found little work (relative to the studies of basic damage modes) investigating interactions of modes, making it difficult to identify effects of interactions on lengthscales. The current failure criteria used to predict damage in composites are discussed in the section on "Prediction of Damage and Failure." While the majority of failure criteria are non-mechanistic, a few criteria exist based on mechanistic methods and incorporate lengthscales into the prediction models. The concept of lengthscales associated with composites is presented in the section on "Lengthscales in Composites." The lengthscales associated with the basic damage modes, mode interactions, design, and failure criteria are summarized in this section. The next steps to reaching a better understanding of composite failure are to determine whether the existing lengthscales are sufficient to describe the governing mechanisms of damage/failure and to identify the critical lengthscale (or possibly lengthscales) controlling the damage process across the multiple scales of composite structures.

4. The Question Tree

As discussed, the first step taken during this work was to investigate the background of the topics related to the project and plan an approach to accomplish the project goals. The extensive literature review that was conducted, as described in the previous section, was used to pull together more recent and past literature dealing with the project topics. Using the information and knowledge determined from the literature review, a question tree was developed. This question tree was formed to help guide the process of accomplishing the three primary tasks involved in: assessing current failure models; developing an overall methodology to work through the lengthscale levels through to full-scale structures; and planning the experimental programs to acquire needed knowledge and to work chosen failure approaches and the overall methodology.

The overall goal of the high level, complex question of developing the overall methodology was broken down into two primary branches in the question tree. Branch A, shown in Figure 12, focused on the manifestation of different damage mechanisms within a composite material, laminate, and structure, and the lengthscales associated with such mechanisms. Branch B, shown in Figure 13, focused on the predictive capabilities to calculate stress states, predict failure, and assess overall structural behavior. From these two primary points, which addressed the overall question of developing the methodology, further breakdowns were made into branches with questions needed to answer the higher-level question. Initial focus was on determining answers to the A.3 branch, which addressed lengthscale factors in composites. Answers to A.3.3 were of particular importance as this addresses the contributing factors that have effect on composite damage and how these factors change across lengthscales. In particular, these factors were used when setting up the documentation procedures, ensuring that the contributing lengthscale factors effecting damage were all documented so that key relations could be found.

In working this question tree, further literature was reviewed, primarily addressing damage and failure theories as related to composite materials and structures. One of the focuses in reviewing the literature was on identifying lengthscale issues as encountered in previous works. While most previous works do not specifically identify lengthscale issues and effects, these effects do have influence on testing and are often partially explored and information can be garnered from what is reported. An example of such is work that observes a failure mode transition when the thicknesses of flexural test specimens are increased [e.g. 70]. The failure modes and associated thicknesses were identified in the work, but the mechanisms controlling the transition were not investigated. Such work supports the need to better understand the lengthscale effects occurring in composite materials. The better categorization of this information in concert with other information may lead to the ability to answer questions as posed.

Damage and failure within composites has been of great interest to composite engineers, designers, and researchers, and there are multiple questions in the tree associated with this. The significant research that has been done studying the damage modes present in composites was considered in the literature review. Due to the complex nature of composites and the structures of such, many different damage modes can occur. Damage at the level of the ply to the laminate can be categorized into two areas: in-plane and out-of-plane. In-plane damage modes include fiber fracture, matrix cracking, fiber microbuckling, and interfacial debonding. The out-of-plane damage mode is delamination. The literature review spanned from the specifics associated with studies of each damage mode in isolation to interactions among damage modes, particularly as the lengthscale under consideration increases. The review revealed the need to identify the characteristic lengthscale(s) of each mode, and showed that these are not well documented or understood, particularly as damage grows and mode interactions become present. In particular, the literature review helped identify the needs to be addressed.

An important aspect of using the full potential of composites as a structural material is the ability to predict the conditions under which the structure will fail. There have been many proposed failure theories that work to capture such response of composites. The literature review supported the task, being performed by the research team under the overall effort, of considering various failure theories. It showed that the majority of failure theories are empirically dominated, that most do not address damage type, and that no one theory is able to fully capture failure in composites. These limitations were particularly shown by the World Wide Failure Exercise [1, 85-90], discussed in the literature review. The existing theories are typically able to predict/correlate failure for certain loading cases, but lose their capability for other loading scenarios. It was found that overall, no one theory outperformed other theories across all loading cases. The Dissipated Energy Density approach of NRL continues to be addressed in such.

In addition to the damage and failure work considered, the methodology of the Building Block Approach (BBA) was carefully reviewed and considered to better understand and characterize the current certification/validation procedure used in designing composite structures. The BBA is currently how information is transferred through structural scales in the overall design and certification process. The method requires the identification and isolation of an initial lengthscale associated with a specific damage mode and the determination of "material allowables" associated with such. This lengthscale and its information must be passed to the higher structural level(s) of testing, and only the isolated damage/failure modes accounted for at the lower levels may be present in the higher level testing. The results between the two levels are compared to established "knockdown factors" to use with the baseline data. These "knockdown factors" in some sense blindly account for lengthscale issues introduced at higher structural levels. Furthermore, the levels introduced in this approach are linked to the particulars of manufacturing, assembly, and testing techniques/issues, as opposed to the particulars of the damage lengthscales and their manifestations. Interaction of damage modes are often not accounted for in the overall approach as well. This leads to key overall questions in working toward a better methodology. Further specifics of the Building Block Approach are discussed in Section 3.3 of the literature review.

5. Research Specifics

The details of the research specifics for this part of the overall project are provided herein. These specifics were largely guided by the question tree, both by answers to questions found during the literature review, and by unanswered questions needing investigation during this project in order to work towards answers. Initial effort defined a planned test matrix to investigate lengthscale effects. Effort then focused on developing procedures to characterize damage in tested specimens in such a way to allow lengthscale effects to be identified across specimen levels. Refinements to these procedures were made over the course of this project as lessons were learned. A damage comparison database was then established to gather the information collected during the characterization. Further investigation of damage modes and damage paths

in the tested specimens was made capable through the application of computed microtomography.

5.1 *Planning Test Matrices*

An important aspect of the effort was the coordinated planning among the three primary groups involved in the overall effort in designing test specimens and associated test matrices. Initial plans were made for test specimens to clearly investigate issues that arise as the lengthscale ladder is maneuvered. Many of these details were dependent upon the results for the baseline behavior of the material as determined via the NRL mechatronic loading machine. This machine works to identify the mechanical behavior and failure mechanisms that are manifested at that baseline level and that must be accounted for in moving higher in lengthscales, and then incorporating the issues introduced by the details of the larger lengthscales.

This effort continued throughout the project to support the specimen and test matrix design for the characterization specimens, and even more so for the higher levels of testing. Particular aspects focused on the definition of refinement in the test details for further testing based on the results from initial tests. The higher levels of testing are the specimens with an open hole, the specimens with ply drop-offs, and the stiffened panel specimens. These specimens represent an increase in structural complexity from the baseline characterization tests and allow an investigation of how the mechanisms controlling damage are affected at an increased structural level. In particular, the inclusion of the structural details, the open hole, the ply dropoffs, and the stiffeners, changes the stress-field gradients within the structure and thus the material. These gradients change the forcing lengthscales and introduce the possibility of inducing damage mechanisms and interactions associated with different lengthscales. The details concerning the issues of lengthscales and their importance were part of this consideration in supporting and being a part of this effort. In the design of the overall test matrix, effort was made to account for probabilistic variation. This work, with other members of the team, led to fully defined test specimens and a test matrix (involving test matrices for each of the specimens defined).

In total, four different specimen types were designed for the project: double-notched, open-hole tension, ply-drop, and stiffened panels. All specimens were to be made of the same composite material, AS4/3501-6 carbon/epoxy. The double-notched specimens were designed to be tested in the custom-built six degree-of-freedom loader system (6DLS) of NRL, and were the base-level specimens for this overall project. These specimens were made with eight different stacking sequences: $[+\theta/-\theta]_{16T}$ or $[+\theta_4/-\theta_4]_{4T}$ where $\theta = 15°$, 30°, 60°, and 75°. The specimens have a rectangular geometry of 3 inches by 2 inches and a thickness of 0.175 inches. Notches, with a width of 0.11 inches, are cut at the mid-length on both sides of the specimen. The notches are cut into the specimen 0.45 inches from the edge, ending with a semi-circular notch. This geometry, along with the six degree-of-freedom loader system, allows three-dimensional stress states to be imposed on the specimen, permitting investigation of the mechanisms controlling damage at the base level.

The open-hole tension specimens and the ply-drop specimens represented an increase in structural complexity from the base-level characterization tests and were designed to allow an investigation on how the mechanisms controlling damage are affected at an increased structural level. In particular, the inclusion of the structural details, the open hole or ply drop, changes the stress-field gradients within the structure and thus the material. This changes the forcing lengthscales and may include damage mechanisms and interactions associated with different lengthscales.

The open-hole tension (OHT) specimens were made with three different geometries and two different laminate stacking sequences. The three geometries were a specimen with overall dimensions of 7.5 inches by 1.0 inches by 0.126 inches containing no hole (referred to as a hole of diameter of 0 inches), a specimen with overall dimensions of 7.5 inches by 1.0 inches by 0.126 inches containing a hole of diameter of 0.5 inches, and a specimen with overall dimensions of 13.5 inches by 4.0 inches by 0.126 inches containing a hole of diameter of 1.0 inches. The hole in each specimen is through the thickness and centered on the length and width of the specimen. These three different geometries were selected to allow investigation on the influences due to scaling. The two laminate stacking sequences used in the specimens were $[+45/0/-45]_{4S}$ and $[+45_4/0_4/-45_4]_S$. These two stacking sequences were selected to investigate the influences of effective ply thickness. Most test specimens were to be tested to ultimate failure, with testing on a few specimens to be stopped at the detectable initiation of damage. All OHT specimens were to be tested at CRC-ACS.

The ply-drop (PD) specimens were made with two different laminate stacking sequences, similar in nature to those used in the open-hole tension specimens. The overall dimensions of the specimen are 8.0 inches in length by 1.5 inches in width with thickness at one end of 0.189 inches ranging to 0.126 inches at the dropped end. There is a 2 inch long grip bonded onto each end of the specimen along with compensation for thickness differential at the dropped end. The plies are dropped in a 0.5 inch region in the middle of the specimen. The overall laminate configuration is a layup of $[X, X_D, X]_T$ where the subscript 'D' indicates dropped plies. The two sublaminates used in the specimens are $[+45/0/-45]_{2S}$ and $[+45_2/0_2/-45_2]_S$. These selections allow investigation of the influences of effective ply thickness in this configuration of greater structural complexity. These test specimens were also to be tested to ultimate failure, with the possibility of testing of a few specimens to be stopped at the detectable initiation of damage. All PD specimens were to be tested at CRC-ACS.

The stiffened panel specimens represented another increase in structural complexity beyond the single structural features of an open hole or ply drop. The stiffened panel specimens incorporate multiple structural features, each creating stress-field gradients within the structure and thus the material. The overall dimensions of the specimen are 12.25 inches in length by 10.75 inches in width. The base plate (i.e. skin) has two different layups, with one of each type to be constructed and tested. One is symmetrical, $[\pm45/90/0]_S$, and the other unsymmetrical, $[+45/-45/90/0/0/90/+45/-45]_T$. There are three blade stiffeners located lengthwise on the panel. The center stiffener is centered widthwise, with each other stiffener being located 3.125 inches to the side of the center stiffener. These stiffeners are 1.0 inches in height with layups of $[-45/+45/90/0/0/-45/+45/0]_S$. The lengthwise edges of the

specimen are to be potted for testing. Testing is to be conducted in a test rig to yield clamped conditions for the lengthwise edges and simply-supported conditions for the widthwise edges. It was intended that these two test specimens would be tested to ultimate failure. The specimens were to be tested at CRC-ACS.

5.2 *Need for Damage Documentation*

Once the question tree was fully established and the project specimens defined, the primary focus was on development of procedures to document and characterize damage for use in the overall project and on producing an initial comparison database to investigate the effects of lengthscale on damage. Due to delays at the other locations, specimens for this project were not available to M.I.T. at the expected time. As later defined, a number were not available before the close of this part of the project and are thus not considered herein. In order to continue progress on the development of damage documentation procedures, specimens from a previous project were utilized. In particular, specimens from a previous NRL project [109] were used in the initial development and refinement of these procedures such that the procedures were finalized and ready to be applied to the specimens from this project once the experimental testing began and specimens were available. The decision to use the previous specimens from the NRL was made primarily because these tested specimens and the associated results were immediately available to aid in the development of procedures to use with the current project. In addition, these specimens were made of a material similar to that being used in the current project, were at the baseline level being used in the current project and of similar geometry, and exhibit multiple composite damage modes thereby allowing diverse characterization. The developed procedures offer ways to compare damage both qualitatively and quantitatively, and allow effects to be investigated across the lengthscales as the procedures were applied throughout the project.

The procedures capture the visual state of a specimen with a photograph and then create two images to document the damage. The first image is the damage grid, which is used to quantitatively document the extent of damage in the specimen. The second image is the damage sketch, which captures the qualitative features of the damage. The damage information collected from the previous NRL specimens served as the lowest length characterization for the initial comparison database. Damage information from the specimens of the current project was added to this database as testing was completed and the procedures were applied. The comparison database allows lengthscale effects to be investigated among all specimen levels, including beyond this project, based on the factors identified and utilized. Information exposed by the database was used to answer questions from the question tree.

The procedures to document and characterize damage are critical in the investigation of lengthscale effects in composites. Due to the complex nature of composites, the lengthscale effects may not be revealed without good procedures. Therefore, the development of documentation and characterization procedures was a primary accomplishment during this project. These procedures were developed for use in the current project, but are also for application to composite damage testing more generally. The first step in developing the procedures was in identifying and

considering the factors involved in composite damage. Literature on composite damage was reviewed to investigate the A.3.3 branch of the question tree, shown in Figure 12. This particular branch addresses the question of what the contributing factors of composite damage are at each of the various levels. This helped to identify factors involved with damage at various lengthscales. Examples of such factors are the influence of ply thickness on matrix cracks, the influence of neighboring ply angles on delamination, and effects of the level of specimen size [5, 6, 70]. In order to completely investigate all factors that could be associated with lengthscale effects, it is important to be able to completely document these factors using the established procedures. Factors such as the specifics of the fiber and matrix materials, laminate stacking sequences, specimen geometries and features (e.g., holes, ply drops, strain risers), and load histories of the specimens were determined important to document. It was also desirable to document the damage initiation, progression, and final failure. Nondestructive inspection techniques were then used to investigate the damage initiation points and damage propagation paths in the experimentally tested specimens.

5.3 *Documentation Procedure Development*

The procedure developed to document the factors of each test has a number of primary steps. The characterization portion of the procedure investigates the 'active' damage modes, where an 'active' damage mode refers to a mode of damage present ("turned on"/"at work") in the specimen. Answers from the question tree were used to identify the damage modes possible in composites, and also to distinguish the visual appearance of each of the modes. The goal of the characterization procedures is to provide a quantitative and qualitative description of the damage in the specimens. The extent of damage is compared across the specimens using the quantitative piece. Active damage modes, mode interactions, and damage paths are identified and compared using the qualitative piece. The procedures developed to document specimen testing for lengthscale investigation include taking digital photographs of the specimens, documenting the damage from these photos by creating damage grids and damage sketches, and then placing the gathered information from the documentation into a comparison database. The details of these procedures are further described and the application of these procedures to the NRL IPL and CRC-ACS open hole tension specimens is discussed.

As noted, the first part of the documentation procedure involves photographing each of the surfaces of the tested specimen. Using digital photos, instead of the physical specimens, to perform visual inspection has the key advantage of the ability to look at the specimens from any location. This provides an easy means to discuss specimen damage details with researchers at other locations without having to send the specimens. Another advantage of using the photos is the ability to zoom in (up to the resolution limit when the image gets too pixilated) on areas of interest, such as areas showing possible damage. In addition, the details are preserved and can be further examined even once destructive examination, allowing more detailed documentation, has been done.

Several components are needed for a setup for such photographing. The first component is a camera. The key in choosing a camera is to look towards maximizing

the resolution, and hence detail, of the specimen surface. One should look to provide a few pixels of resolution below the lengthscale of the damage to be encountered and/or of interest. In addition, specimen size, or size of structural detail of interest comes into consideration when setting focal length, and is a mix with the size of the specimen to be captured within one picture, and thus the numbers of pictures that must be taken in order to capture the full area(s) of interest. The number of pictures, of course, also relates to amount of time needed, and ease of the work. The next component necessary to the documentation procedure is the lighting of the specimen. A direct light source, such as a flood light or a flash, will produce glare in the surface photograph, thereby interfering with the specimen documentation. Therefore, a diffuse light should be used, as this allows damage to be more easily and better seen in the photographs. In cases where the specimen are small in scale (as are the baseline specimens in this project), the specimen may be placed in a photographer's light tent to produce diffuse lighting on the surfaces. For larger specimens, the use of a photographer's softbox can provide the necessary lighting. The final component necessary for the setup of the camera is a fixed stand. By fixing the distance between the camera and the specimen, photos of the same scale will be produced. To capture the scale of the photographs, it is also important to provide a length reference in each photo. This length reference will depend on the size of the specimens. If large numbers of specimens of the same geometry are being documented, using the same setup (e.g., camera settings, lighting) allows downstream processing of the photos to be systematic. In addition to the camera setup, the specimen orientation must also be consistent. A reference to some angle pertinent to the specimens must be established. This reference depends upon the type of specimens to be characterized. This selection is specifically described later for the specimens of this work. In general, it is suggested to be relative to ply angles and/or associated directions.

Once the documentation via photographing is complete, the digital photos are transferred from the camera to a computer. A photo editing software can be used to edit the digital photos. This allows simple manipulation of the stored photographic information. However, it is very important not to alter the documentation of the specimens while using the editing software. Editing actions should be limited to operations that do not change the appearance of the specimen. For example, it can be found that the documentation photos had excess white space around the specimen faces. The photo editing software can be used to remove this irrelevant area by cropping the photos to the size of the specimen face. Other such procedures can take place to process large batches of photos automatically. A computer code can be developed that runs within the photo editing software. The specifics of the code are dependent on the details of the specimen.

After completion of the photo documentation, the photos are used to begin characterization of damage. An objective approach is taken by first documenting the damage without considering the cause (e.g., type of loading, stacking sequence, material). The damage is determined by visual inspection of the photos and the specimens are inspected when clarification is needed. The damage modes that can be determined by visual inspection are limited by the lengthscale of the damage. This limits visual inspection to determining the following modes: matrix cracking, fiber fracture, and delamination. The inspector makes the determination of the type and

extent of damage in the specimens. The goal of the damage characterization is to document the extent and paths of the 'active' damage modes to allow investigation of the lengthscale effects.

The first means of documenting damage in the specimens is the use of damage grids. The damage grids provide the quantitative damage measure, allowing an objective comparison of the extent of damage across specimens via specific definitions of the amount of damage. The images from the photo documentation of the specimen serve as the base for the damage documentation. Additional 'layers' are added to the top of the images using photo editing software. The layers can be thought of as transparencies being placed on top of the images. These layers have the advantage of being modified separately from the documentation photo, thus preserving the documentation of the specimen. The first layer added contains a coordinate system, with the location of the axes placed manually on the layer at a defined reference location. The coordinate system allows specifics of the specimen to be described, such as ply orientation and specimen geometry. The second layer added contains a grid to quantify damage. The grid origin is related to the coordinate system of the first layer. The grid spacing is selected based on the lengths associated with the damage types, not on the size of the specimen. It was learned from the work on the NRL "In-Plane Loader" (IPL) specimens that a finer grid spacing is necessary through the thickness of the specimens due to the lengthscales of the damage, and the geometric scale of the specimen on these surfaces. The through-thickness damage is typically interply (delamination) and/or intraply (matrix) cracks. These appear as line cracks along the side surfaces of the specimens during visual inspection. The finer grid spacing provides better quantification of the damage compared to using the coarser in-plane grid spacing. One can argue to go down to the level of ply thickness, but levels that small push the visible limits of unaided visual inspection, as well as the ability to determine the actual location of plies and the same z-location of a ply throughout a specimen.

Once the grid is placed on the images, each grid square is examined visually and characterized as being "undamaged", "partially damaged", or "completely damaged." The three levels are chosen to provide specific levels of quantification in characterizing the damage extent. In most cases where damage is present, the damage partially 'clips' the corner of the grid square. Because the damage grids are providing the quantification for damage extent, classifying a partially damaged square as "undamaged" would underestimate the extent, while classifying it as "damaged" would overestimate the extent. This is the reason that a third classifier is used. Assigning the classifier to the grids is made by the inspector according to the following definitions. This converts the subjective assignment (captured via the definitions) to objective classification. For a grid with damage, the determination between "partially damaged" or "completely damaged" is made based on the damage mode and the amount of the grid that is damaged. For delamination, the grid is assigned "partially damaged" if less than half the grid square is delaminated; otherwise, it is assigned "completely damaged". For matrix cracking and fiber fracture, which typically occur as linear damage, the grid is assigned "partially damaged" if the damage does not completely span the grid square or if the damage only 'clips' the corner of a grid; other damage results in an assignment of "completely damaged." The "undamaged"

classifier means there was no damage observed in the grid. From these damage grids, the extent of damage of each specimen is quantified.

Although the damage grids are used in this quantification of damage, this characterization is not able to fully capture details of the damage type and damage shape. Therefore, another means of documenting damage was developed. This second means is the use of damage sketches. The damage sketches are developed to provide more information about the damage in a single image. Another layer is added to each of the images for the damage sketches. The damage sketches are designed to capture the 'active' damage modes, the damage paths, and the extent of damage, all in a single image. Classifiers for the damage modes are selected to convey the damage type. For the damage to be addressed as previously described, matrix cracking is represented as a black line, delamination is a filled gray area, and fiber fracture is an area filled with a "divot" pattern (a specific hatch pattern). The classifiers were selected to be similar to the damage modes. For example, matrix cracking usually occurs in a straight line, delamination occurs in an area when viewed in the plane of the ply and as a crack between plies when viewed from the side, and fiber fracture occurs in a jagged line creating an area of damage. With this classification scheme, the damage sketches can easily show the damage paths and lead to questions of mode interaction by displaying all 'active' damage modes in the same region.

5.4 *Refinement of Damage Documentation Procedures*

The initial development of procedures to document and characterize damage in composites was developed using specimens from a previous NRL project due to the unavailability of specimens from the current effort as described in Section 5.2. The details of these specimens are described in Section 6.1. These initial procedures were then implemented on the twenty-one open-hole tension specimens that were received before the closure of this part of the overall effort. During these implementations, three areas in the initial procedure were identified where improvements were needed. These three areas were: one, a consistent means to handle specimens that had failed into two or more pieces during testing; two, a consistent manipulation of specimen images and/or documentation procedures in order to return the planar dimensions to the virgin (untested) dimensions; and, three, better identification of the size of the damage grid and damage sketch dimensions within specimen types to maintain comparable regimes of documentation of damage. These refinements were identified after applying the initial procedure to the open-hole tension specimens and anomalies appearing in the results. The aim of the refinements was to make the procedures more generally applicable, and thereby capable of being implemented across a wide range of composite specimens.

The first refinement pursued was a means to more consistently and clearly handle specimens that had failed and pulled apart into two or more pieces during the testing. Following the original documentation procedure, each individual specimen face was photographed. With failed specimens, additional surfaces below the original specimen surfaces are exposed due to the manner in which the laminated composite specimens fail (e.g., combination/interaction of the basic damage modes through the specimen thickness). Specimens can be separated into two, or more, pieces during

failure. This separation can result in multiple ply surfaces being exposed. Such a case is shown in Figure 14. This is an open-hole specimen, as received from CRC-ACS, that had been loaded to ultimate failure, resulting in the specimen being broken into two pieces. As is visible in these photographs, due to the complex failure paths of composites, there are jagged edges at multiple layers. In order to set up the photos for implementation of the damage grids and damage sketches, it is necessary to recombine the broken pieces back into a "single" specimen.

Three basic methods for rejoining the specimens were considered. The first was to physically work to puzzle the broken specimen pieces back together. However, due to the extent of damage and deformation in individual layers of the composite, physically puzzling the two specimen pieces back into one would have been a difficult task and would have likely resulted in additional damage being introduced. The second idea was to modify the damage grid and damage sketch procedures to accommodate broken specimens. However, doing this would have resulted in inconsistencies (e.g., noncontinuous damage paths, possible overcounting/ undercounting of damage grids) that would make comparison between unbroken and broken specimens misleading.

The third idea, which was selected for inclusion in the documentation procedure, involves "virtually joining" the individual pieces of the specimens. It begins with taking surface photographs of each of the broken specimen pieces, being sure to include consistent length references. The specimen pieces are then "digitally joined" using photo-editing software. This requires establishing a "joining template" to recombine the photographs of the broken surface. This joining template is established for a/the primary plane of the specimen using the dimensions of the virgin (original) specimen. It is desirable to use a width and length dimension based on preselected references on the specimen. The actual width of the specimen was used herein. However, since this procedure did not exist when these specimens were tested, a general length reference on the specimens did not exist. In the case of open-hole specimens, the hole can be used as a length reference in combination with a lengthwise edge of the specimen. The joining template for an open hole specimen using its back face and these references is illustrated in Figure 15. Dashed lines represent the template references.

The next step in the "virtual joining" procedure involves positioning the surface photographs from this perspective into the template. Each individual photograph is positioned within the template using the template references in relation to that dimension of the specimen in the photograph. A different "layer" within the photo-editing software is used for each photograph at this stage to allow for individual positioning.

The first photograph to be positioned was that of the piece containing the lengthwise edge that was used in referencing the position of the hole. The widthwise edge of the specimen is placed against a ruler with the lengthwise edge placed against a square at the point of "0" on the ruler. The joining template is moved relative to the photograph of the specimen so that the reference of the hole is placed against the hole edges visible in this photograph. This repositioning allows the location of the midpoint of the hole to be determined relative to the ruler in the photograph. This ruler is

digitally placed along the width of specimen pieces in other photographs using the midpoint of the circle of the joining template as a reference relative to the ruler and then positioning the specimen hole edges aligned with the circle of the joining template.

These individual layers are subsequently overlapped using the joining template as a guide. This results in overlaps of the surface photographs similar to overlapping photographic slides, projecting light through them and viewing that result. The measurement item (ruler in these cases) in the photographs is used to determine the distance that the individual photographs were moved in this process by comparing the ruler point that the midpoint of the circle intersects. This distance is then used to join the other photographs of the specimen surfaces. In the case of the open hole specimen, there are three other surfaces – front, left, and right.

However, since the purpose of this process is to document damage, the individual photographs are not brought together completely to their original length. A slight "offset" is required in order to clearly show damage for subsequent consideration. It was found that completely returning the specimens to their original length would often "mask" the damage, making it difficult to see the damage in the documentation photos. In setting this "offset," there needs to be a balance between clearly showing the damage that occurs, while properly representing the damage that would be visible. Final refinement of the size of this "offset" was still being considered at the closure of this project. An offset of 0.01 inches was used for the OHT specimens that were "virtually joined" during this work. For these cases, this offset achieved a balance in maintaining a visible damage path in the documentation photos while minimizing the "opening" of the specimen.

The final step in the "virtual joining" procedure involves the determination of the surfaces that would be exposed based on their place in the specimen relative to the outer surface being considered. This process requires an objective judgment to determine which layers would be visible (determined by considering the stacking sequence and which layers are closer to the surface) and cropping out the material that would not be visible. Items determined to be below/under items are digitally deleted from the two images until only the item closest to the surface of consideration remains. This process results in one final view of that particular surface. Although this view is one integrated view, it is only integrated through the imaging of the software. The individual photographic pieces remain, and can later be consulted as needed.

An example of this "virtual joining" procedure is shown using the open hole tension specimen, as tested at CRC-ACS, with a hole diameter of 1.0 inches. The original photographs of the two pieces of the back surface as failed are shown in Figure 14. The joining template, using the measured specimen width and the measured hole diameter as references, is shown in Figure 15. The individual layers as positioned within the joining template are shown in Figure 16. Portions of these layers were then digitally deleted until only outer layers that would have been visible could be seen. The resulting "virtually joined" back face of this specimen is shown in Figure 17.

With this virtual joining process, the damage documentation procedure can be applied to specimens that break during testing. This allows the damage data from such

tests to be worked in order to be included in the comparison database with a consistent reference.

A second refinement to the damage documentation procedures was the normalization of the damage grid and damage sketch dimensions. In specimens containing damage paths through their entire thickness, it was found that a change in planar dimensions from the virgin (untested) dimensions often occurs. This is, of course, also true in all specimens that separate into more than one piece upon failure. This change in dimensions can result in a change in the surface area being characterized by the damage grids and damage sketches. The change in area would result in the extent of damage being compared across the same specimen type to be inconsistent. An example of such a specimen is shown in Figure 18. This is an open-hole tension specimen, as tested at CRC-ACS, with a hole diameter of 0.5 inches. The hole in this failed specimen has become slightly elongated due to failure. This elongation can be ascertained by considering the photograph in Figure 19 where a black circle with the same diameter of 0.50 inches has been superposed on the original photograph.

In order to eliminate this inconsistency from the damage documentation procedure, a new process was added. This new process involves digitally editing the damage grids and damage sketches of the specimens back to virgin dimensions. This process is similar to the digital process of the first refinement of "virtual joining", with the change that grids and sketches of specimens that may still be in one piece may need to be "digitally cut" to return the specimen to the original (pre-tested) dimensions.

As previously established, the damage grids are overlaid and the grids recorded and sketches made. The overall size of these grids, generally in the direction of loading, can be altered due to the failure process as the specimen has slightly changed size. The grids and sketches must therefore be digitally edited to return them to virgin dimensions. As is required in the first refinement, virgin dimensions of the specimen are needed. In addition, the virgin dimensions of any structural details (e.g. open hole) can be an asset in the process. Using these references, the recordings of the post-tested specimen can be digitally returned to the virgin dimensions, thus allowing a consistent surface area comparison across specimens of the same geometries.

A key difficulty in this process was determining the locations at which to "digitally cut" the specimen grid and sketch and then return the recordings back to the virgin dimensions. These locations generally needed to coincide with dominant damage as manifested at the multiple surfaces of the specimen. In the process, each surface of the specimen would be considered individually as to location of cutting, although the distance that pieces are moved would be consistent across all surfaces. For example, in some specimens, a dominant matrix crack ran along the surface plies of the specimen with a combination of damage (i.e., delaminations, matrix cracks, fiber fractures) occurring in plies below the surface. This combination of damage allowed the specimen to be "pulled apart", with two sections of the specimen opening along the dominant matrix crack. In such cases, the digital cut was to be made along the dominant matrix crack allowing the crack to be "closed", thereby returning the specimen to its virgin dimensions. In other specimens, there was no clear matrix crack on the surface, but rather a series of parallel matrix cracks that can "bend" to allow the

surface ply to comply with the plies below the surface which "open." In these cases, a mapping procedure was developed to map the surface damage from the stretched specimen back to the virgin dimensions.

This overall mapping procedure was developed and used for the few specimens that exhibited such a failure. Final refinements on the mapping procedures were not able to be conducted due to the insufficient number of specimens showing such failure. The specific length of the adjustment was one particular issue that may require final refinements. In the case where the specimen requires the first refinement of "virtual joining", this adjustment length was defined by the offset length as previously discussed. When a structural detail exists in the specimen, the apparent change in this structural detail after failure can be used as the adjustment length. However, there are other situations, such as an unnotched specimen, that will require a length reference to be placed on the specimen surface before testing. Such details were not able to be worked into the current project testing as the specimens were received too late to incorporate changes.

As an example of the mapping procedure, one of the OHT specimens exhibited a dominant matrix crack propagating from the hole to the outer edge on one side of the specimen but had a series of parallel matrix cracks that "bent" to allow the specimen to "open" on the other side. The documentation of the specimen is shown in Figure 20. As can be seen on the front surface (indicated in the figure), there is a dominant matrix crack, propagating on the right side of the hole, with an "opening" where the specimen has been partially pulled apart. However, there is not a single dominant matrix crack to the left of the hole. Instead, a serious of parallel matrix cracks have formed and allowed the top ply to "bend" in that vicinity. In order to maintain consistent damage grids and damage sketches, the mapping procedure maps this damage back to a "closed" specimen. The damage sketch of this specimen, shown in Figure 21, has mapped the damage back to a "closed" configuration. This can be seen by observing the location of the dominant matrix crack, which, in the damage sketch, is now a single matrix crack (as opposed to the "opened" matrix crack observed in the documentation photograph, Figure 20). Also, the bent matrix cracks to the left of the hole have been mapped back to straight matrix cracks.

A third refinement to the damage documentation procedures addresses a lengthscale issue introduced by varying specimen geometries. In order for the damage grids and damage sketches to cover consistent areas within sets of tested specimens, a lengthscale is introduced to the specimen. This lengthscale is selected based on the overall dimensions of the specimen, dimensions of any pertinent structural details in the specimen, and initial observations of the extent of the damage in the specimens. The objective of this refinement is the definition of a "bounding area" for each specimen surface that will contain the damage for all specimens of that set. This "bounding area" should be defined such that it is applicable for all specimens of the same geometry. However, the reality of damage initiation and propagation is such that the pertinent area for observation can be quite different depending upon the laminate of the specimen as well as the loading condition applied. The applicability of a specific "bounding area" is therefore generally limited to a particular specimen set.

This refinement was made after consideration of the various stress fields introduced by the different structural details, which act as stress/strain concentrators and generally are the location of damage initiation. From these initiation points, damage propagates into the specimen. It is critical to focus the damage documentation on regions surrounding the structural detail because these regions are most likely to experience damage during testing. The distance beyond the structural detail that is contained within the bounding area is also dependent on the specimen laminate and loading conditions, as these influence the damage behavior and propagation. This refinement is a change from the original documentation procedures that extended the damage grids and damage sketches across the entire face of the smallest level specimens (NRL IPL) for all cases without consideration of the specifics of the specimen and the damage as manifested.

As an example of this documentation refinement, the hole diameter was used for the open hole specimens as a primary reference length in determining the dimensions of the bounding area for the damage grids and damage sketches. In order to establish a consistent region for the damage grids and damage sketches across all open-hole tension specimens in the set, visual inspections were made to determine the extent of damage that occurred in the specimens received. From the inspections, it was determined that a square bounding area with sides of length equal to four times the hole diameter, and being centered on the center of the hole, would fully encompass the damage observed in this specimen type and set.

The three refinements to the damage documentation procedures were made to make the overall procedures for damage documentation more robust and to enable the procedures to be implemented on a broader class of composites specimens. This includes specimens that break into multiple pieces during the testing, specimens that are "stretched" during the loading, and specimens across a broader range of lengths and configurations. With the refined procedures in place, consistent comparisons across specimen types are ensured.

5.5 *Establishment of Damage Comparison Database*

Another important component of the procedure to investigate lengthscale effects in composites is the use of the damage comparison database. A key accomplishment of this project was the establishment of this initial damage comparison database via the damage documentation procedure implementation on the NRL IPL and open hole specimens. This database continued to grow throughout the project as specimens became available and the damage documentation procedure was applied.

The comparison database was established to allow investigation of lengthscale effects in composites across multiple specimen types (e.g., different geometries, laminates, loadings). The database contains all the information gathered from the damage documentation procedures (damage extent from the damage grids, damage paths and damage modes from the damage sketches, etc.) as well as specifics on the specimens (fiber and epoxy type, laminate layups, loading history, etc.). By organizing all this information into a sortable/searchable database, comparisons can be made to find trends and expose differences in damage as the level of testing is changed. For

example, a researcher may be interested in the change in damage extent caused by varying only the size of a structural feature (e.g., hole). From the comparison database, one can select the fixed parameters (e.g., material, laminate stacking sequence, etc.) and investigate how the damage extent varies as the size of the structural feature varies.

The advantage of this comparison database is that it represents a new focus, investigating lengthscale effects, whereas previous databases on composites were used in determining material allowables for specific laminates. Damage information was lacking from these previous databases, partially due to absence of a damage documentation procedure, making it nearly impossible for researchers to use the contained information to study failure trends, which ultimately limits the ability to design the most efficient structures. The comparison database was developed and populated using the damage documentation data from the experimental specimens of the project. This database provides researchers with a standard platform to investigate damage trends and lengthscale effects across multiple specimen types while also allowing damage/failure data to be shared with one another.

The database contains all the information gathered from the procedures as described. The test specifics (fiber and epoxy type, laminate layups, etc.) and damage specifics (extent, 'active' modes, paths, etc.) are all included in the database. A sample excerpt of the database is shown in Table 2. The first column specifies the specimen identifier (specimen ID number). The next three columns capture the test inputs; material type, stacking sequence, and load paths. The material type is indicated by a classifier corresponding to the fiber and matrix (e.g., 1 corresponds to AS1/3501-6). The stacking sequence of the specimen laminate is indicated by a classifier assigned to each sequence. In a similar fashion, each load path is assigned a unique classifier. The following four columns capture the visually observed damage modes: delamination, matrix cracking, fiber fracture, and zig-zags. The classifiers in these columns are binary, where a 1 or 0 indicates whether or not the damage mode was visually observed. An exception is the "zig-zags" column, where the number in that column represents the number of zig-zag failures observed in the specimen. The next three columns summarize the visual damage/failure observations. The "failure present" column indicates via the binary value, 1 or 0, whether damage (any mode) was visually observed in the specimen. The next column indicates the number of "active" damage modes, which is a summation of the cells from the "visually observed damage modes" columns. The "zig-zag present" column indicates with the binary value, 1 or 0, whether zig-zags were visually observed. The final two columns capture the damage quantification results from the damage grids. Additional columns may be added to the database if other unique damage patterns are observed in future work. However, the damage characterizers should be kept to a minimum to allow data to be as widely applicable as possible. Incorporating project specific classifiers would begin to limit the usefulness of such a comparison database.

With the collected information, comparisons were made to find trends and expose differences in damage as the scale of testing was changed. The database has the results from application of the procedures on the 182 previously tested NRL IPL specimens as well as the 21 CRC-ACS open hole specimens received from this project. Although this portion of the project has ended, the database will continue to grow as

results from the continued experimental testing (NRL and CRC-ACS) are documented. The culmination of the database will be summarized as part of a doctoral thesis using this work.

Table 2 Example excerpt of the Damage Comparison Database

	Test Parameters			Visually Observed Damage Modes				...
Specimen #	Matrl	Stack	Load Path	Delam	Matrix Cracking	Fiber Fracture	Zig-Zags	...
001-33	1	1	1	1	0	0	0	...
001-34	1	1	2	1	1	0	0	...
001-36	1	1	4	1	0	0	0	...

...	Failure Summary			Damage Quantification	
...	Failure Present	# Active Modes	Zig-Zag Present	Partial	Complete
...	1	1	0	3%	1%
...	1	2	0	5%	8%
...	1	1	0	3%	1%

5.6 *Damage Investigation using Computed Microtomography*

A major achievement during this project involved finding and utilizing the methodology of computed microtomography (CμT) in investigating damage in composite specimens. While computed tomography has been in use for many years in the medical field (CAT-scans), it is only recently that this technology has been applied to composites [105-108]. There have been very limited studies using CμT to investigate damage in composites. However, the recent advances in this technology allow composite damage to be investigated as never before. Information can be gathered from specimens without any specimen preparation (e.g., use of dyes, access to interior damage). From the CμT scans, damage paths and the interaction of damage modes throughout the volume of the specimen can be investigated with greater detail than ever before.

Computed microtomography allows damage in composite specimens to be fully investigated in three dimensions without any specimen preparation and therefore requires no destructive sectioning, knowledge of damage location, coupling fluid for ultrasonic inspection, etc. This technique creates a digital representation of three-dimensional (3-D) volumes from scans of physical/experimental composite specimens. From these 3-D volumes, lengthscale effects associated with composite damage were

studied in greater detail than ever before. The 3-D volumes are manipulated via a graphics software program. Thus, "virtual cuts" could be made through any plane of a specimen and the damage on that plane examined with resolution down to the order of several microns. This allowed visualization of damage paths and damage extent anywhere within the volume as well as observations of damage mode interactions throughout the volume of the specimen.

Three-dimensional volume scans of specimens were conducted via a closed X-ray computed microtomography system. A specimen would be mounted on a turntable in the X-ray cabinet and then individual X-ray projections were captured as the specimen was rotated. An algorithm then used these projections to recreate a virtual volume of the scanned specimen. The researchers at M.I.T. have access to the computed microtomography machine at Harvard University's Center for Nanoscale Systems (CNS) located in Cambridge, Massachusetts.

The machine is an X-Tek HMXST225 computed microtomography X-ray imaging system. The system has an open source X-ray tube capable of a maximum resolution of 3 to 5 microns in reflection mode and 2 microns in transition mode. The achievable scan resolution is a function of specimen dimensions and decreases as specimen size increases (the geometric magnification used in the system results in the inverse relationship). Specifically, the resolution is proportional to the width, thickness, and height of the specimen as per:

$$\text{Resolution} \propto \frac{1}{C_1\sqrt{w^2+t^2}+C_2 h}$$

where w, t, and h are the specimen width, thickness, and height, and C_1 and C_2 are constants dependent on the CμT machine. The machine can accommodate a specimen up to 6 inches by 6 inches by 6 inches with the limitation that X-rays must be able to fully penetrate the specimen (dependent on the X-ray attenuation of the specimen). Targets of molybdenum (Mo), tungsten (W), silver (Ag), and copper (Cu) are available in order to optimize the X-ray spectrum for specimens of different materials. Each target produces a unique spectrum of X-ray wavelengths (and hence X-ray energy levels). The multiple targets allow a spectrum to be selected to optimize the attenuation of X-rays through a specimen. This attenuation is a function of the X-ray wavelength and the material. The CT algorithm calculates the attenuation from changes in intensity sensed at the X-ray detector (XRD). For example, a spectrum with short wavelength (high energy) X-rays will not have sufficient attenuation through a 'soft' material to detect fine changes within the volume. However, a spectrum with long wavelength (low energy) X-rays will have too much attenuation through a 'hard' (e.g., metal) material and may result in zero intensity (X-rays not fully penetrating material) at the X-ray detector. A Perkin Elmer X-ray detector 1621 X-ray panel provides 2000 by 2000 pixel (16 inch by 16 inch) field of view with 7.5 frames per second readout. The machine can be used to image a wide range of materials from organic materials to plastics, metals, and composites.

6. Results

The results from this portion of the overall project are presented within this section. The procedures described in Section 5 were applied to the originally tested NRL IPL specimens and to all specimens from the current project that were received in time to process before the end of this portion of the project. Observations on lengthscales involved with damage are discussed. All damage characterization information collected from the procedures was added to the comparison database and findings are discussed. Results from further investigation of damage paths and mode interactions utilizing computed microtomography are presented.

6.1 *Applying Damage Documentation Procedures to NRL IPL Specimens*

A key accomplishment of this project was the use of the established procedures to document and characterize the damage of the previously tested NRL IPL specimens. The overall photo documentation layout for these specimens can be seen in Figure 22. The specimens are rectangular with nominal in-plane dimensions of 1.5 inches in length and 1.0 inches in width. The thickness of these specimens is on the order of 0.14 inches, depending on the material (AS1 or AS4 as fiber) and the number of plies. In all specimens, there is a rectangular-shaped strain riser cut into the specimen in the direction of the width and halfway along the length. This strain riser is 0.04 inches wide and 0.6 inches in length. The specimens from the original DED (Dissipated Energy Density) study made from the AS1/3501-6 and AS4/3501-6 materials were chosen for investigation since they best related to the material being used in the current overall project. Specimens of each material with four different stacking sequences had been used. Each combination of material and stacking sequence is referred to as a particular item. Further details on the specimens can be found in the NRL report: NRL/FR/6383--92-9369, "Experimental Determination of Dissipated Energy Density as a Measure of Strain-Induced Damage in Composites" [109].

The specimens from the original DED work chosen for investigation were sent from the NRL to M.I.T. In total, seven different items (four with AS1 fibers and three with AS4 fibers) were sent with a total of 210 specimens. Some items had missing specimens (unaccounted for after 20 years), but all remaining specimens from these items were sent. The specifics of these items are shown in Table 3. One issue found while inspecting the specimens was the lack of knowledge of the laminate stacking sequence. The layups were reported as +/- θ and the number of plies were not specified. However, visual inspection of the sides of the specimens revealed that the laminates were not a simple layup of +/- θ. In order to properly determine the stacking sequence for each item, a matrix burn-off was conducted on one sample for each item. The determined stacking sequences are listed in Table 3. The results from items 001 and 004 showed these specimens to have two extra plies, making these laminates unsymmetric. All the other items were determined to be balanced and symmetric laminates as indicated.

Once the laminate stacking sequences were determined for each item, the angle ply directions on the surface had to be determined for each specimen. All specimens

received from the NRL were separated by item in plastic bags, and each specimen had a numbered label taped on it corresponding to its specimen number. This specimen number corresponds to the experimental load path to which the specimen was exposed and with regard to a data file. However, the orientation of the fiber stacking sequence was not marked. Therefore, the specimen item number (refer to Table 3) and specimen number were written on each specimen using a silver paint pen (e.g., 002-34 is the label for item 002 and specimen number 34) and the numbered labels were removed. In some cases, the labels left a discoloration on the specimen surface. After all specimens had been labeled with the silver pen, each was then viewed under an optical microscope to determine the outer layer fiber orientation. It was found that the outer layer fibers could be seen under an optical microscope at 100X magnification. At lower magnifications, an artifact due to the peel-ply used during the manufacturing process of the composite plates gave the surface of the specimens an appearance similar to a composite fabric ply. The 'front' surface of each specimen was chosen such that the rectangular strain riser was oriented to the left (as in [109]) and that the top ply had a positive fiber angle. A silver arrow was drawn on the 'front' surface along the 0°-direction.

Table 3 Originally tested Naval Research Laboratory (NRL) In-Plane Loader (IPL) specimens sent to M.I.T. for investigation and characterization

NRL Item	Resin	Fiber	Reported Layup	NRL File	# of Specimens Received	Determined Stacking Sequence
001	3501-6	AS1	+/-15	mt-1	30	$[+15/-15_2/+15_3/(-/+15)_2/-15_3/(\pm15)_2/+15]_T$
002	3501-6	AS1	+/-30	mt-2	19	$[(+30/-30_2/+30_2/-30)_S]_S$
003	3501-6	AS1	+/-60	mt-3	36	$[(+60/-60_2/+60_2/-60)_S]_S$
004	3501-6	AS1	+/-75	mt-4	35	$[+75/-75_2/+75_3/(-/+75)_2/-75_3/(\pm75)_2/+75]_T$
005	3501-6	AS4	+/-15	mt-5	30	$[(+30/-30_2/+30_2/-30)_S]_S$
007	3501-6	AS4	+/-60	mt-7	30	$[(+60/-60_2/+60_2/-60)_S]_S$
008	3501-6	AS4	+/-75	mt-8	30	$[(+75/-75_2/+75_2/-75)_S]_S$

Once the specimens were all labeled and the outer ply orientations determined, each of the six faces of the 210 specimens were photographed. This yields a total of 1260 surface photos. A Nikon D60 DSLR camera with a NIKKOR DX AF-S 18-55mm lens, a Nikon Close-up.c No.2 filter, and a generic ultraviolet filter was mounted on a photo stand within a photographer's light tent. The light tent provided a diffuse light source. The lens was extended to 55 mm and focused 1.54 inches above the table of the light tent. The distance between this focal plane and the film plane of the camera was 11.9 inches. The camera was placed in "Close Up" mode with the flash and active D-lighting turned 'off', focus mode set to 'manual,' image quality and size set to 'fine' and 'large,' respectively, and the ISO sensitivity set to 'automatic.' These settings are used

in all the documentation photos, thus maintaining the same photograph sizes throughout the process, and thereby making processing of the photos systematic. In order to give the length reference for this specimen size, a right angle ruler, marked in inches, was placed inside the light tent and was positioned to coincide with the focal plane of the camera. Two back spacers were sized and made to place under the specimens to bring each face of the specimens into the focal plane (1.54 inches above the table). The spacer used while photographing the 'front' and 'back' surfaces was 1.39 inches tall and the spacer used while photographing the 'left' and 'right' surfaces was 0.52 inches tall (refer to Figure 22 for surface definitions). No spacer was required to photograph the 'top' and 'bottom' surfaces since the focal plane was set to coincide with the length of the specimens. The small variations in specimen thickness due to the differences in ply thickness between the items did not bring the 'front' and 'back' surfaces out of focus. The spacers allowed each face of the specimen to be quickly placed and photographed without having to adjust the camera. On average, it required less than one minute per specimen to do this photographing (including placement).

After the documentation via photographing was complete, the photos were transferred from the camera to a computer. These photos, however, had excess area (white space) around the specimen faces that was not relevant to the documentation. Therefore, the photos were cropped and oriented using the picture editing software GIMP (GNU Image Manipulation Program). A computer code that ran within GIMP (a scheme file) was written to automate this process. The code was implemented from within GIMP and automatically cropped the unedited surface photographs to size and then combined the six specimen face photos into a single image. The layout for the single specimen image is similar to an engineering drawing, showing an unfolded multiview projection. The image shown in Figure 22 is an example of the layout used for the photo documentation. As in an engineering multiview projection drawing, each face is shown at the same scale. The image shown in Figure 23 is an example of the final photo documentation created for each of the 210 NRL IPL specimens.

After completion of the photo documentation of the NRL IPL specimens, the damage characterization procedures were applied. The coordinate layer was added first. The coordinate axes were placed at the tip of the strain riser, with the axes labels (x, y, and z) corresponding to the axes used in [109]. That previous NRL work did not address through-thickness damage and placed the origin of the x-y axes at the tip of the strain raiser. The z-axis is added here and is placed at the midplane of the laminate. The coordinate axes can be seen in Figure 24. The axes are placed in the computer files manually through visual inspection. The second layer containing the damage grid was then added to the photo. The origins of the grids for each surface were coincident with the coordinate axes on that surface. The grid spacing was selected to be 0.05 inches for the in-plane dimensions, and 0.025 inches through the thickness of the specimen. These spacings were chosen to provide the resolution with regard to damage and damage paths as previously described. The finer grid spacing through the thickness was selected to better quantify the damage along the side surfaces. Once the grids were placed, the grid squares were classified as either "undamaged", "partially damaged", or "completely damaged" as previously defined. An example of a damage grid is shown in Figure 25. From the damage grid, the extent of damage is quantified. The third layer containing the damage sketch was then added to the photo. The damage paths were

drawn on this layer, including the damage classifying scheme. An example of a damage sketch using these classifiers is shown Figure 26.

With particular reference to the figures, but with regard to all work in this overall coordinated project, there is a need to have consistent reference as to fiber angle within plies. Fiber angle is considered positive counterclockwise (+CCW) from the established 0°-axis/direction. In all figures, this 0°-direction is indicated. However, it must be noted that the positive counterclockwise reference is with reference to viewing the specimen from its front face. In viewing a specimen from a back face, one has rotated the specimen by 180°. This causes the positive direction to now be negative counterclockwise, or positive clockwise (+CW). This must be considered in all figures presented herein. Furthermore, one must take this rotation of viewing into account when considering the view of any specimen. Such is more obvious when viewing the specimens from a side view, although the angle will again take on a negative or positive aspect when considering a left or right face, or a top or bottom face.

All documentation photos of the originally tested NRL IPL specimens were completed, the damage grids were implemented, with the damage classified for all 210 specimens, and the damage sketches were drawn for all 210 specimens. Of the 210 specimens received from NRL, only 182 specimens were determined to have been tested (loaded) and 28 were virgin (unloaded without grip marks). Of the 182 specimens that had been loaded, only 106 showed visual signs of damage, while the other 76 had visual signs only of the grip marks. Within the 106 specimens that showed visual damage, some exhibited obvious damage while others had barely visible damage only found after very close inspection with a trained eye. Nondestructive investigation via computed microtomography was conducted on some of the NRL IPL specimens to further investigate damage paths and mode interactions, the process and results of which are discussed later.

6.2 *Applying Damage Documentation Procedures to CRC-ACS Specimens*

Another key accomplishment of this project was the application of the damage documentation procedures to document and characterize the damage in the open-hole tension specimens tested thus far in the associated efforts at CRC-ACS. This included work around the needed refinements that were identified as discussed in Section 5.4. The work on these specimens was the primary driver in identifying the three areas requiring refinements of the damage documentation procedures.

In total, twenty-one open hole specimens were received from CRC-ACS for documentation and characterization, with another 30 specimens just received but that could not be documented since the time on this grant expired. (NOTE: This exceeds the total number of specimens originally planned for testing as reported in Table 5. This is due to manufacturing issues encountered at CRC-ACS.) Within the received specimens, there were three different geometries and two different laminate stacking sequences. The three geometries were a specimen with overall dimensions of 7.5 inches by 1.0 inches by 0.126 inches containing no hole (referred to as a hole of diameter of 0 inches), a specimen with overall dimensions of 7.5 inches by 1.0 inches by 0.126 inches containing a hole of diameter of 0.5 inches, and a specimen with overall dimensions of

13.5 inches by 4.0 inches by 0.126 inches containing a hole of diameter of 1.0 inches. The hole in each specimen is through the thickness and centered on the length and width of the specimen. The two laminate stacking sequences used in the specimens were $[+45/0/-45]_{4S}$ and $[+45_4/0_4/-45_4]_S$. The combinations of geometries and laminates of the received specimens are listed in Table 4. The specimen IDs listed in the table contain information on the specimen geometry and laminate as well as the specimen number (listed as "##" after the last hyphen) for the specific combination of geometry and laminate.

Table 4 Open-hole test specimens tested at CRC-ACS and received by M.I.T. for damage documentation and characterization

Specimen ID	Geometry	Laminate	# of Specimens
OH-A001-##	7.5" x 1.0" x 0.126" 0" Dia. Hole	$[+45/0/-45]_{4S}$	3
OH-A051-##	7.5" x 2.0" x 0.126" 0.5" Dia. Hole	$[+45/0/-45]_{4S}$	4
OH-A101-##	13.5" x 4.0" x 0.126" 1.0" Dia. Hole	$[+45/0/-45]_{4S}$	4
OH-B004-##	7.5" x 1.0" x 0.126" 0" Dia. Hole	$[+45_4/0_4/-45_4]_S$	3
OH-B054-##	7.5" x 2.0" x 0.126" 0.5" Dia. Hole	$[+45_4/0_4/-45_4]_S$	3
OH-B104-##	13.5" x 4.0" x 0.126" 1.0" Dia. Hole	$[+45_4/0_4/-45_4]_S$	4

The overall photo documentation layout of these specimens is illustrated in Figure 27. Following the documentation procedures, a photograph of each specimen face was taken. If needed, the digital adjustment of "virtual joining" was made, and the individual surface photos were combined with axes added to each face. Once this set-up was complete, the damage grid and damage sketch layers were overlaid, and the grid and sketch filled following the objective instructions of the documentation procedures. The quantified information collected from the damage grids and damage sketches for each specimen was then added to the comparison database.

As an example, the application of the damage documentation procedures to an open-hole tension specimen, as tested at CRC-ACS, is described here. The optical documentation photographs are shown in Figure 28. From these photographs, quantitative and qualitative data are then documented through the use of the damage grids and damage sketches, respectively. The damage grids and damage sketches were both developed to capture damage information about a specimen according to objective criteria. The extent of visible damage on the surface of the open-hole tension specimen is quantified by using the damage grid shown for this specimen in Figure 29. As can be seen in this figure, damage appears to initiate at the edge of the hole and to propagate in a line tangent to the hole at a +45° angle. However, the damage grid is not able to capture the damage type and the more precise shape of the damage. The 'active'

damage type(s), as well as the shape and direction of damage, is captured via the damage sketch, as shown in Figure 30 for this specimen. As previously defined, an 'active' damage mode refers to a mode of damage present ("turned on" / "at work") in the specimen. Through visual inspection of the specimen photographs (or of the specimens themselves when further clarity is needed), the damage modes of matrix cracking, delamination, and fiber fracture are able to be identified and placed in the damage sketches. From the damage sketches for the specimen in Figure 30, one can see that the main type of damage in this open-hole tension specimen is that of matrix cracks running along the fiber direction of +45° on the front and back surfaces, and a mixture of matrix cracks and delaminations on the left and right surfaces. The damage sketches also contain detailed information on the spacing of the matrix cracks. All the observed damage is contained within the area selected for the damage grids and sketches.

The implementation of the damage documentation procedures worked well on all twenty-one open hole specimens received and processed. While the initial implementation of the original documentation procedures on these open hole specimens showed needed improvements in these procedures, the refinements were made and enhanced these procedures. These refined procedures are more generic and capable of being applied to a wider range of damaged composite specimens due to the lessons learned from the specimens worked during this project.

Preparation to implement the damage documentation procedures on the other specimens that were to be tested in associated parts of this overall program was completed. This included the ply-drop specimens from CRC-ACS and the double-notch specimens from NRL. This preparation included initial camera settings to photograph each specimen face as well as the set-up of the computer code to combine these individual surface photographs and place the documentation layers (axes layer, damage grid layer, and damage sketch layer) on the combined image. The preparation was done in order to expedite the implementation of the damage documentation procedure had the specimens been tested and shipped to M.I.T.

6.3 *Comparison Database Results*

The comparison database allowed lengthscale effects in composites to be investigated. An initial damage comparison database was established via the implementation of the damage documentation procedures on the originally tested NRL IPL and on the open hole specimens received. This database continued to grow throughout the project as specimens became available and the damage documentation procedures were applied. As results from the damage documentation of specimens of different geometries were added to the database, investigation of lengthscale effects across specimen types (e.g., different geometries, laminates, loadings) was conducted.

The database contains all the information gathered from the damage documentation procedures (damage extent from the damage grids, damage paths and damage modes from the damage sketches, etc.) as well as specifics on the specimens (fiber and epoxy type, laminate layups, loading history, etc.). At the end of this piece of the project, 203 tested specimens were entered into the database. This included the 182 originally tested NRL IPL specimens and the 21 OHT specimens from this project. By

organizing all this information into a sortable/searchable database, comparisons were made to find trends and expose differences in damage as the level of testing was changed.

The initial specimens to be documented and entered into the database were the originally tested NRL IPL specimens. Comparisons in the damage trends within these specimens were initially conducted. One finding was that fiber fracture only occurred in 23 of the specimens and was always associated with the fiber angle. Another was that matrix cracking was the most common observed failure mode, occurring in 92 of the 106 specimens that showed visual damage. This result was expected as matrix cracking is the most commonly observed damage mode reported in the literature. It was also noted that matrix cracking was present in all but 9 specimens that exhibited delamination (a total of 43 specimens exhibited delamination), although it did occur without delamination (in 58 specimens). One observation of mode interaction commonly found in these specimens was an interaction between matrix cracking and delamination occurring through the thickness. Therefore, this interaction was named a 'zig-zag' damage mode since the result was a zig-zag pattern through the thickness of the specimen with alternating through-ply matrix cracks and small delaminations interconnecting the matrix cracks in $+\theta$ and $-\theta$ plies. It should be noted that the small delaminations associated with the zig-zag damage mode were not counted toward the number of specimens exhibiting delamination as they have this special geometry. An example of the zig-zag damage mode is shown in Figure 31. The zig-zag pattern was observed in 52 of the specimens with the damage initiating at the tip of the strain riser and progressing to the "right surface" (as defined in Figure 22) along the fiber angles, either as a single zig-zag or symmetrical zig-zags. The example seen in Figure 31 shows a zig-zag failure that is symmetric about the strain riser. An important lengthscale issue observed in the NRL IPL testing was the influence of the boundaries (grips). In some cases the damage modes appeared to be unaffected by the boundary grips. However, in other cases the damage appeared to change direction right at the boundaries. This is shown in Figure 32. Another mode interaction observed in a few cases was the change of damage mode along the progression path. As seen in Figure 33, the specimen exhibits a zig-zag failure along the fiber angles with matrix cracking occurring on the "front" surface when the damage mode abruptly changes to fiber fracture.

Upon receiving the first batch of twenty-one open hole specimens from CRC-ACS, the damage documentation procedures were applied and the results from these specimens were added to the comparison database. An initial trend found within the open-hole tension specimens is the presence of matrix cracking in the outer layers of all specimens, with the cracks running along the outer-ply fiber angle of +45°. Another trend common across all the open-hole tension specimens is that the dominant surface matrix crack runs tangent to the hole edge along the outer ply angle of +45°. This can clearly be seen in the damage captured in Figure 29 and Figure 30. A third trend from the open-hole tension specimens is that the $[+45_4/0_4/-45_4]_S$ specimens broke into two separate pieces at final failure, whereas those of the $[+45/0/-45]_{4S}$ laminate did not. Additional open hole specimens were received from CRC-ACS during the last month of the project. The damage documentation procedures were being implemented and the damage information being added to the database, but the specimens were not received

in time to fully investigate damage trends. Initial observations from the second batch of open hole specimens revealed similar trends as the first batch of specimens.

Comparisons were also made across specimen types. The zig-zag damage mode observed in the originally tested NRL IPL specimens was not found in any of the CRC-ACS open hole specimens. This may be due to the open hole specimens having 0° plies which influence the damage paths through the thickness of the laminate. Another observation made between specimen types was that the stitch cracking (observed via CμT) present in some originally tested NRL IPL specimens was not found in any of the open hole specimens. Again, the absence of this damage mode in the open hole specimens is likely attributed to the presence of 0° plies which change the damage mechanisms in the vicinity of matrix cracks in the angled plies. An additional observation made between specimen types was the greater damage extent (primarily matrix cracking and delaminations) through the thickness of the open hole specimens compared to the damage observed in the originally tested NRL IPL specimens. However, this may be attributed to the experimental loading conditions, with the open hole specimens being tested further into the damage regime (continued loading after significant damage development) than the NRL IPL specimens. Continued comparisons will be made across specimen types and reported as part of a doctoral thesis involving this work.

6.4 *Results from Computed Microtomography Investigation*

Over the course of the project, thirty-one specimens were scanned using the CμT. This included scans of ten of the base-level originally tested NRL IPL specimens, and scans of twenty-one of the open-hole tension specimens, as tested at CRC-ACS. Many observations about damage and damage paths were made from these scans. From the originally tested NRL IPL specimens, one of the most interesting damage characteristics was the presence of a "zig-zag" damage mode. This "zig-zag" damage mode consists of alternating through-thickness matrix cracks and short delaminations, resulting in a zig-zag damage path. This damage mode was observed in 52 of the 106 NRL IPL specimens that exhibited visual damage. From the CμT scans, it was observed that this damage mode initiated near the tip of the strain-riser and propagated along the same angle as one of the plies (however the damage went through multiple plies).

An example of a CμT scan and observed results of a NRL IPL specimen follows. This specimen is made of AS4/3501-6 with a stacking sequence of $[(+15/-15_2/+15_2/-15)_5]_S$. The 0°-axis is defined as parallel to the X-axis, which is parallel to the strain-riser (see [109] for description of strain riser). The overall specimen dimensions are 1.5 inch by 1.0 inch by 0.14 inch (length by width by thickness) with a 0.6-inch long and 0.04-inch wide strain riser (notch) cut into the specimen. This specimen had been loaded using the NRL IPL. The loading on this specimen was comprised of an extensional load along the Y-axis (length) and an in-plane counterclockwise rotation about the specimen center. Further details of the specimen and loading conditions can be found in [109]. Optical photographs (which are part of the documentation procedure) of the faces of the failed specimen are shown in Figure 34.

Virtual images taken of the specimen and created via the CμT process are shown in Figure 35 and Figure 36 as examples of such created 3-D volumes. The volume shown in Figure 35 represents the specimen material between the dashed lines of Figure 34. These dashed lines encompass the damaged region as determined from the damage grid of the specimen. This specimen exhibits multiple damage modes (fiber fracture, matrix cracking, and delamination), all of which are observable in the recreated 3-D volume. One of the most powerful features of this process is the ability to investigate damage within the specimen without sectioning (cutting) the specimen, but instead "virtually cutting" the 3-D volume. An example of a virtual cut of the specimen is shown in Figure 36. The cutting plane (location of cut) is that shown in Figure 35 as a shaded plane intersecting the volume. This is the end of the piece shown in Figure 36 with the shaded plane still there to help in its identification. This is emphasized in a two-dimensional presentation of the cutting plane in Figure 37. It was observed in this specimen that the damage on the outer right-face of the specimen consisted of matrix cracks and short delaminations alternating through the thickness. This can be seen upon close observation of the photographs shown in Figure 34. As can be seen in Figure 36 and Figure 37, this damage at the "virtually cut" face has the same pattern as on the outer right face (also more clearly seen in Figure 35 than in Figure 34). Taking additional cuts, shown in Figure 38a and Figure 38b, it is found that the damage initiates at the strain riser and propagates along the positive and negative fiber directions until reaching the outer right face. As can be seen in these two figures, the damage alternates between the positive and negative oriented plies. In order to get this same information with traditional methods, multiple cuts of finite width would need to have been made, along with the analysis of each face exposed from this sectioning. This would have made it impossible to do further work/testing on that sectioned specimen, as well as destroying parts of the actual damage volume via the sectioning. With the virtual cutting, further work can be done quite easily, and no details are affected.

Scans of the open-hole tension specimens, as tested at CRC-ACS, also revealed observations about the damage. A unique and unexpected failure was found in a few of these specimens, where damage was occurring at the top and bottom of the hole in addition to the expected damage location (at the maximum stress/strain concentration). There are two thoughts as to the cause of this damage at this location. One is that damage initiates from the high stress/strain concentrator and propagates to the top/bottom of the hole and creates a new stress/strain concentrator where further damage initiates. A second is that there is preexisting damage due to the specimen manufacturing procedure, specifically the drilling procedure to produce the open hole. This damage can cause large stress concentrations and resulting stress gradients beyond those from the structural detail (hole), thereby creating multiple, unexpected initiation points for damage. These observations were to be investigated further in the second round of open hole specimens tested by CRC-ACS. This included a change in the manufacturing procedure of CRC-ACS, particularly the process used to drill the holes. Scans were planned of open hole specimens manufactured with the modified drilling procedure, but these specimens were not received prior to the end of this part of the project.

An example of a CμT scan and observed results of a CRC-ACS specimen follows. The specimen is made of AS4/3501-6 with a stacking sequence of $[+45_4/0_4/-45_4]_S$. The 0°-axis is defined parallel to the Y-axis, which is parallel to the direction of loading. The overall specimen dimensions are 13.5 inches by 4.0 inches by 0.126 inches containing a hole of diameter of 1.0 inches. This specimen had been loaded in tension until ultimate failure, resulting in the specimen breaking into two pieces. Optical photographs, from the documentation process, of the faces of the failed specimen are shown in Figure 39. Note that the entire length of the specimen is not shown in these photos. The virtual joining procedure was used during the documentation process to recombine the broken specimen pieces, as shown in Figure 39. The individual specimen pieces were scanned with the CμT resulting in two 3-D volumes. Virtual images, with an orientation normal to the back surfaces of the 3-D volumes, of these two pieces are shown in Figure 40 and Figure 41. As can be seen in these figures, this specimen exhibits different damage modes (fiber fracture, fiber pull-out, matrix crack, and delamination) through the thickness of the specimen. The spotted pattern observed on the outer plies is an artifact from the optical strain mapping technique. The changes in damage mode and damage paths were investigated by "virtually cutting" (previously described for NRL IPL specimen) material in a ply-by-ply manner. The ply-by-ply virtual cuts of the top half of the specimen are shown in Figure 42. A three-dimensional view of both specimen pieces combined into a single image, as shown in Figure 43, allows one to easily see the failure paths, on a ply-by-ply basis, that resulted in the specimen separating into two pieces. It was observed in this specimen that the dominant damage mode varied through the thickness of the laminate (thus, a dependence on fiber orientation). Similar observations were made in the other OHT specimens.

7. Unaddressed Items

Very few of the planned project specimens were completed by the end of time of this portion of the overall project. Because a large portion of the work to be performed by M.I.T. was dependent on these project specimens, the delays in testing resulted in the inability to perform some of the proposed work. A summary of the specimens planned and those actually completed as of the completion of this piece of the overall project are shown in Table 5.

Table 5 Planned and completed specimens

Specimen Type	Test Location	Number of Specimens Tested	
		Planned	Completed
Open-Hole Tension	CRC-ACS	36	21
Ply-Drop	CRC-ACS	12	0
Double-Notched	NRL	1152	0
Stiffened Panels	CRC-ACS	2	0
In-Plane Loader*	NRL*	0	210

*In-Plane Loader specimens from a previous NRL project.

In order to move forward with other aspects of this project, specimens readily available from a previous NRL project were used as previously described. These were the NRL In-Plane Loader (IPL) specimens. The NRL IPL specimens were made of similar material (AS1 and AS4 fibers with 3501-6 matrix) and stacking sequences as the planned project specimens (AS4/3501-6). The NRL IPL specimens were also very similar in geometry to the double-notched specimens planned for the current project. The use of the NRL IPL specimens allowed initial development of the damage documentation procedure and comparison database as well as some initial investigations on lengthscale effects.

One item that was unable to be investigated due to the delays in specimen testing was the lengthscale effects of stress-field gradients. Finite element models of the project specimens were developed at MIT to study the analytical stress fields. However, an insufficient number of experimental specimens were tested in order to compare and analyze results between the analytical and experimental tests. At the conclusion of the project, the NRL was working on composing videos with the strain mapping, and hence the experimental strain fields, for some of the open-hole tension specimens tested at CRC-ACS. As that data became available, the experimental gradients were investigated. However, too few of the specimens were completed by the close of the project to draw meaningful conclusions. Had more specimens been available, the results from analytical models would have been validated and verified via comparison to the experimental results. The information would then be added to the damage comparison database and used for further consideration. This would have allowed trends between the stress-field gradients and the 'active' damage modes, damage extent, and damage paths to be investigated for lengthscale effects. The NRL IPL specimens that were used to help develop the damage documentation procedures could not be used to study experimental stress-field gradients as those specimens were not designed for such a study, and hence, there was no experimental data on the stress fields. Therefore, due to delayed specimen production and testing, a complete investigation to identify lengthscales associated with stress-field gradients was not complete.

8. Summary

Over the course of the project, many key steps were taken working towards the three primary tasks: assessing current failure models; developing an overall methodology to work through the lengthscale levels through to full-scale structures; and planning the experimental programs to acquire needed knowledge and to work chosen failure approaches and the overall methodology. A question tree was developed using information and knowledge from an extensive literature review. Answers from the question tree helped in planning the test program for the project.

A key contribution from the project includes procedures to document and characterize damage for use in the overall project. Baseline procedures were established using specimens from a previous NRL project and then refinements were made while applying the initial procedures to the open hole specimens of this project. In particular, the procedures as previously established were implemented on current

project specimens and three areas in the initial procedures were identified where improvements were needed. The first of these is a consistent means to handle specimens that had failed into two or more pieces during testing. The second area is a consistent manipulation of specimen images and/or documentation procedures in order to return the planar dimensions to the virgin (untested) dimensions. The third of these is a better identification of the size of the damage grid and damage sketch dimensions within specimen types to maintain comparable regimes of documentation of damage. The aim of these refinements is to make the overall procedures more robust and to enable the procedures to be implemented on a broader class of composite specimens. This will ensure consistent comparisons across specimens of various lengths and configurations. These refinements were pursued in parallel with the use of the damage documentation procedures to document and characterize the damage in the open-hole tension specimens tested. By the close of the project, the procedures were applied to 210 previously tested NRL IPL specimens and twenty-one open-hole tension specimens.

An additional thirty specimens were received from CRC-ACS during the last weeks of the project. Damage documentation of these specimens was begun but did not conclude by the end of the project. Preparation to implement the damage documentation procedures on the other project specimens that were to be tested in associated parts of this overall program was also completed. However, due to the delays in specimen production and testing, these were not worked. This includes the remaining open-hole tension and ply-drop specimens from CRC-ACS, the stiffened panel specimens, and the basic level double-notch characterization specimens from NRL. The preparation was done to expedite the implementation of the damage documentation procedure once the specimens had been tested and shipped to M.I.T.

A major achievement made during the course of this project involved finding and utilizing the methodology of computed microtomography (CμT) in investigating damage in the composite specimens. This technique creates a digital representation of three-dimensional volumes from scans of physical/experimental composite specimens. Therefore, damage, damage paths, and interaction of damage modes throughout the volume of the specimen can be investigated without any specimen preparation and with no destructive sectioning. During the course of the project, scans of thirty-one specimens were made; ten which were base-level previously tested NRL IPL specimens, and twenty-one which were open-hole tension specimens from CRC-ACS. From these scans, damage mode interactions as well as damage paths were studied throughout the volume of the specimen. Without the CμT scans, the stitch cracking in the NRL IPL specimens would not have been identified, and the identification of improper manufacturing techniques of the OHT specimens, resulting in unanticipated damage locations, may not have been made.

Damage information collected from all the specimens was added to the Damage Comparison Database. This comparison database allowed damage trends and lengthscale effects to be investigated across specimens of varying structural levels, a task that was previously inaccessible. Although the database was primarily filled with the originally tested NRL IPL specimens, results showing lengthscale effects were able to be initially identified from this database.

Overall, the work performed during the course of the project advanced the knowledge and methodology of utilizing lengthscales to better understand how damage mechanisms change as the level of testing changes. While few of the planned levels of testing were complete by the close of this part of the project, promising results were emerging from the limited data in the comparison database. An outcome that is ready for use in future projects is the damage documentation procedure, which allows damage to be characterized in a standardized process for various composite specimens (i.e., specimens of different geometries, structural features, loadings). This will allow means to readily identify issues associated with lengthscales and levels of testing. It is recommended to continue pursuing the methodology of lengthscales as a means to reach an understanding of the changes in mechanisms affecting the material response and damage process in composite structures.

References

1. M.J. Hinton, A.S. Kaddour, and P.D. Soden. "A Comparison of the Predictive Capabilities of Current Failure Theories for Composite Laminates, Judged Against Experimental Evidence", *Composites Science and Technology*, Vol. 62, 2002, pp.1725-1797.

2. S.M. Spearing, P.A. Lagacé, and H.L.N. McManus. "On the Role of Lengthscale in the Prediction of Failure of Composite Structures: Assessment and Needs", *Applied Composite Materials*, Vol. 5, 1998, pp. 139-149.

3. P. Beaumont, ed., "*Proceedings of the Conference on Advances in Multi-Scale Modelling of Composite Material Systems of Components*", Monterey, CA, 2005.

4. NICOP Submission "Methodology for Determination of Mechanical Behavior and Failure in Composite Structures", Perez, Herszberg, Kelly, Furukawa, Mourtiz, Wang, Michopolous, and Lagacé, August, 2006.

5. D.L. Flaggs and M.H. Kural. "Experimental Determination of the In Situ Transverse Lamina Strength in Graphite/Epoxy Laminates", *Journal of Composite Materials*, Vol. 16, No. 2, 1982, pp. 103-116.

6. N.J. Pagano and R.B. Pipes. "The Influence of Stacking Sequence on Laminate Strength", *Journal of Composite Materials*, Vol. 5, No. 1, 1971, pp. 50-57.

7. B.W. Rosen. "Mechanics of Composite Strengthening", *Fiber Composite Materials*, pp. 37-75, American Society of Metals, Metals Park, Ohio, 1965.

8. S.L. Phoenix. "Statistical Analysis of Flaw Strength Spectra of High-Modulus Fibers", *Composite Reliability, ASTM STP 580*, 1975, pp. 77-89.

9. T.K. O'Brein. "Characterization of Delamination Onset and Growth in a Composite Laminate", *Damage in Composite Materials, ASTM STP 775*, 1982, pp. 140-167.

10. I.M. Daniel and O. Ishai. *Engineering Mechanics of Composite Materials*, Oxford University Press, New York, 1994.

11. B.D. Coleman. "On the Strength of Classical Fibres and Fibre Bundles", *Journal of the Mechanics and Physics of Solids*, Vol. 7, No. 1, 1958, pp. 60-70.

12. S.L. Phoenix and H.H. Taylor. "The Asymptotic Strength Distribution of a General Fiber Bundle", *Advances in Applied Probability*, Vol. 5, No. 2, 1973, pp. 200-216.

13. W.A. Weibull. "A Statistical Theory of the Strength of Materials", *Ingvetensk. Akad. Handl.*, Vol. 151, 1939, pp. 5-45.

14. S.L. Phoenix. "Stochastic Strength and Fatigue of Fiber Bundles", *International Journal of Fracture*, Vol. 14, No. 3, June 1978, pp. 327-344.

15. D.G. Harlow and S.L. Phoenix. "The Chain-of-Bundles Probability Model for the Strength of Fibrous Materials I: Analysis and Conjectures", *Journal of Composite Materials*, Vol. 12, No. 2, 1978, pp. 195-214.

16. H.T. Hahn and J.G. Williams. "Compression Failure Mechanisms in Unidirectional Composites". NASA-TM-85834, NASA, August 1984.

17. B.W. Rosen. "Tensile Failure of Fibrous Composites", *AIAA Journal*, Vol. 2, No. 11, 1964, pp. 1985-1991.

18. M.H.R. Jen, Y.S. Kau, and J.M. Hsu. "Initiation and Propagation of Delamination in a Centrally Notched Composite Laminate", *Journal of Composite Materials*, Vol. 27, No. 3, 1993, pp. 272-302.

19. R.Y. Kim and H.T. Hahn. "Effect of Curing Stresses on the First Ply-failure in Composite Laminates", *Journal of Composite Materials*, Vol. 13, 1979, pp. 2-16.

20. S.L. Phoenix. "Probabilistic Strength Analysis of Fibre Bundle Structures", *Fibre Science and Technology*, Vol. 7, 1974, pp. 15-31.

21. P.S. Theocaris and C.A. Stassinakis. "Crack Propagation in Fibrous Composite Materials Studied by SEM", *Journal of Composite Materials*, Vol. 15, 1981, pp. 133-141.

22. E. Altus and O. Ishai. "Transverse Cracking and Delamination Interaction in the Failure Process of Composite Laminates", *Composites Science and Technology*, Vol. 26, No. 1, 1986, pp. 59-77.

23. C.E. Harris, D.H. Allen, and E.W. Nottorf. "Predictions of Poisson's Ratio in Cross-Ply Laminates Containing Matrix Cracks and Delaminations", *Journal of Composite Technology and Research*, Vol. 11, No. 2, 1989, pp. 53-58.

24. A. Rotem and Z. Hashin. "Failure Modes of Angle Ply Laminates", *Journal of Composite Materials*, Vol. 9, 1975, pp. 191-206.

25. H.T. Hahn and S.W. Tsai. "On the Behavior of Composite Laminates After Initial Failures", *Journal of Composite Materials*, Vol. 8, 1974, pp. 288-305.

26. A.K. Ditcher and J.P.H.Webber. "Edge Effects in Uniaxial Compression Testing of Cross-Ply Carbon-Fiber Laminates", *Journal of Composite Materials*, Vol. 16, May 1982, pp. 228-243.

27. D.W. Wilson. "Evaluation of the V-Notched Beam Shear Test Through an Interlaboratory Study", *Journal of Composite Technology and Research*, Vol. 12, No. 3, 1990, pp. 131-138.

28. S.A. Salpekar and T.K. O'Brien. "Analysis of Matrix Cracking and Local Delamination in $(0/+\theta/-\theta)$s Graphite Epoxy Laminates Under Tension Load", In

Proceedings of the 8th International Conference on Composite Materials, Volume 3, Honolulu, HI, 1991, 28-G.

29. N.A. Fleck, L.Deng, and B. Budiansky. "Prediction of Kink Width in Compressed Fiber Composites", *Journal of Applied Mechanics*, Vol. 62, June 1995, pp. 329-337.

30. P.M. Jelf and N.A. Fleck. "Compression Failure Mechanisms in Unidirectional Composites", *Journal of Composite Materials*, Vol. 26, No. 18, 1992, pp. 2706-2726.

31. P. Berbinau, C. Soutis, and I.A. Guz. "Compressive Failure of 0° Unidirectional Carbon-Fibre-Reinforced Plastic (CFRP) Laminates by Fibre Microbuckling", *Composites Science and Technology*, Vol. 59, 1999, pp. 1451-1455.

32. A.S. Argon. "Fracture of Composites", *Treatise on Materials Science and Technology*, Vol. 1, 1972, pp. 79-114.

33. B. Budiansky and N.A. Fleck. "Compressive Failure of Fibre Composites", *Journal of the Mechanics and Physics of Solids*, Vol. 41, No. 1, 1993, pp. 183-211.

34. A.G. Evans and W.F. Adler. "Kinking as a Mode of Structural Degradation in Carbon Fiber Composites", *Acta Metallurgica*, Vol. 26, 1978, pp. 725-738.

35. B. Budiansky. "Micromechanics", *Computers and Structures*, Vol. 16, No. 1-4, 1983, pp. 3-12.

36. A. Maewal. "Postbuckling Behavior of a Periodically Laminated Medium in Compression", *International Journal of Solids and Structures*, Vol. 17, 1981, pp. 335-344.

37. C.A. Berg and M. Salama. "Fatige of Graphite Fibre-Reinforced Epoxy in Compression", *Fibre Science and Technology*, Vol. 6, 1973, pp. 79-118.

38. C.W. Weaver and J.G. Williams. "Deformation of a Carbon-Epoxy Composite under Hydrostatic Pressure", *Journal of Materials Science*, Vol. 10, 1975, pp. 1323-1333.

39. C.R. Chaplin. "Compressive Fracture in Undirectional Glass-Reinforced Plastics", *Journal of Materials Science*, Vol. 12, 1977, pp. 347-352.

40. C. Soutis, P.T. Curtis, and N.A. Fleck. "Compressive Failure of Notched Carbon Fibre Composites", *Proceedings of the Royal Society of London, Series A*, Vol. 440, 1993, pp. 241-256.

41. A. Kelly. "Interface Effects and the Work of Fracture of a Fibrous Composite", *Proceedings of the Royal Society of London, Series A*, Vol. 319, July 1970, pp. 95-116.

42. A. Takaku and R.G.C. Arridge. "The Effect of Interfacial Radial and Shear Stress on Fibre Pull-Out in Composite Materials", *Journal of Physics D: Applied Physics*, Vol. 6,

1973, pp. 2038-2047.

43. J.W. Hutchinson and H.M. Jensen. "Models of Fiber Debonding and Pullout in Brittle Composites with Friction", *Mechanics of Materials*, Vol. 9, 1990, pp. 139-163.

44. P. Lawrence. "Some Theoretical Considerations of Fibre Pull-Out from an Elastic Matrix", *Journal of Materials Science*, Vol. 7, 1972, pp. 1-6.

45. L.S. Sigl and A.G. Evans. "Effects of Residual Stress and Frictional Sliding on Cracking and Pull-Out in Brittle Matrix Composites", *Mechanics of Materials*, Vol. 8, 1989, pp. 1-12.

46. C. Liang and J.W. Hutchinson. "Mechanics of the Fiber Pushout Test", *Mechanics of Materials*, Vol. 14, 1993, pp. 207-221.

47. G. Lin, P.H. Geubelle, and N.R. Sottos. "Simulation of Fiber Debonding with Friction in a Model Composite Pushout Test", *International Journal of Solids and Structures*, Vol. 38, 2001, pp. 8547-8562.

48. A. Kelly and W.R. Tyson. "Tensile Properties of Fibre-Reinfoced Metals: Copper/Tungsten and Copper/Molybdenum", *Journal of the Mechanics and Physics of Solids*, Vol. 13, 1965, pp. 329-350.

49. P.B. Bowden. "The Effect of Hydrostatic Pressure on the Fibre-Matrix Bond in a Steel-Resin Model Composite", *Journal of Materials Science*, Vol. 5, 1970, pp. 517-520.

50. P.W.R. Beaumont and D.C. Phillips. "Tensile Strengths of Notched Composites", *Journal of Composite Materials*, Vol. 6, 1972, pp. 32-46.

51. M.S. El-Zein and K.L. Reifsnider. "The Strength Prediction of Composite Laminates Containing a Circular Hole", *Journal of Composites Technology and Research*, Vol. 12, No. 1, 1990, pp. 24-30.

52. N.J. Pagano and R.B. Pipes. "Some Observation on the Interlaminar Strength of Composite Laminates", *International Journal of Mechanical Sciences*, Vol. 15, 1973, pp. 679-688.

53. T.K. O'Brien. "Analysis of Local Delaminations and Their Influence on Composite Laminate Behavior", *Delamination and Debonding of Materials, ASTM 876*, 1985, pp. 282-297.

54. T.K. O'Brien. "Interlaminar Fracture of Composites", NASA Technical Memorandum 85768, June 1984. N84-27835.

55. S.R. Soni and R.Y. Kim. "Delamination of Composite Laminates Stimulated by Interlaminar Shear", *Composite Materials: Testing and Design, ASTM STP 893*, 1986, pp. 286-307.

56. J.C. Brewer and P.A. Lagacé. "Quadratic Stress Criterion for Initiation of Free Edge Delamination", *Journal of Composite Materials*, Vol. 22, December 1988, pp. 1141-1155.

57. R.Y. Kim and S.R. Soni. "Experimental and Analytical Studies On the Onset of Delamination in Laminated Composites", *Journal of Composite Materials*, Vol. 18, January 1984, pp. 70-80.

58. C. Kassapoglou and P.A. Lagacé. "An Efficient Method for the Calculation of Interlaminar Stresses in Composite Materials", *Journal of Applied Mechanics*, Vol. 53, December 1986, pp. 744-750.

59. N.V. Bhat and P.A. Lagacé. "An Analytical Method for the Evaluation of Interlaminar Stresses Due to Material Discontinuities", *Journal of Composite Materials*, Vol. 28, No. 3, 1994, pp. 190-210.

60. K.J. Saeger, P.A. Lagacé, and D.J. Shim. "Interlaminar Stresses Due to In-Plane Gradient Stress Fields", *Journal of Composite Materials*, Vol. 36, No. 2, 2002, pp. 211-227.

61. T.K. O'Brien and S.J. Hooper. "Local Delamination in Laminates with Angle Ply Matrix Crack, Part II: Delamination Fracture Analysis and Fatigue Characterization", *Composite Materials: Fatigue and Fracture, ASTM STP 1156*, Vol. 4, 1993, pp. 507-538.

62. S.S. Wang. "Fracture Mechanics for Delamination Problems in Materials", *Journal of Composite Materials*, Vol. 17, May 1983, pp. 210-223.

63. P.A. Lagacé and N.V. Bhat. "Efficient Use of Film Adhesive Interlayers to Suppress Delamination", *Composite Materials: Testing and Design, ASTM STP 1120*, Vol. 10, 1992, pp. 384-396.

64. E.A. Armanios, L.W. Reheld, and F. Weinstein. "Understanding and Predicting Sublaminate Damage Mechanisms in Composite Structures", *Composite Materials: Testing and Design, ASTM STP 1059*, Philadelphia, 1990.

65. R.A. Kline and F.H. Chang. "Composite Failure Surface Analysis", *Journal of Composite Materials*, Vol. 14, October 1980, pp. 315-324.

66. T.K. O'Brien and S.J. Hooper. "Local Delamination in Laminates with Angle Ply Matrix Crack, Part I: Tension Tests and Stress Analysis", *Composite Materials: Fatigue and Fracture, ASTM STP 1156*, Vol. 4, pp. 491-506.

67. J.D. Whitcomb. "Predicted and Observed Effects of Stacking Sequence and Delamination Size on Instability Related Delamination Growth", *Journal of Composite Technology and Research*, Vol. 11, No. 3, 1989, pp. 94-98.

68. I.M. Daniel, R.E. Rowlands, and J.B. Whiteside. "Effects of Material and Stacking

Sequence on Behavior of Composite Plates with Holes", *Experimental Mechanics*, Vol. 14, No. 1, January 1974, pp. 1-9.

69. J.M. Whitney and C.E. Browning. "Free-Edge Delamination of Tensile Coupons", *Journal of Composite Materials*, Vol. 6 1972, pp. 300-303.

70. K.E. Jackson. "Scaling Effects in the Flexural Response and Failure of Composite Beams", *AIAA Journal*, Vol. 30, No. 8, August 1992, pp. 2099-2105.

71. D.P. Johnson, J. Morton, S. Kellas, and K.E. Jackson. "Scaling Effect in Sublaminate-Level Scaled Composite Laminates", *AIAA Journal*, Vol. 36, No. 3, March 1998, pp. 441-447.

72. C.T. Herakovich. "Influence of Layer Thickness on the Strength of Angle-Ply Laminates", *Journal of Composite Materials*, Vol. 16, May 1982, pp. 216-227.

73. S. Kellas and J. Morton. "Strength Scaling in Fiber Composites", AIAA-91-1144-CP, NASA Contract Report 4335, November 1990.

74. P.A. Lagacé, J.C. Brewer, and C. Kassapoglou. "The Effect of Thickness on Interlaminar Stresses and Delamination in Straight-Edged Laminates", *Journal of Composite Technology and Research*, Vol. 9, No. 3, 1987, pp. 81-87.

75. M.R. Wisnom. "Size Effects in the Testing of Fibre-Composite Materials", *Composites Science and Technology*, Vol. 59, 1999, pp. 1937-1957.

76. T.K. O'Brien and S.A. Salpekar. "Scale Effects on the Transverse Tensile Strength of Graphite Epoxy Composites", US Army Aviation Systems Command, Aviation R&T Activity, National Aeronautics and Space Administration, Langley Research Center, 1992.

77. R.H. Martin. "Incorporating Interlaminar Fracture Mechanics into Design", *Proceedings of the Institution of Mechanical Engineers, Part L: Journal of Materials: Design and Applications*, Vol. 214, No. 2, 2000, pp. 91-97.

78. R.D. Jamison, K. Schulte, K.L. Reifsnider, and W.W. Stinchcomb. "Characterization and Analysis of Damage Mechanisms in Tension-Tension Fatigue of Graphite/Epoxy Laminates", *Effects of Defects in Composite Materials, ASTM STP 836*, 1984, pp. 21-55.

79. J.A. Lavoie and E. Adolfsson. "Stitch Cracks in Constraint Plies Adjacent to Cracked Plies", *Journal of Composite Materials*, Vol. 35, No. 23, 2001, pp. 2077-2097.

80. R.S. Whitehead and R.B. Deo. "A Building Block Approach to Design Verification Testing of Primary Composite Structure", In *Proceedings of the 24th AIAA/ASME/ASCE/AHS Structures, Structural Dynamics, and Materials Conference*, pp. 473-477, Lake Tahoe, NV, 1983. AIAA 83-0947.

81. P.R. Guyett and A.W. Cardrick. "The Certification of Composite Airframe Structures", *Aeronautical Journal*, Vol. 84, No. 830/3, July 1980, pp. 188-203.

82. *Composite Materials Handbook 17* (CMH-17-3F). Polmer Matrix Composites: Materials Usage, Design, and Analysis. Volume 3F, Chapter 4, June 2002.

83. C.E. Harris, J.H. Starnes, Jr., and M.J. Shuart. "Design and Manufacturing of Aerospace Composite Structures, State-of-the-Art Assessment", *Journal of Aircraft*, Vol. 39, No. 4, 2002, pp. 545-560.

84. A. Fawcett, J. Trostle, and S.Ward. "777 Empennage Certification Approach", In *11th International Conference on Composite Materials*, Gold Coast, Australia, July 1997.

85. M.J. Hinton and P.D. Soden. "Predicting Failure in Composite Laminates: The Background to the Exercise", *Composites Science and Technology*, Vol. 58, 1998, pp. 1001-1010.

86. P.D. Soden, M.J. Hinton, and A.S. Kaddour. "A Comparison of the Predictive Capabilities of Current Failure Theories for Composite Laminates", *Composites Science and Technology*, Vol. 58, 1998, pp. 1225-1254.

87. M.J. Hinton, A.S. Kaddour, and P.D. Soden. "Evaluation of Failure in Composite Laminates: Background to Part C of the Exercise", *Composites Science and Technology*, Vol. 64, 2004, pp. 321-327.

88. Special issue of *Composites Science and Technology*, Vol. 64, 2004.

89. A.S. Kaddour, M.J. Hinton, P.D. Soden. "A Comparison of the Predictive Capabilities of Current Failure Theories for Composite Laminates: Additional Contributions", *Composites Science and Technology*, Vol. 64, 2004, pp. 449-476.

90. P.D. Soden, A.S. Kaddour, and M.J. Hinton. "Recommendations for Designers and Researchers Resulting from the World-Wide Failure Exercise", *Composites Science and Technology*, Vol. 64, 2004, pp. 589-604.

91. C.C. Chamis. "Failure Criteria for Filamentary Composites", NASA-TN-D-5367, National Aeronautics and Space Administraion, 1969.

92. T.A. Bogetti, C.P.R. Hoppel, V.M. Harik, J.F. Newill, and B.P. Burns. "Predicting the Nonlinear Response and Progressive Failure of Composite Laminates", *Composites Science and Technology*, Vol. 64, No. 3-4, 2004, pp. 329-342.

93. P.A. Zinoviev, S.V. Grigoriev, O.V. Lebedeva, and L.P. Tairova. "The Strength of Multilayered Composites Under a Plane-Stress State", *Composites Science and Technology*, Vol. 58, No. 7, 1998, pp. 1209-1223.

94. S.W. Tsai and E.M. Wu. "A General Theory of Strength for Anisotropic Materials", *Journal of Composite Materials*, Vol. 5, January 1971, pp. 58-80.

95. A. Puck and H. Schürmann. "Failure Analysis of FRP Laminates by Means of Physically Based Phenomological Models", *Composites Science and Technology*, Vol. 58, 1998, pp. 1045-1067.

96. M.E.Waddoups. "Characterization and Design of Composite Materials", In *Composite Materials Workshop*, S.W. Tsai, J.C. Halpin, and N.J. Pagano, editors, pp. 254-308, Stamford, Connecticut, 1968. Technomic Pub. Co.

97. L.J. Hart-Smith. "Predictions of the Original and Truncated Maximum-Strain Failure Models for Certain Fibrous Composite Laminates", *Composites Science and Technology*, Vol. 58, No. 7, 1997, pp. 1151-1178.

98. T.A. Bogetti, C.P.R. Hoppel, V.M. Harik, J.F. Newill, and B.P. Burns. "Predicting the Nonlinear Response and Failure of Composite Laminates: Correlation with Experimental Results", *Composites Science and Technology*, Vol. 64, No. 3-4, 2004, pp. 477-485.

99. P.A. Zinoviev, O.V. Lebedeva, and L.P. Tairova. "A Coupled Analysis of Experimental and Theoretical Results on the Deformation and Failure of Composite Laminates Under a State of Plane Stress", *Composites Science and Technology*, Vol. 62, No. 12-13, 2002, pp. 1711-1723.

100. A. Puck and H. Schürmann. "Failure Analysis of FRP Laminates by Means of Physically Based Phenomological Models", *Composites Science and Technology*, Vol. 62, 2002, pp. 1633-1662.

101. P.K. Gotis, C.C. Chamis, and L. Minnetyan. "Prediction of Composite Laminate Fracture: Micromechanics and Progressive Failure", *Composites Science and Technology*, Vol. 58, 1998, pp. 1137-1149.

102. P.K. Gotis, C.C. Chamis, and L. Minnetyan. "Application of Progressive Fracture Analysis for Predicting Failure Envelopes and Stress-Strain Behaviors of Composite Laminates: A Comparison with Experimental Results", *Composites Science and Technology*, Vol. 62, 2002, pp. 1545-1559.

103. R.G. Cuntze and A. Freund. "The Predictive Capability of Failure Mode Concept-Based Strength Criteria for Multidirectional Laminates", *Composites Science and Technology*, Vol. 64, No. 3-4, 2004, pp. 343-377.

104. R.G. Cuntze. "The Predictive Capability of Failure Mode Concept-Based Strength Criteria for Multidirectional Laminates - Part B", *Composites Science and Technology*, Vol. 64, No. 3-4, 2004, pp. 487-516.

105. R.H. Bossi and G.E. Georgeson, "Composite Structure Development Decisions Using X-Ray CT Measurements", *Materials Evaluation*, Vol. 53, No. 10, 1995, pp. 1198-1203.

106. R.H. Bossi, "Failure Analysis Using Microfocus X-ray Imaging", *Journal of Testing and Evaluation*, Vol. 27, No. 2, 1999, pp. 137-142.

107. P.J. Schilling, B.-P.R. Karedla, A.K. Tatiparthi, M.A. Verges, and P.D. Herrington, "X-ray Computed Microtomography of Internal Damage in Fiber Reinforced Polymer Matrix Composites", *Composites Science and Technology*, Vol. 65, 2005, pp. 2071-2078.

108. P. Wright, X. Fu, I. Sinclair, and S.M. Spearing. "Ultra High Resolution Computed Tomography of Damage in Notched Carbon Fiber-Epoxy Composites", *Journal of Composite Materials*, Vol. 42, No. 19, 2008, pp. 1993-2002.

109. P.W. Mast, G.E. Nash, J. Michopoulos, R.W. Thomas, R. Badaliance, and I. Wolock. "Experimental Determination of Dissipated Energy Density as a Measure of Strain-Induced Damage in Composites", Naval Research Laboratory, Washington, D.C., 1992, NRL/FR/6383-92-9369.

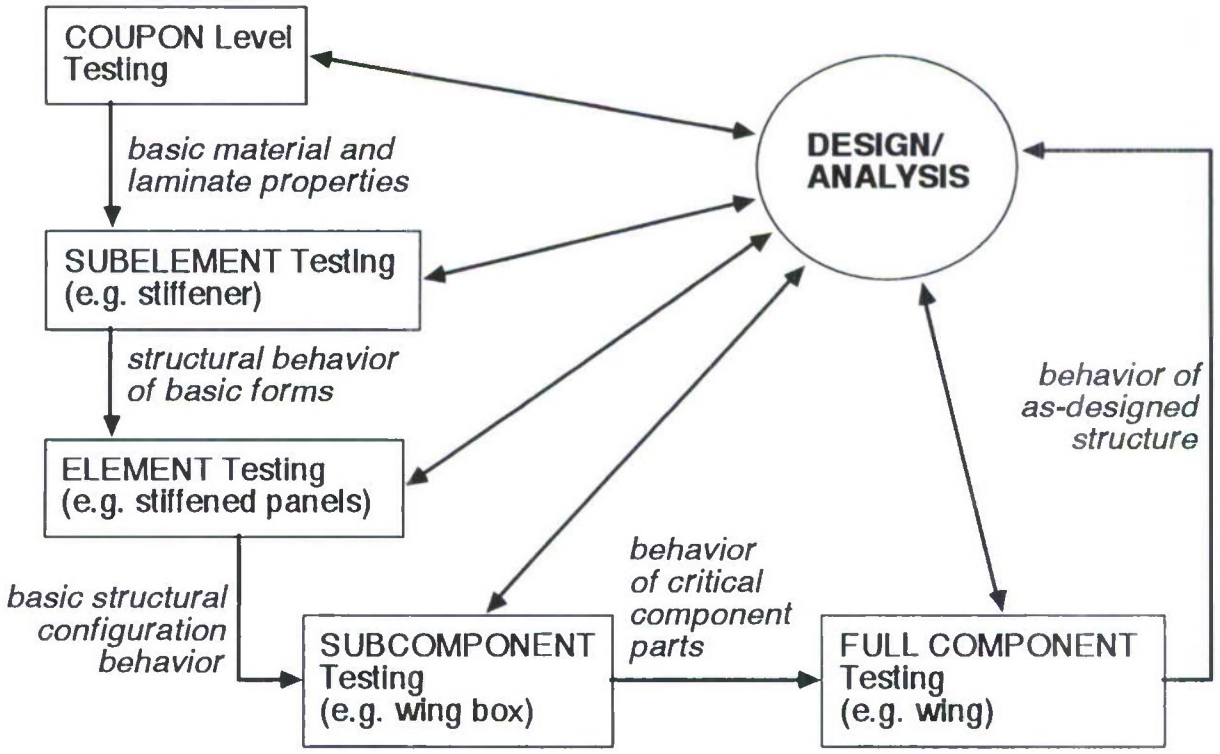

Figure 1. Illustration of the Building Block Approach.

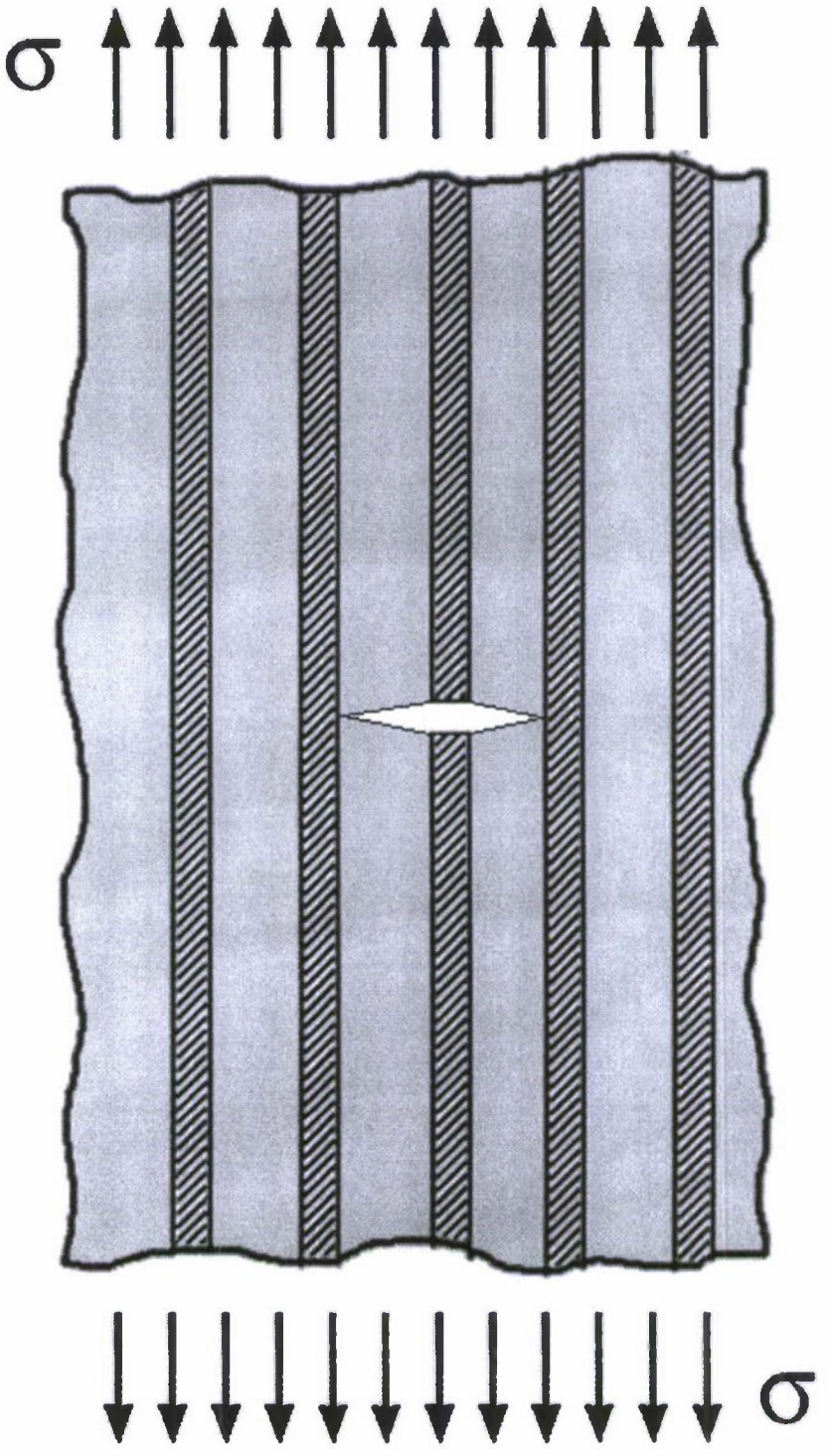

Figure 2. Illustration of a single fiber fracture in a unidirectional lamina under longitudinal tension.

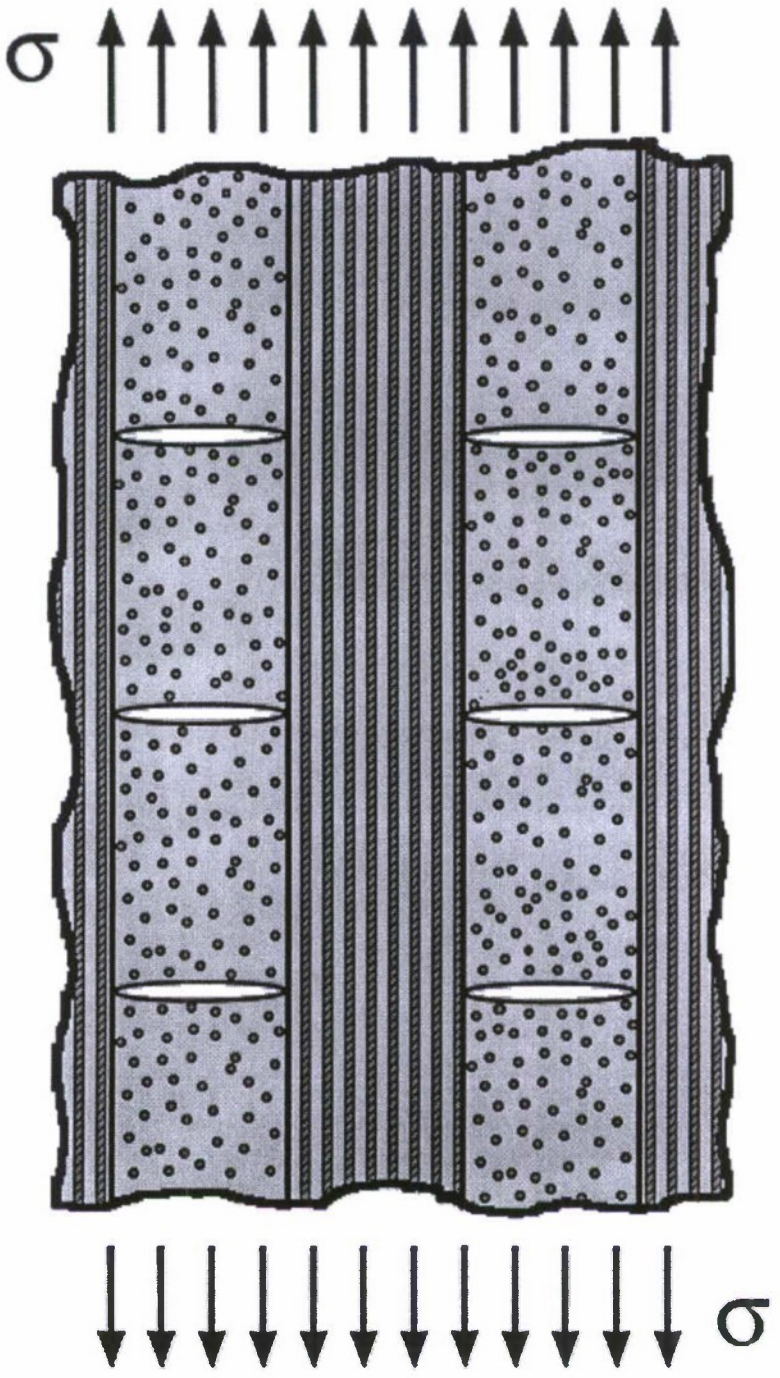

Figure 3. Illustration of matrix cracking in a cross-ply laminate under tensile loading.

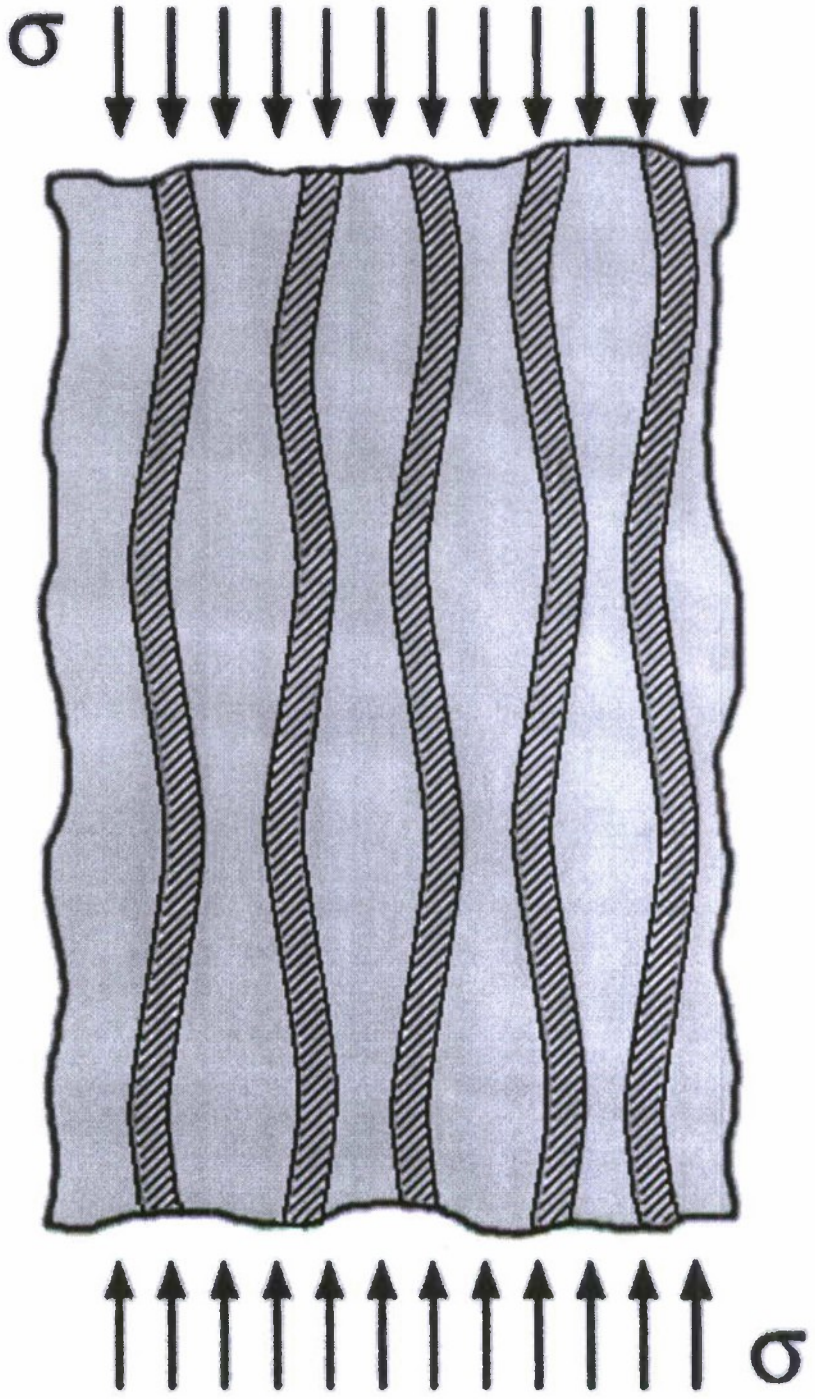

Figure 4. Illustration of out-of-phase elastic microbuckling in a unidirectional composite under longitudinal compressive loading.

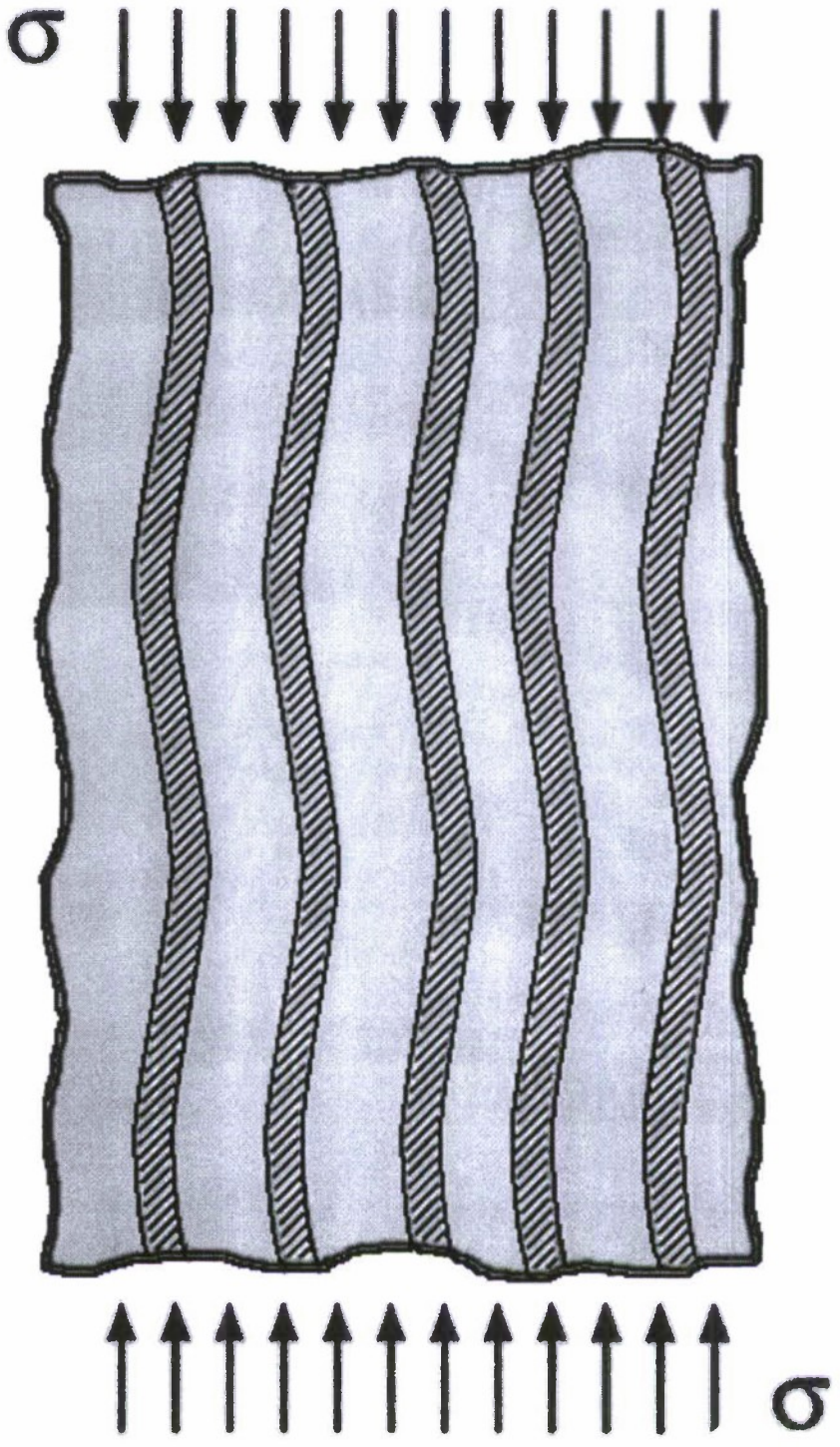

Figure 5. Illustration of in-plane elastic microbuckling in a unidirectional laminate under longitudinal compressive loading.

Figure 6. Illustration of plastic microbuckling and the resulting "kink band" region.

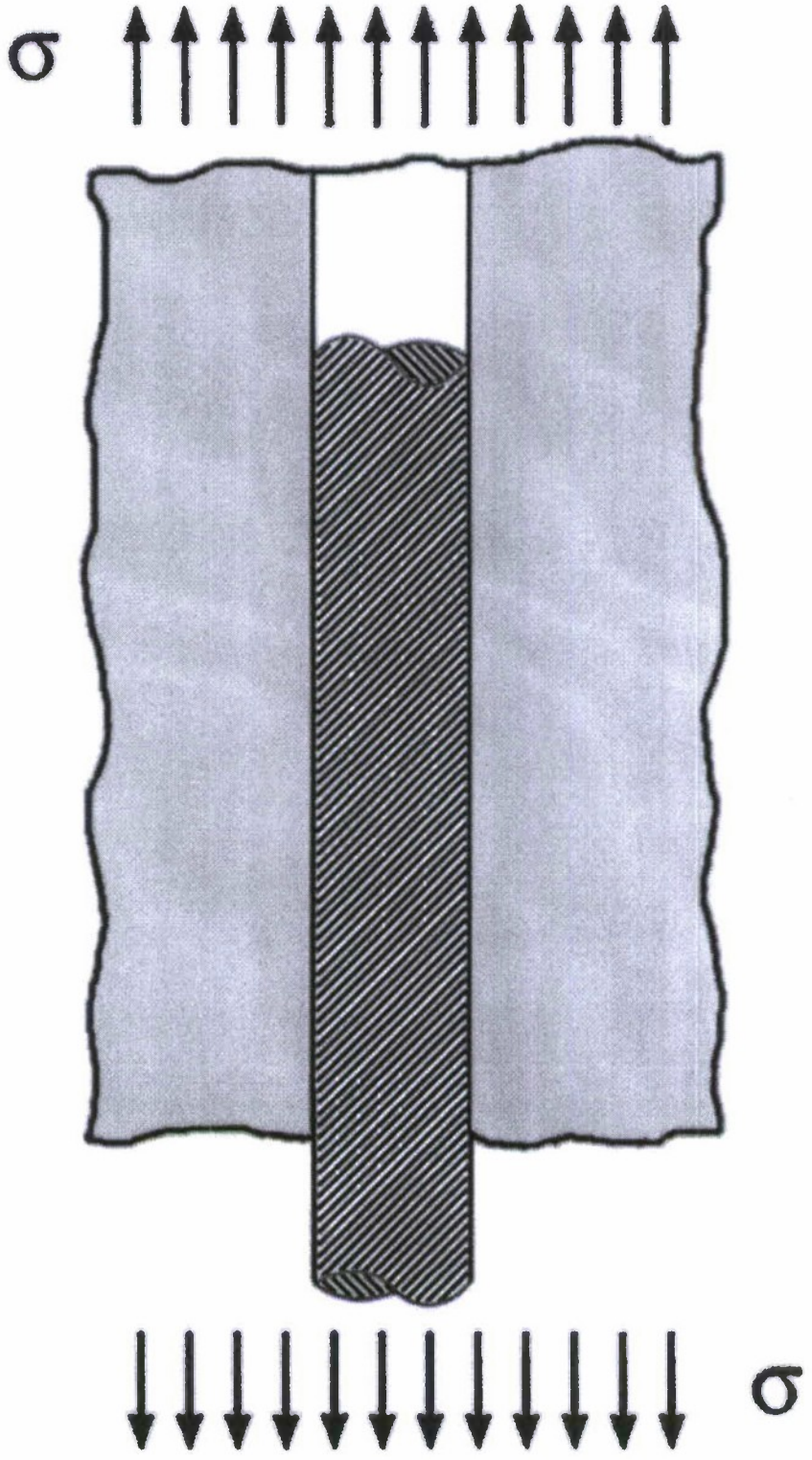

Figure 7. Illustration of interfacial debonding of a fiber from the matrix for a composite in tension.

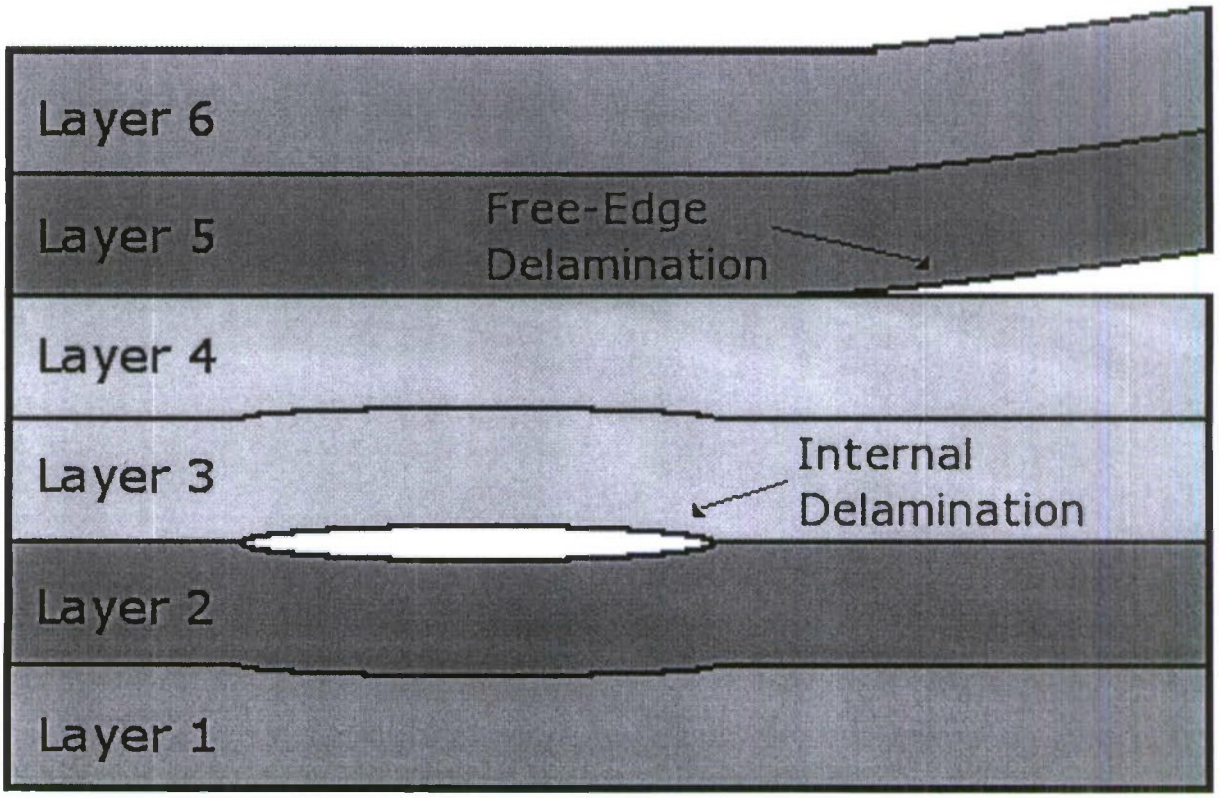

Figure 8. Illustration of a free-edge and internal delamination in a composite laminate.

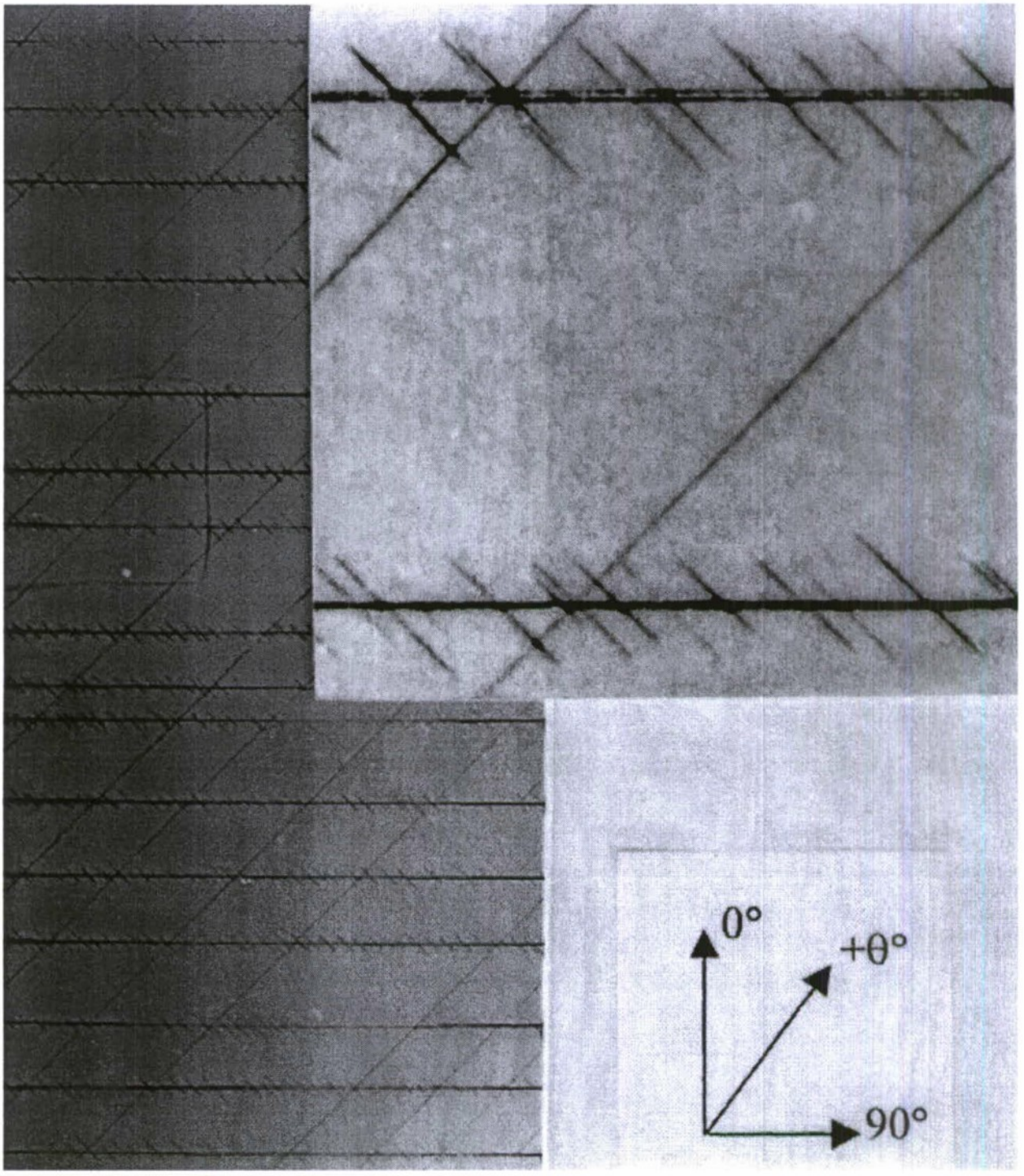

Figure 9. X-radiograph illustrating stitch cracks (along the -45° direction) formed along major matrix cracks (along the 90° direction) in a $[+45_4/-45_4/90_8]_S$ laminate [79].

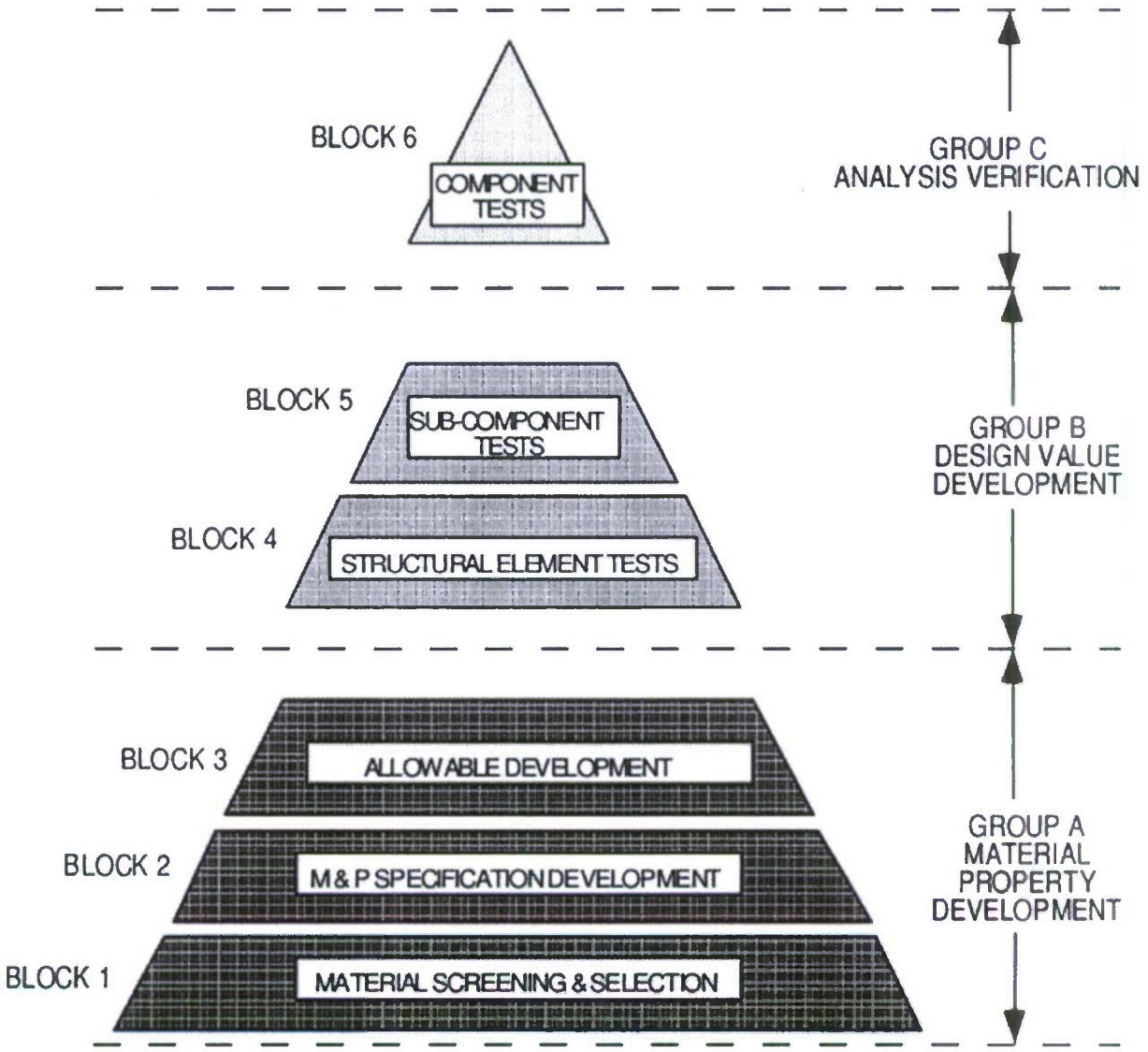

Figure 10. The levels of composite design as defined in the Building Block Approach [82].

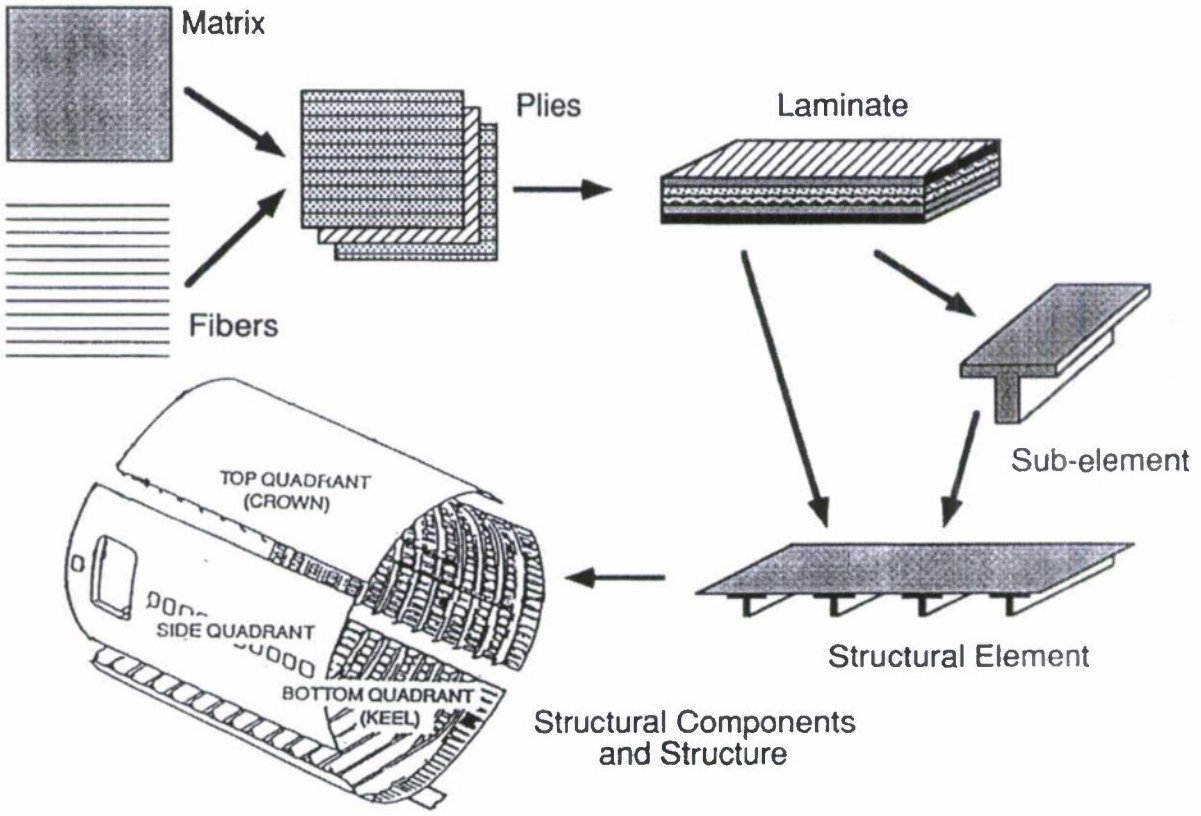

Figure 11. Examples of possible lengthscales in composite structural engineering.

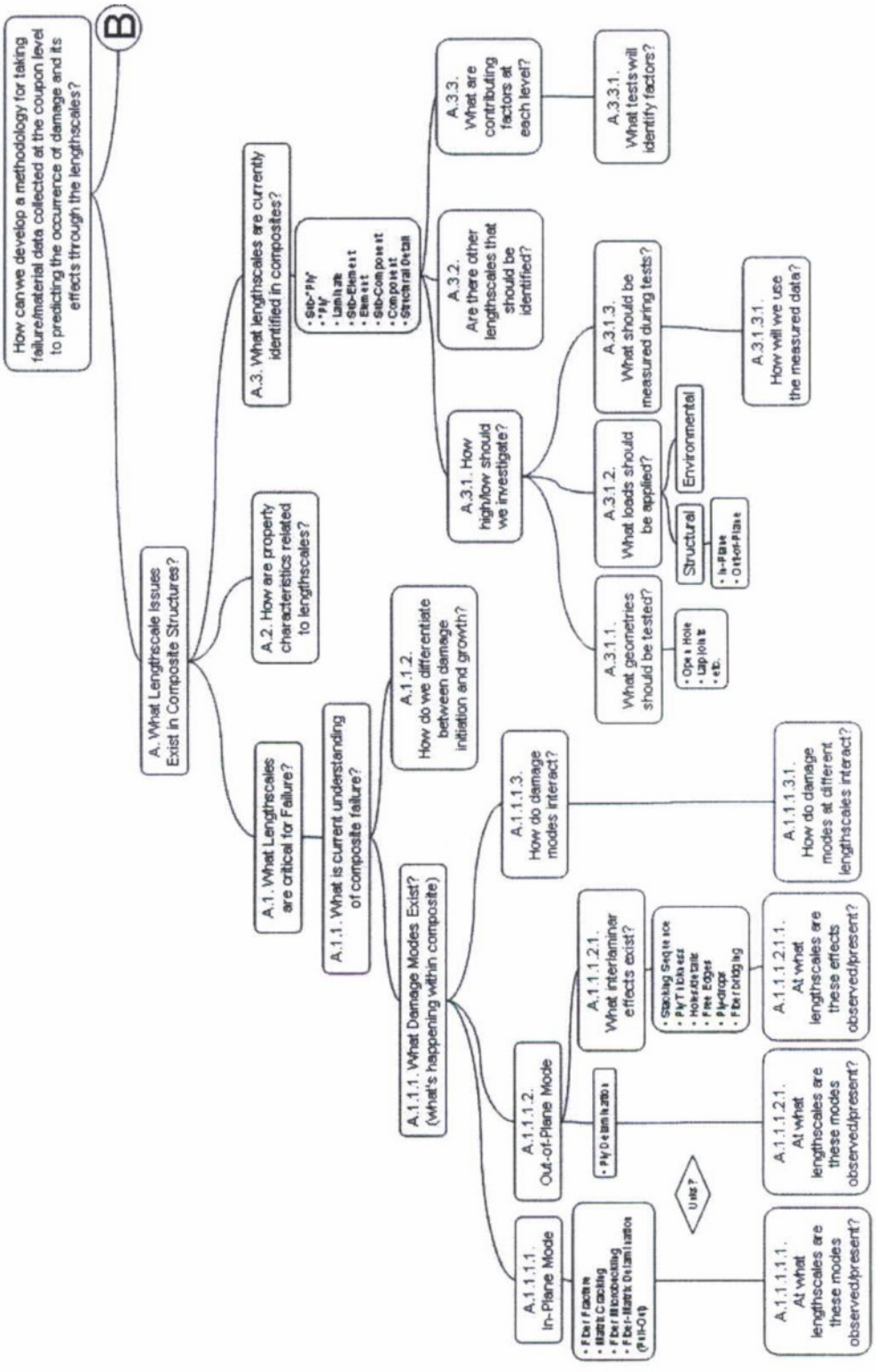

Figure 12. Branch A of Question Tree for the development of an improved methodology for determination of mechanical behavior and failure in composites.

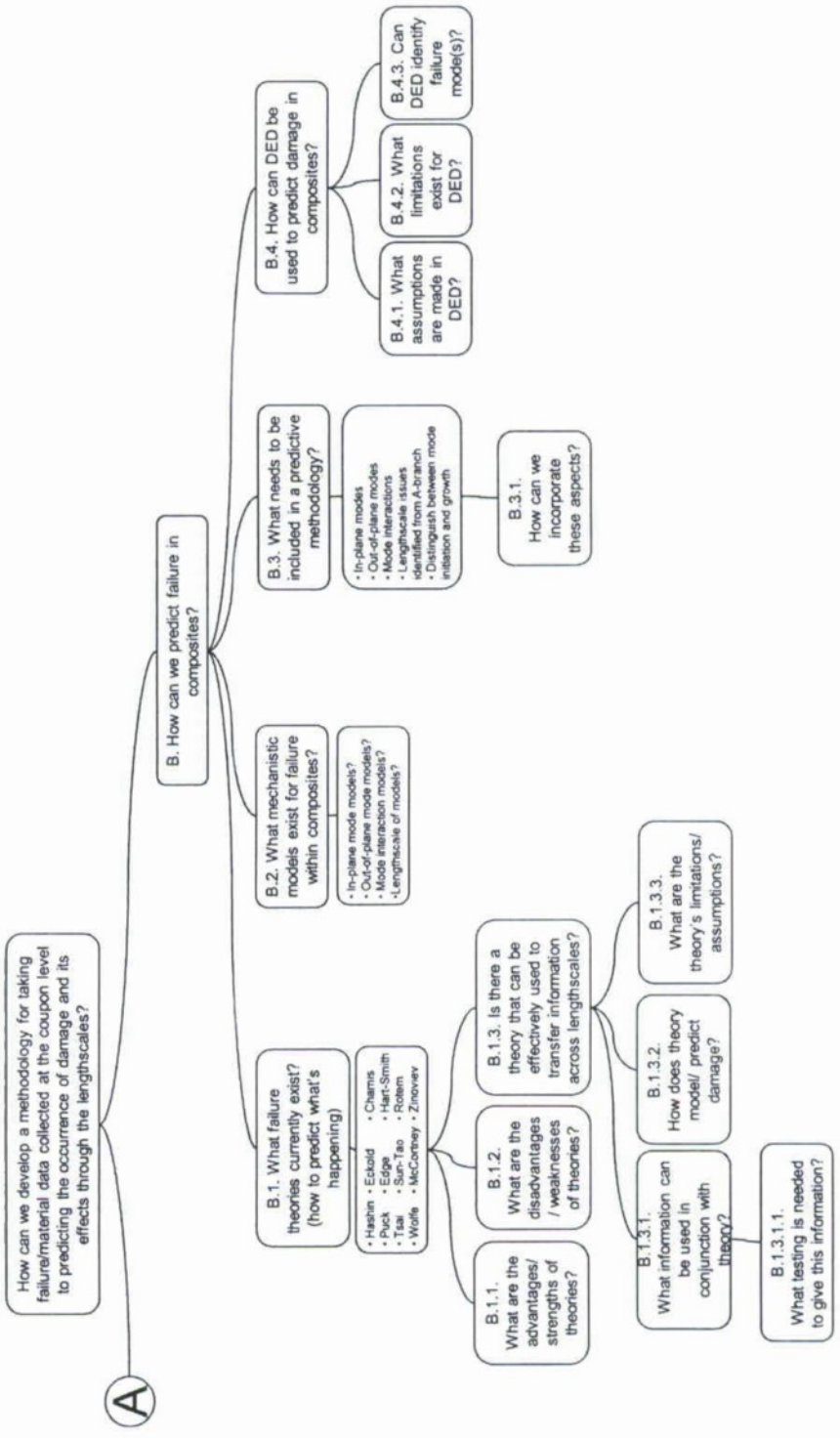

Figure 13. Branch B of Question Tree for the development of an improved methodology for determination of mechanical behavior and failure in composites.

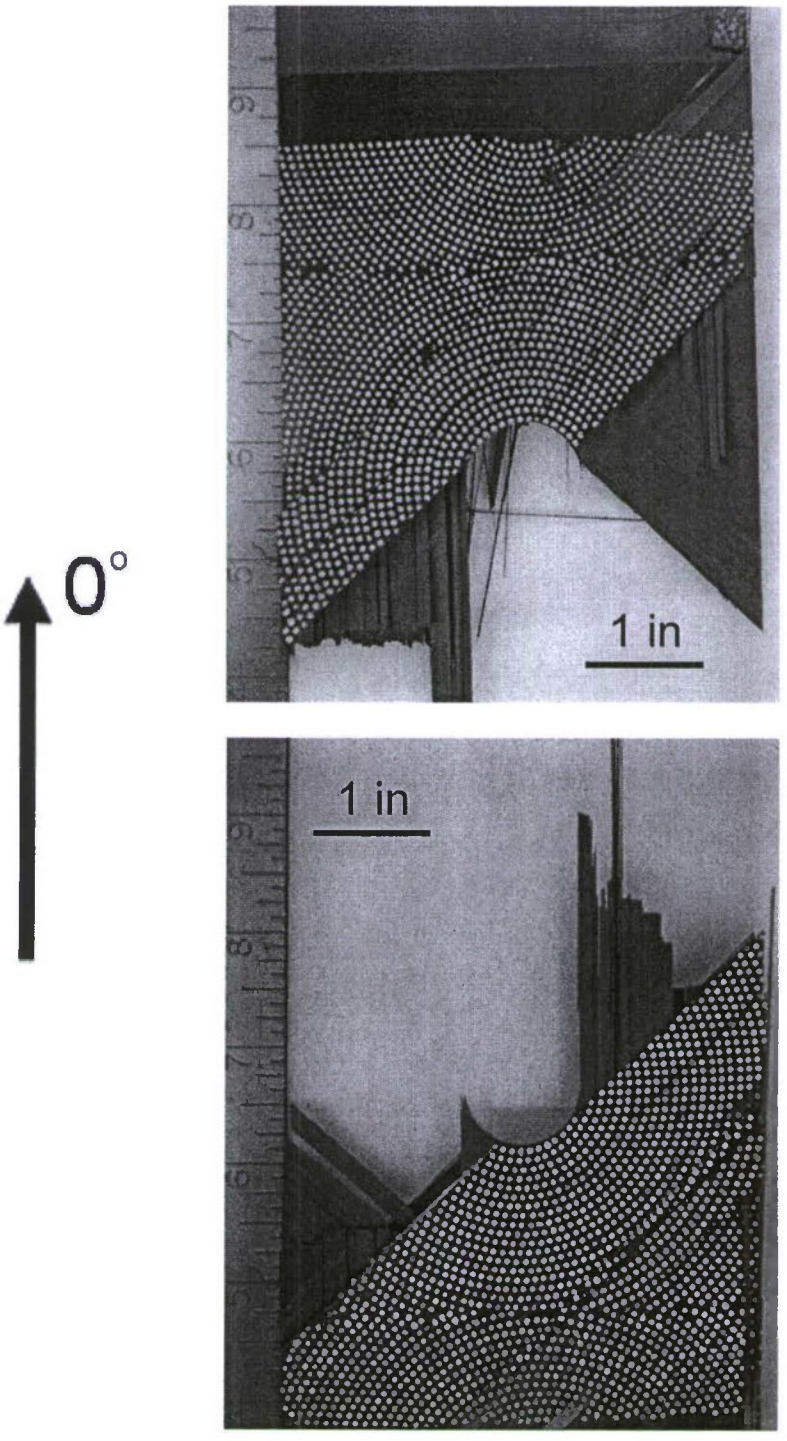

Figure 14. Photographs of the failed open-hole tension specimen OH-B104-04, with hole diameter of 1.0 inches, showing *(upper)* actual back, upper-half face, and *(lower)* actual back, lower-half face.

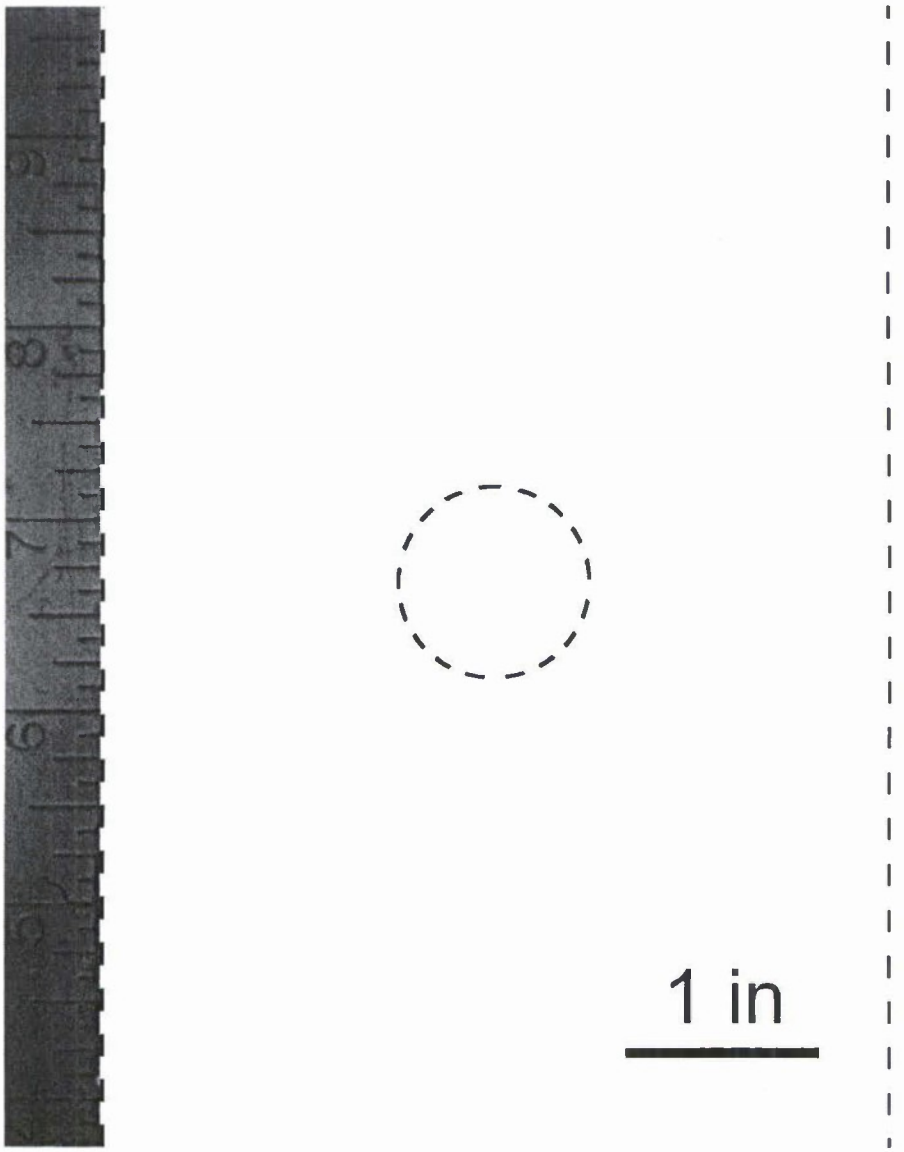

Figure 15. Illustration of "joining template" for open-hole specimen with hole diameter of 1.0 inches.

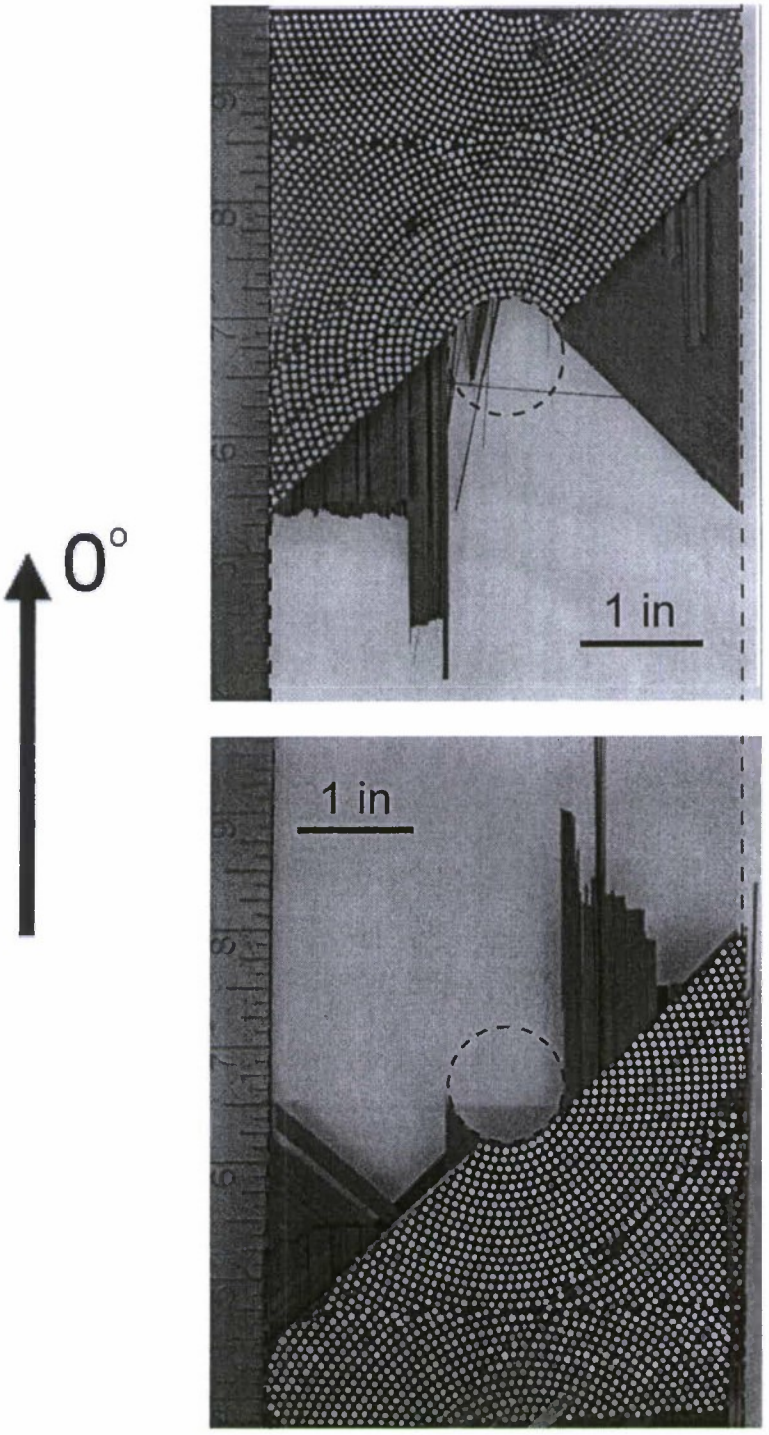

Figure 16. Photographs of the failed open-hole tension specimen OH-B104-04, with hole diameter of 1.0 inches, positioned within the "joining template" showing *(upper)* actual back, upper-half face, and *(lower)* actual back, lower-half face.

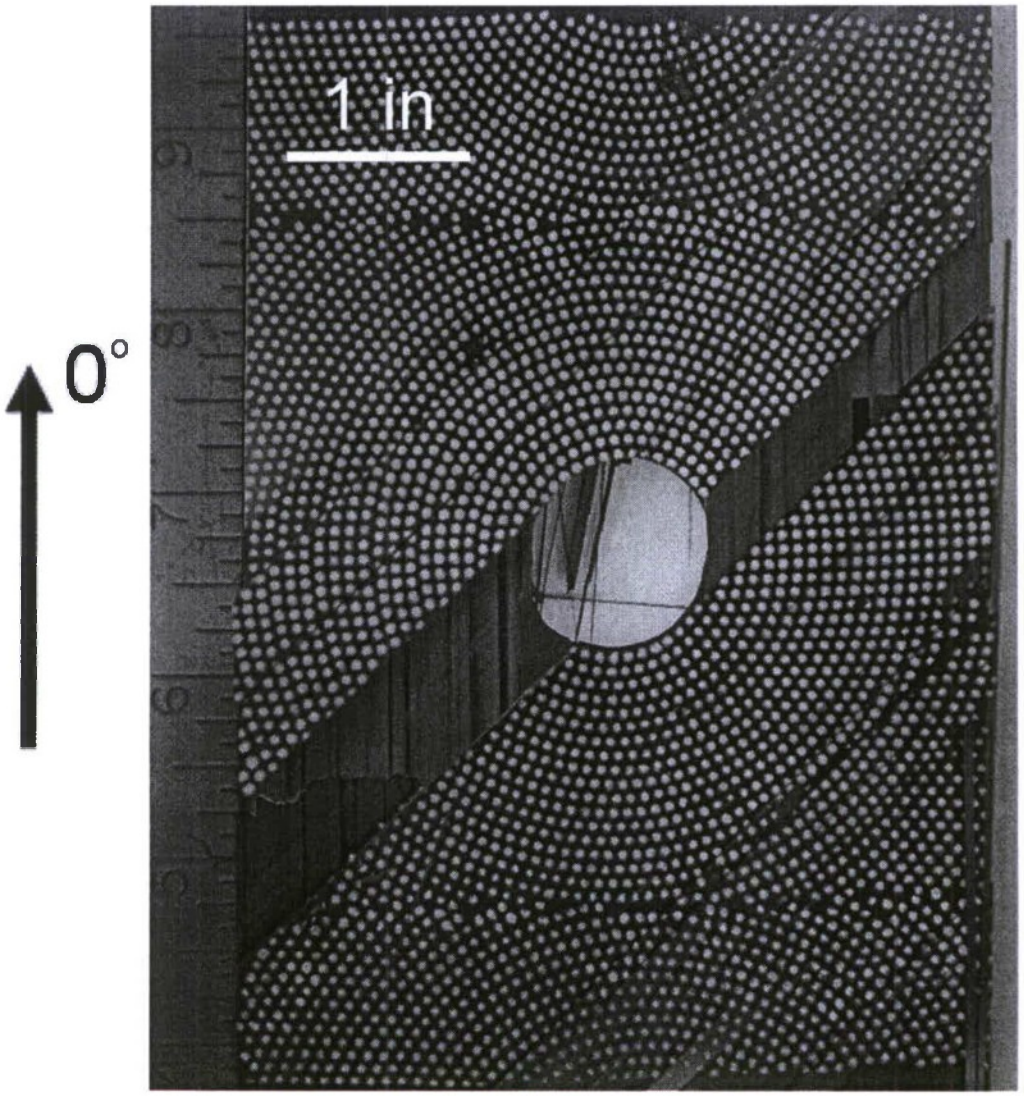

Figure 17. "Virtually joined" photograph of the failed open-hole tension specimen OH-B104-04 with hole diameter of 1.0 inches using "offset" of 0.01 inches.

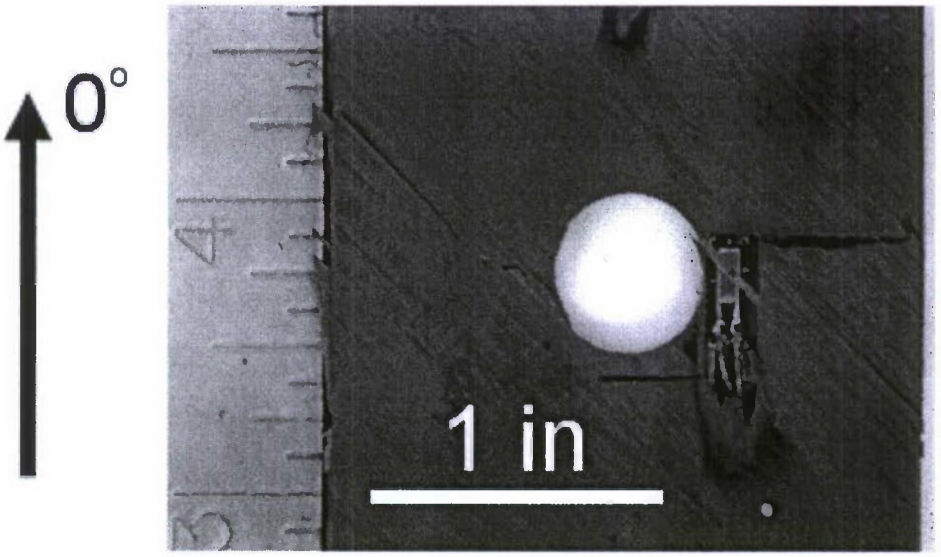

Figure 18. Photograph of the failed open-hole tension specimen OH-A051-01, with hole diameter of 0.5 inches.

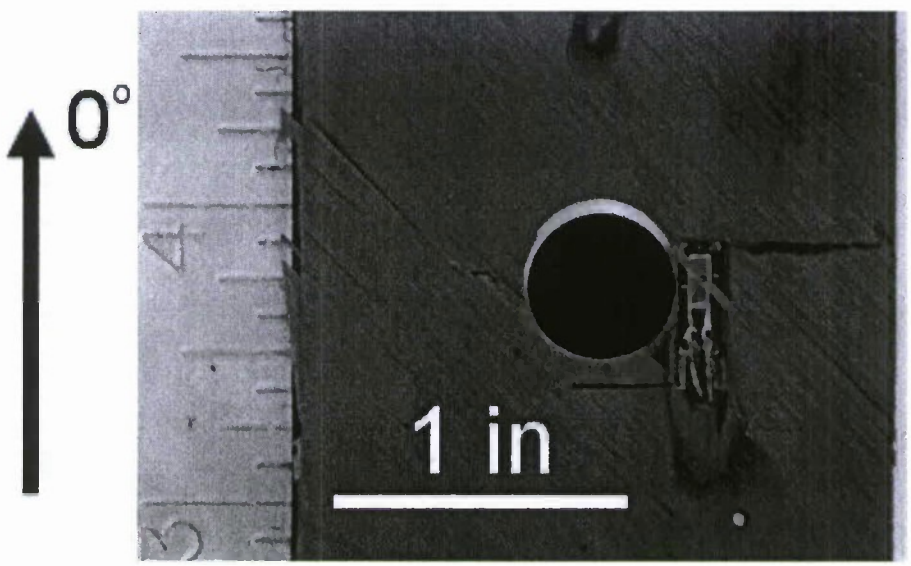

Figure 19. Photograph of the failed open-hole tension specimen OH-A051-01, with hole diameter of 0.5 inches, including superposed black circle of diameter of 0.5 inches.

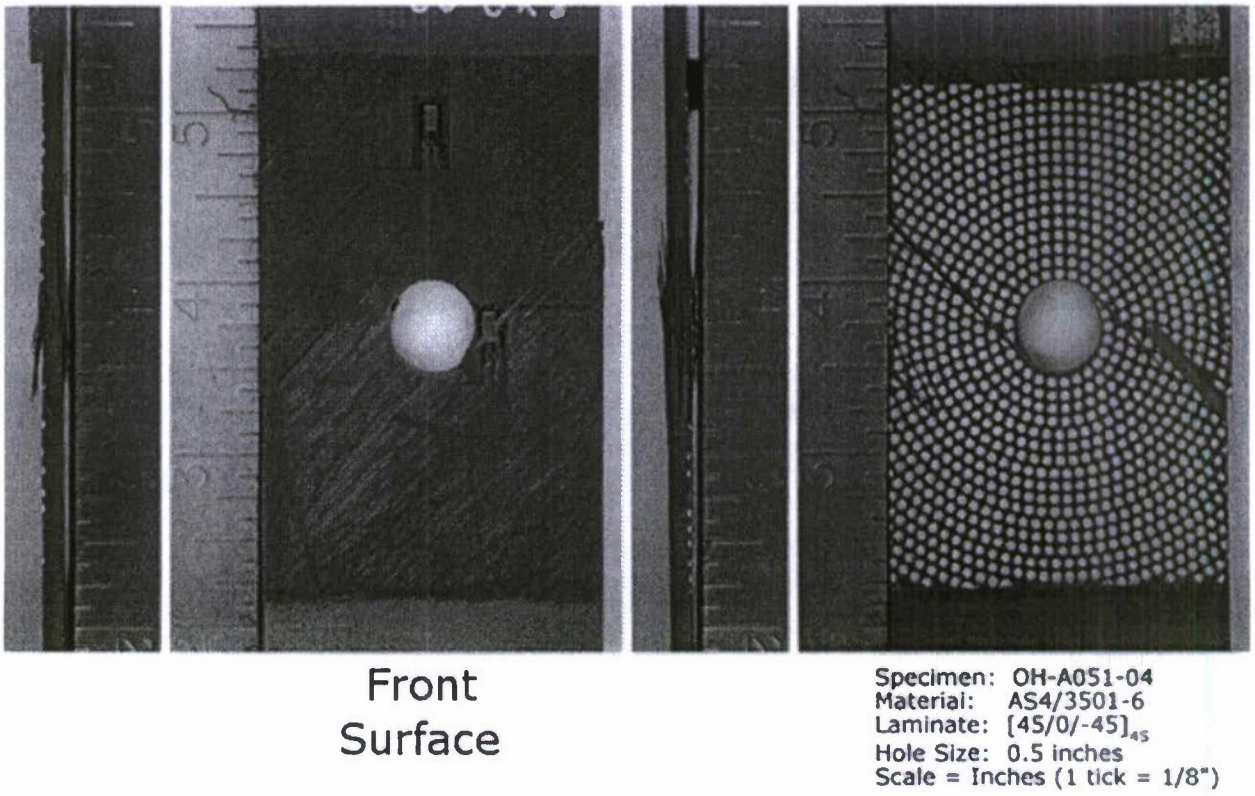

Figure 20. Photo documentation of OHT specimen OH-A051-04.

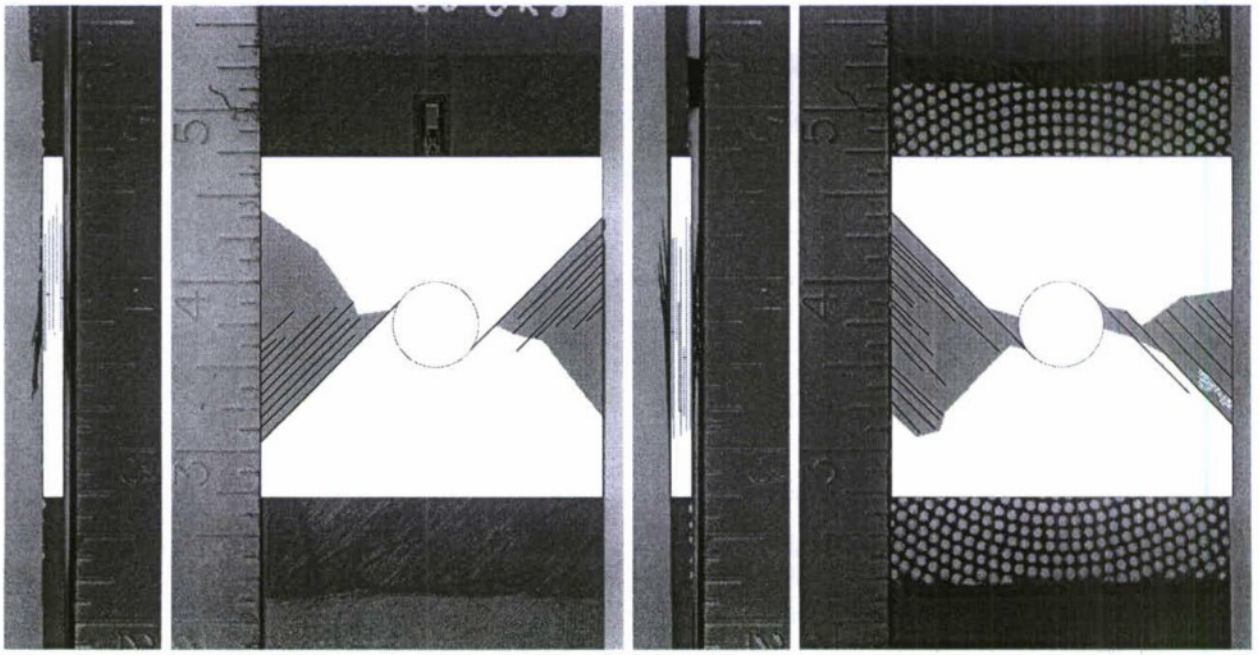

Figure 21. Damage sketch of OHT specimen shown in Figure 20 with mapping procedure applied to damage sketch, resulting in specimen being "closed".

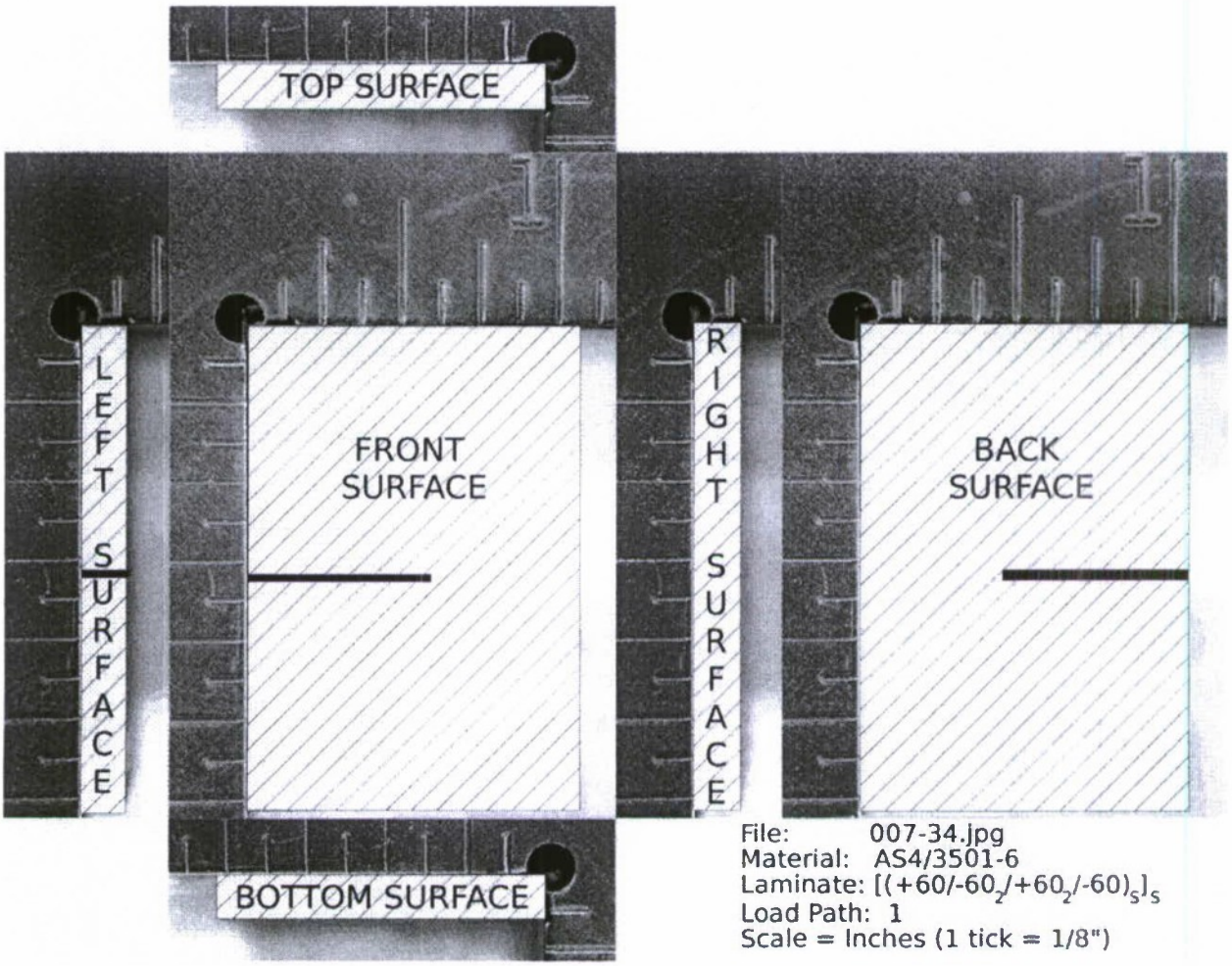

Figure 22. Photo documentation layout for the previously tested NRL IPL specimens.

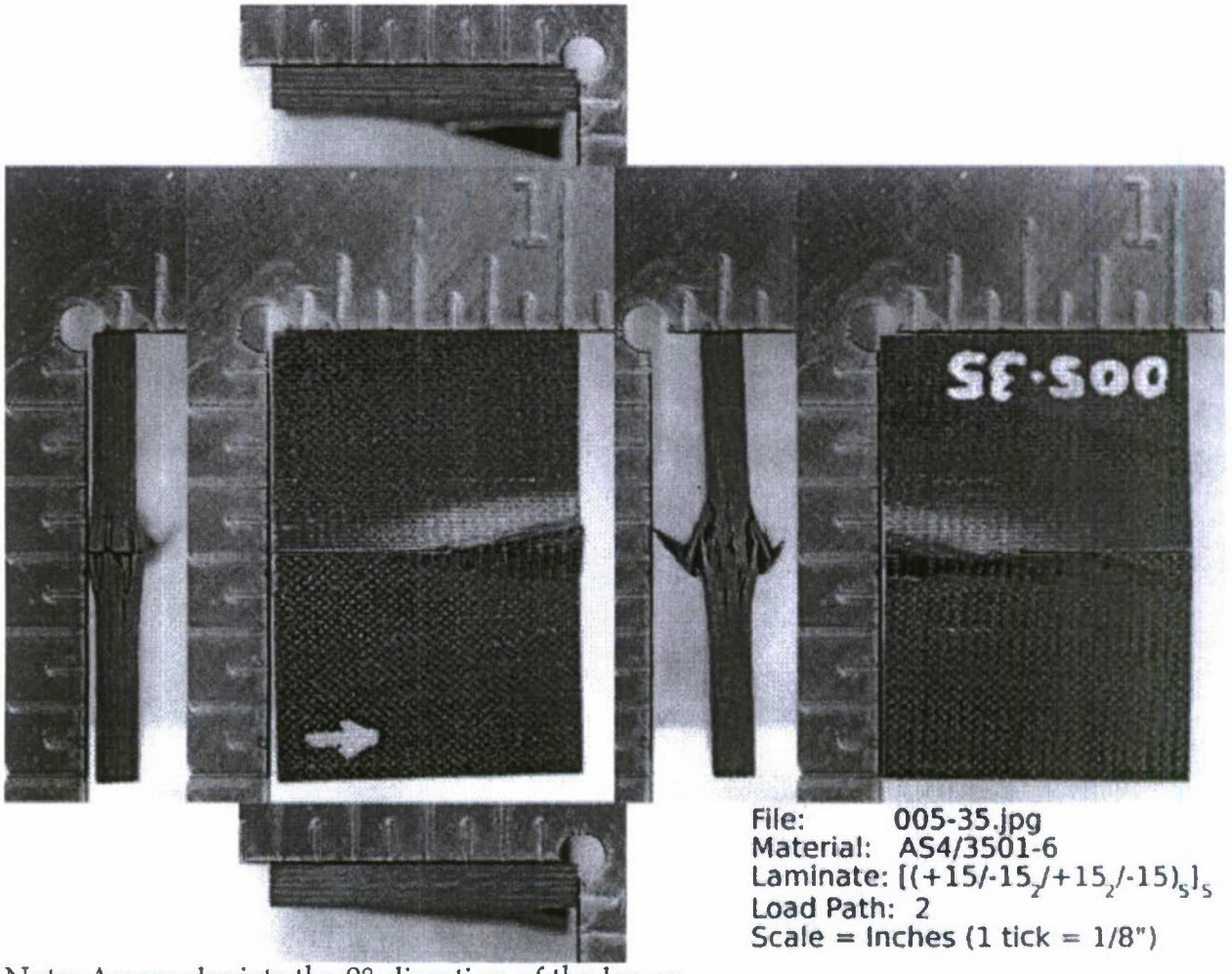

Note: Arrow depicts the 0°-direction of the layup.

Figure 23. Photo documentation of previously tested NRL IPL specimen 005-35 indicating typical layout for each of the 210 IPL specimens received from the NRL.

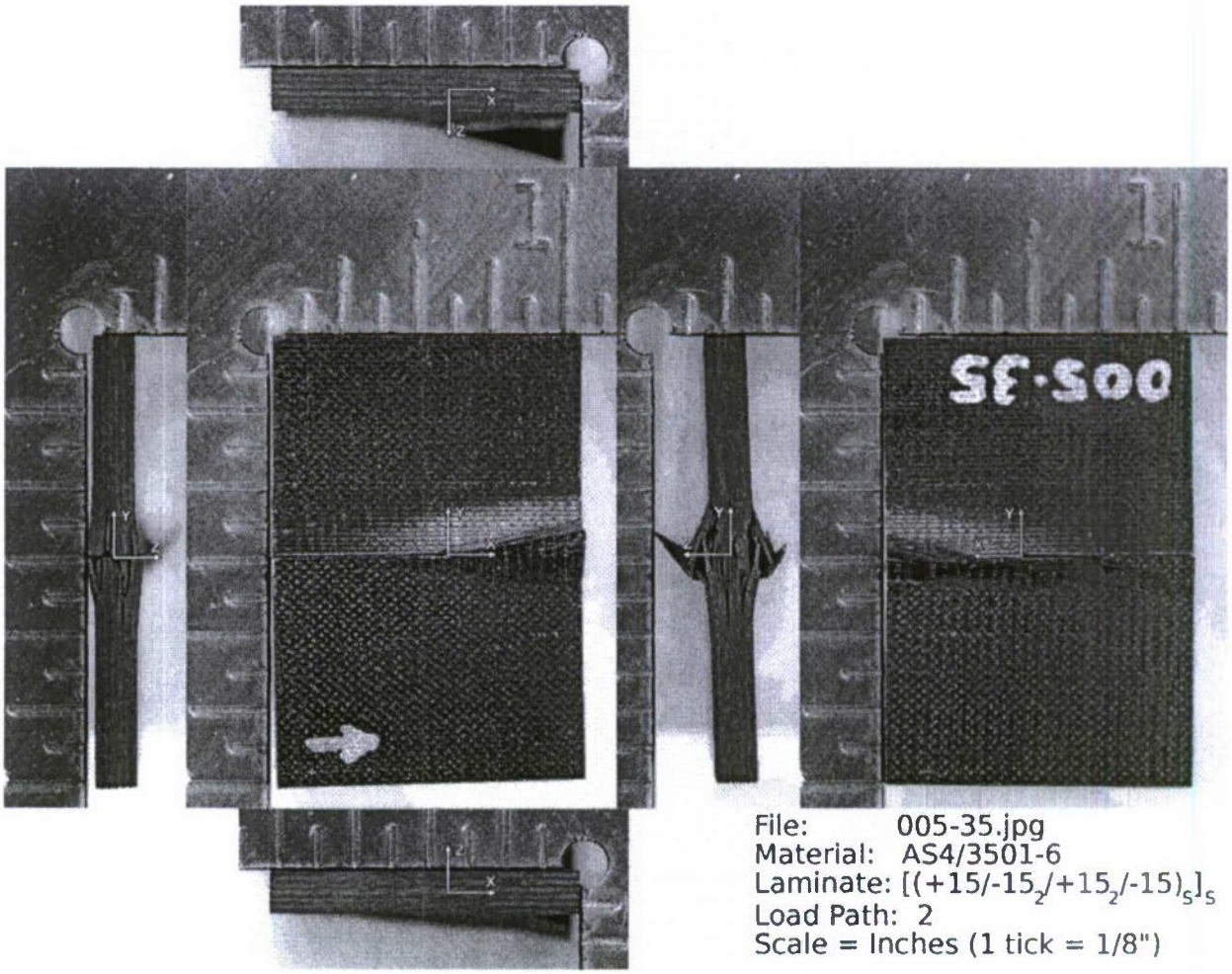

Figure 24. Photo documentation of previously tested NRL IPL specimen 005-35 with coordinate layer visible.

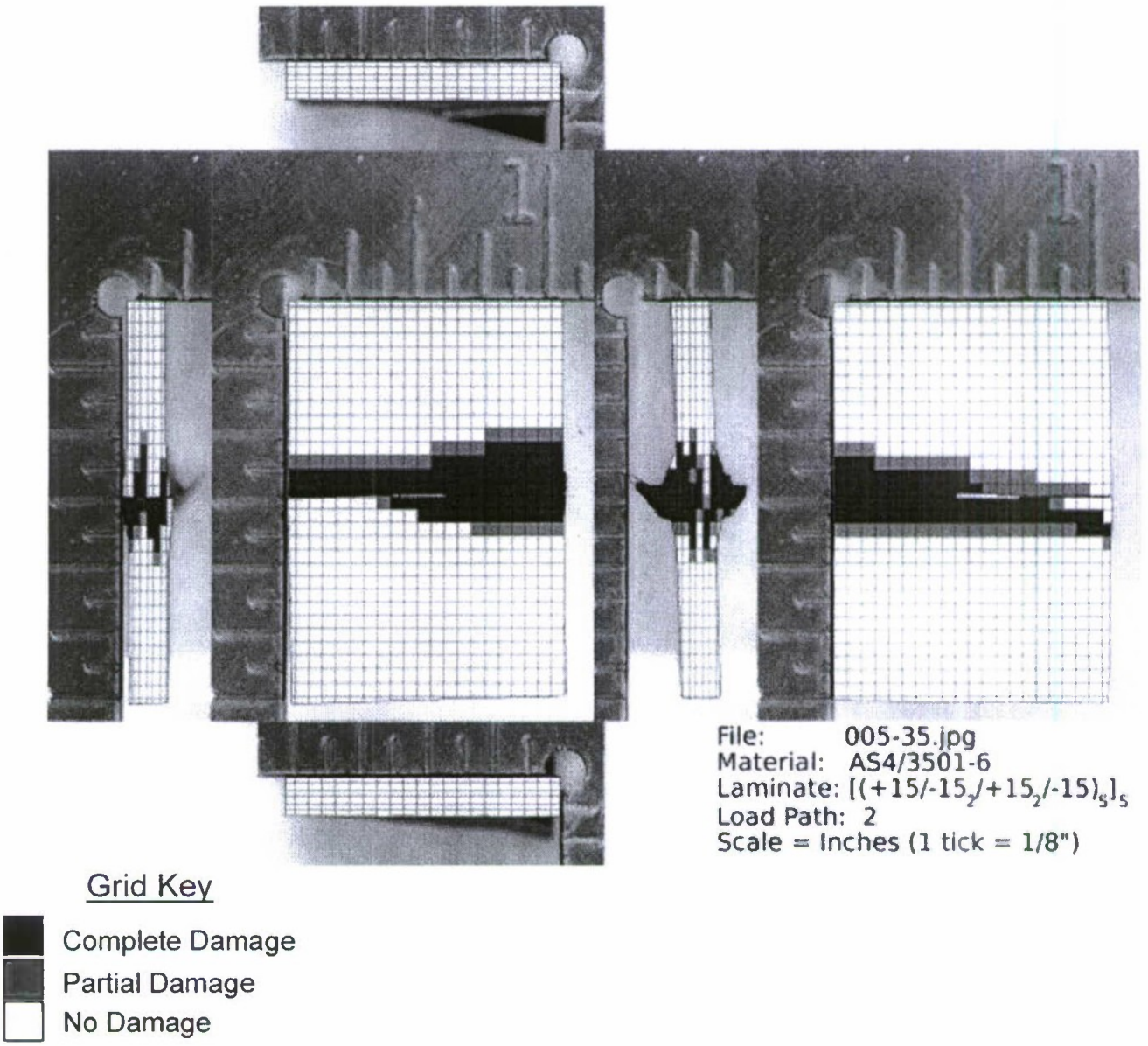

Figure 25. Damage grid of previously tested NRL IPL specimen 005-35 indicating typical visualization of the extent of damage in the specimens.

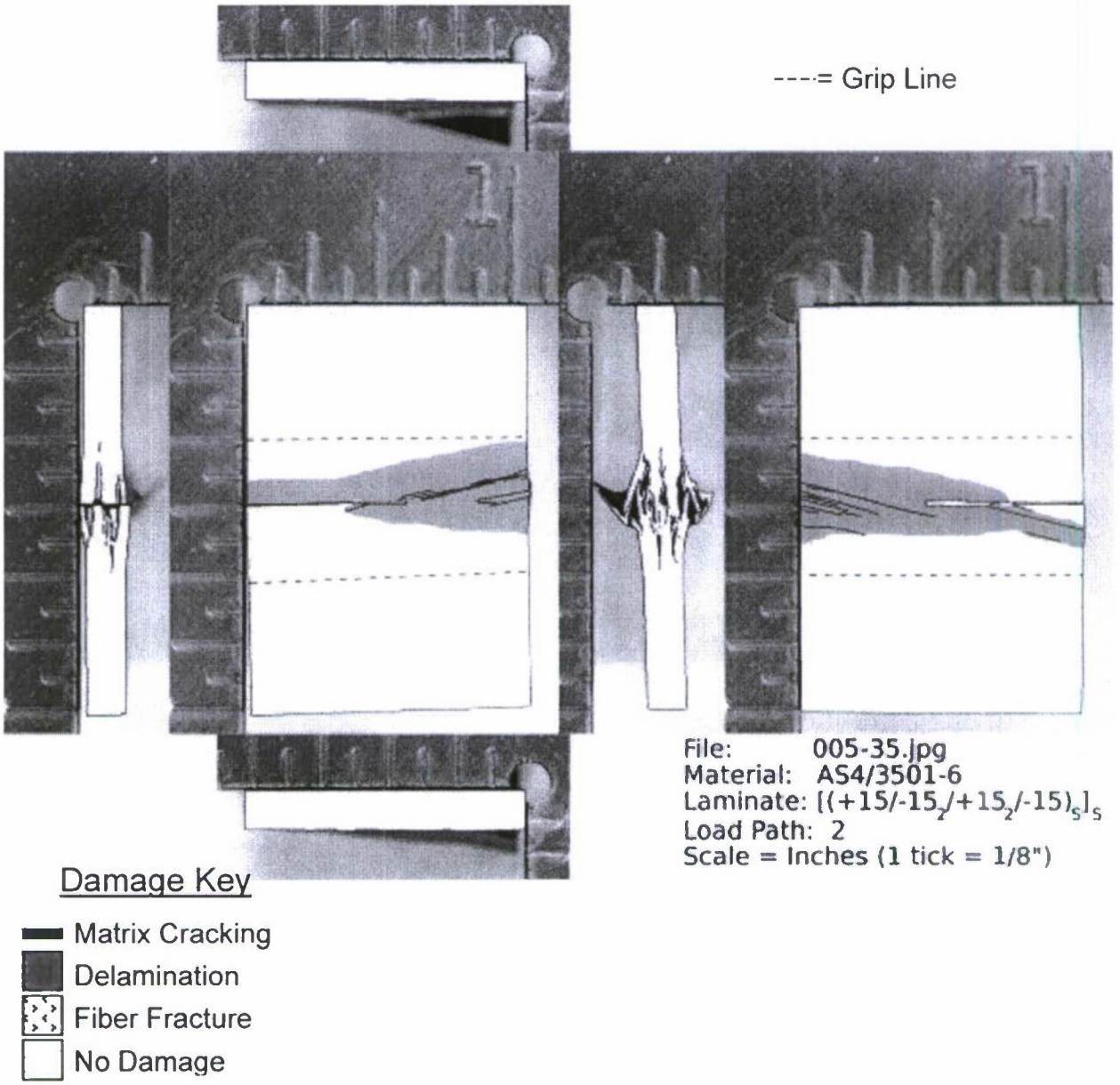

Figure 26. Damage sketch of previously tested NRL IPL specimen 005-35 indicating typical damage in the specimens.

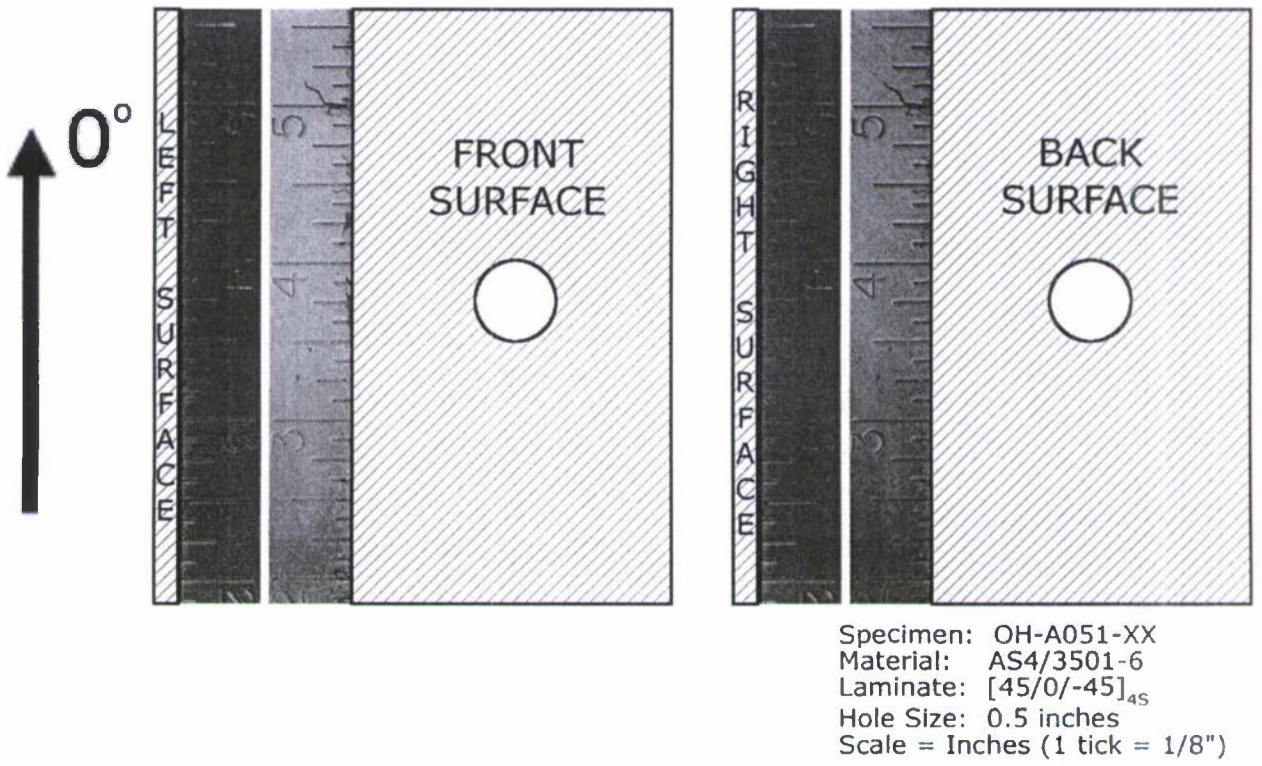

Figure 27. Overall photo documentation layout for the open-hole tension specimens.

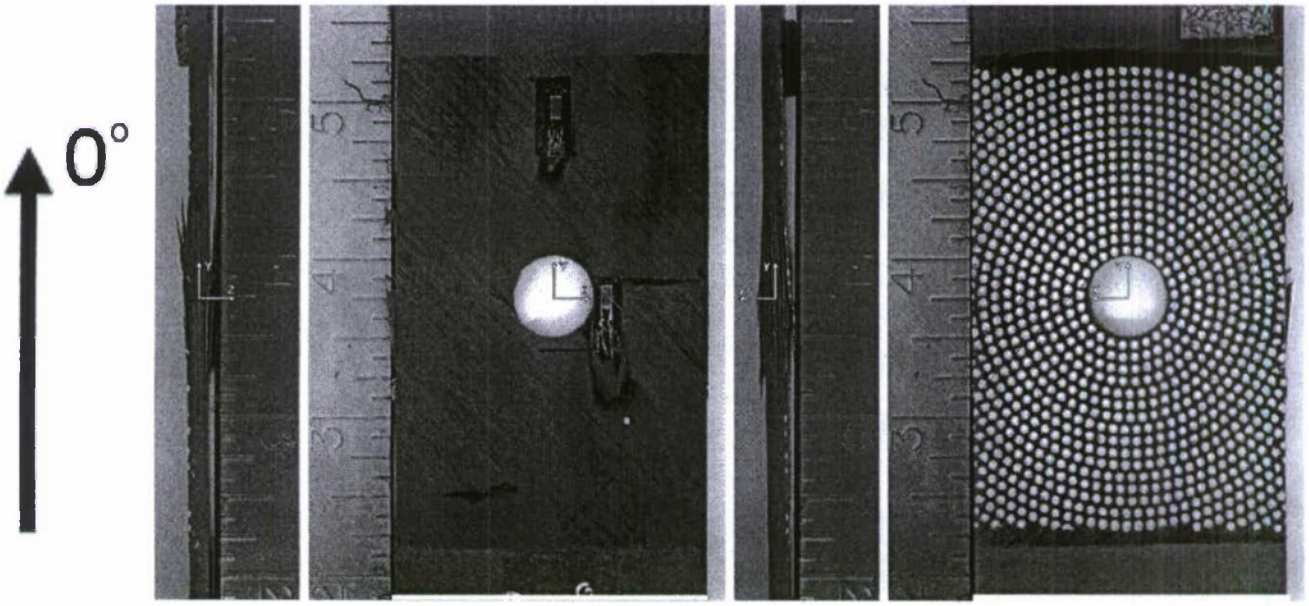

Figure 28. Optical documentation photographs of the failed open-hole tension specimen OH-A051-01, with hole diameter of 0.5 inches.

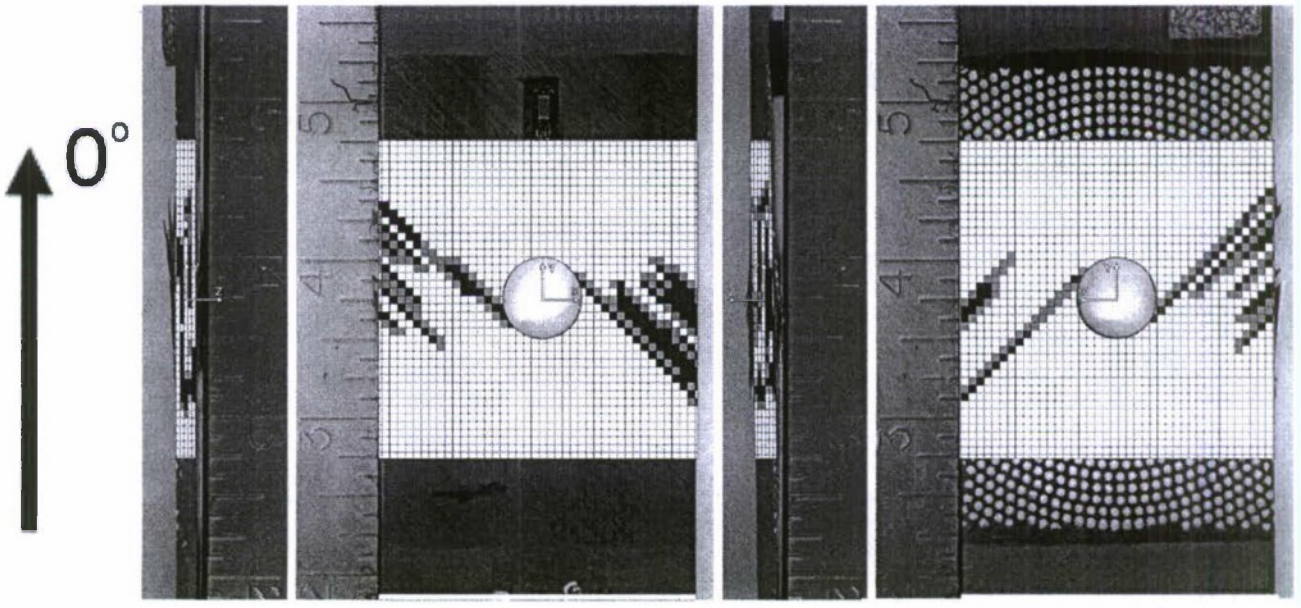

Specimen: OH-A051-01
Material: AS4/3501-6
Laminate: $[45/0/-45]_{4S}$
Hole Size: 0.5 inches
Scale = Inches (1 tick = 1/8")

Grid Key
Complete Damage
Partial Damage
No Damage

Figure 29. Damage grid of the failed open-hole tension specimen OH-A051-01, with hole diameter of 0.5 inches.

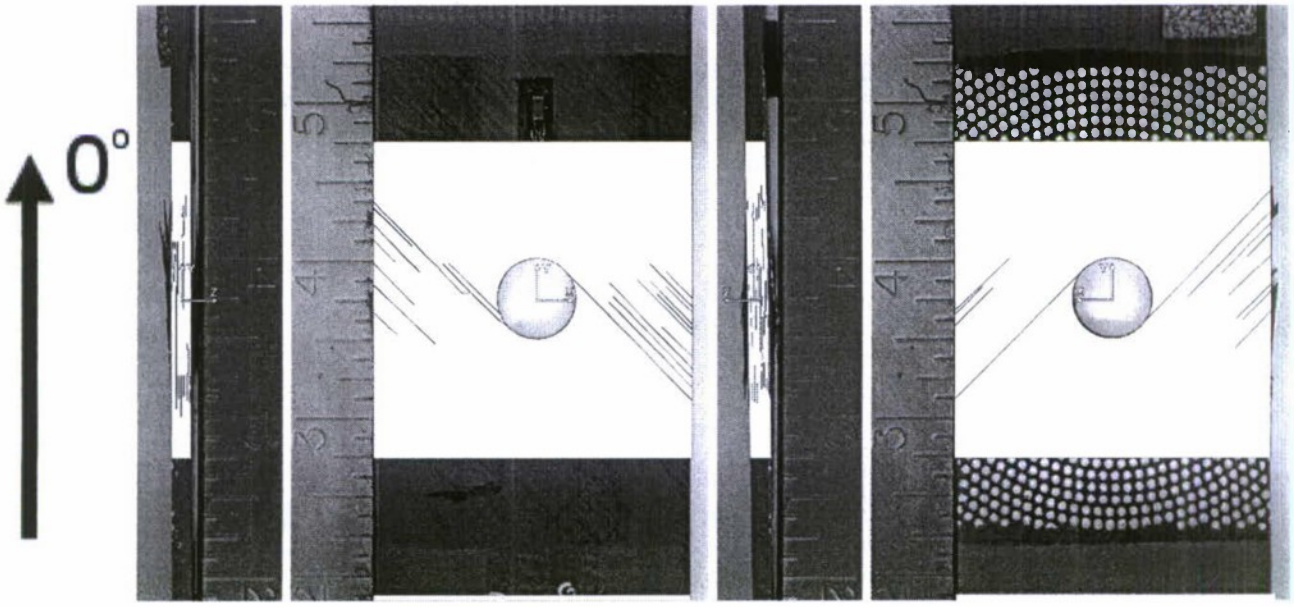

Figure 30. Damage sketch of the failed open-hole tension specimen OH-A051-01, with hole diameter of 0.5 inches.

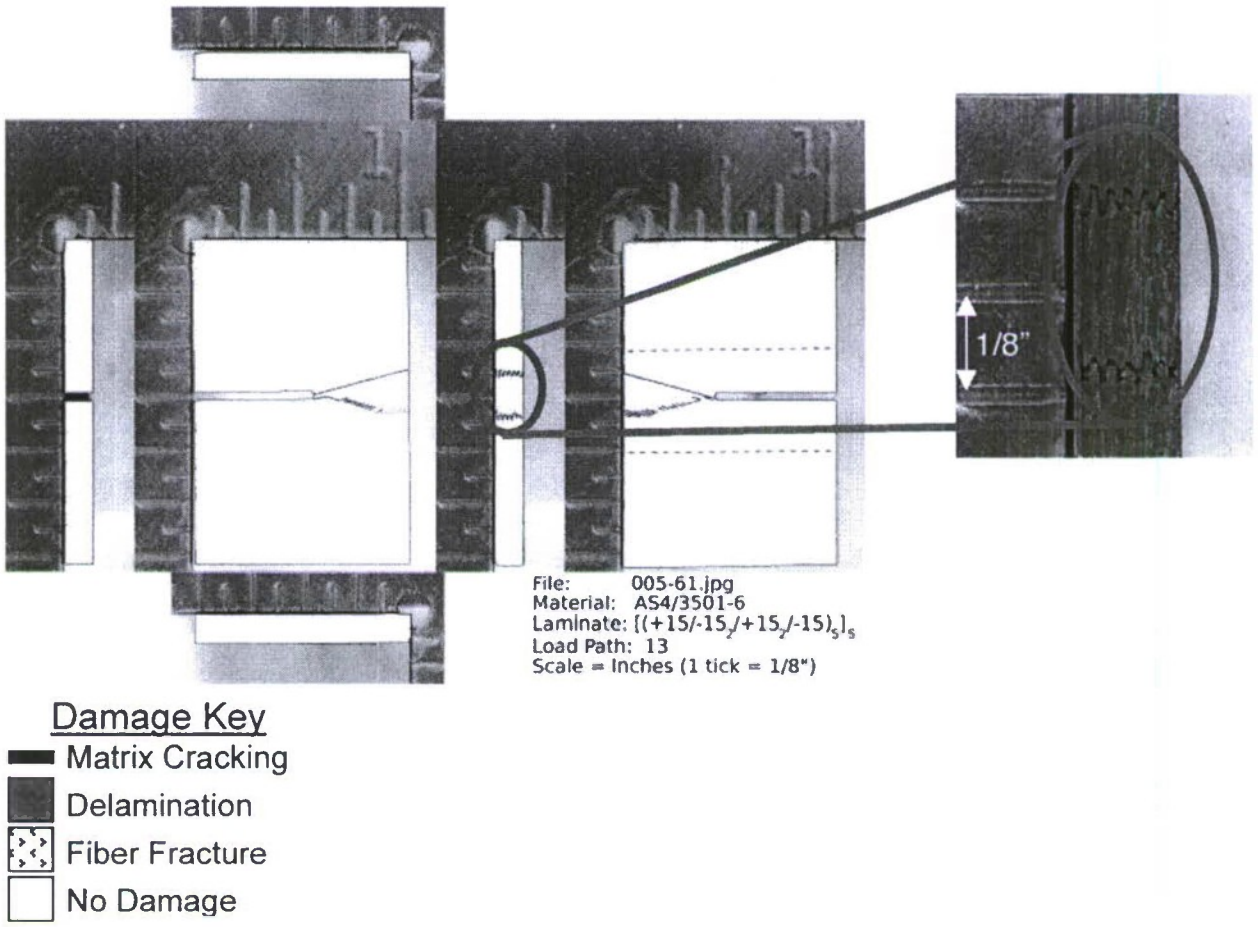

Figure 31. For the NRL IPL specimen 005-61 exhibiting the 'zig-zag' damage mode, *(left)* the overall damage sketch, with *(right)* the enlarged photograph of the 'right face'.

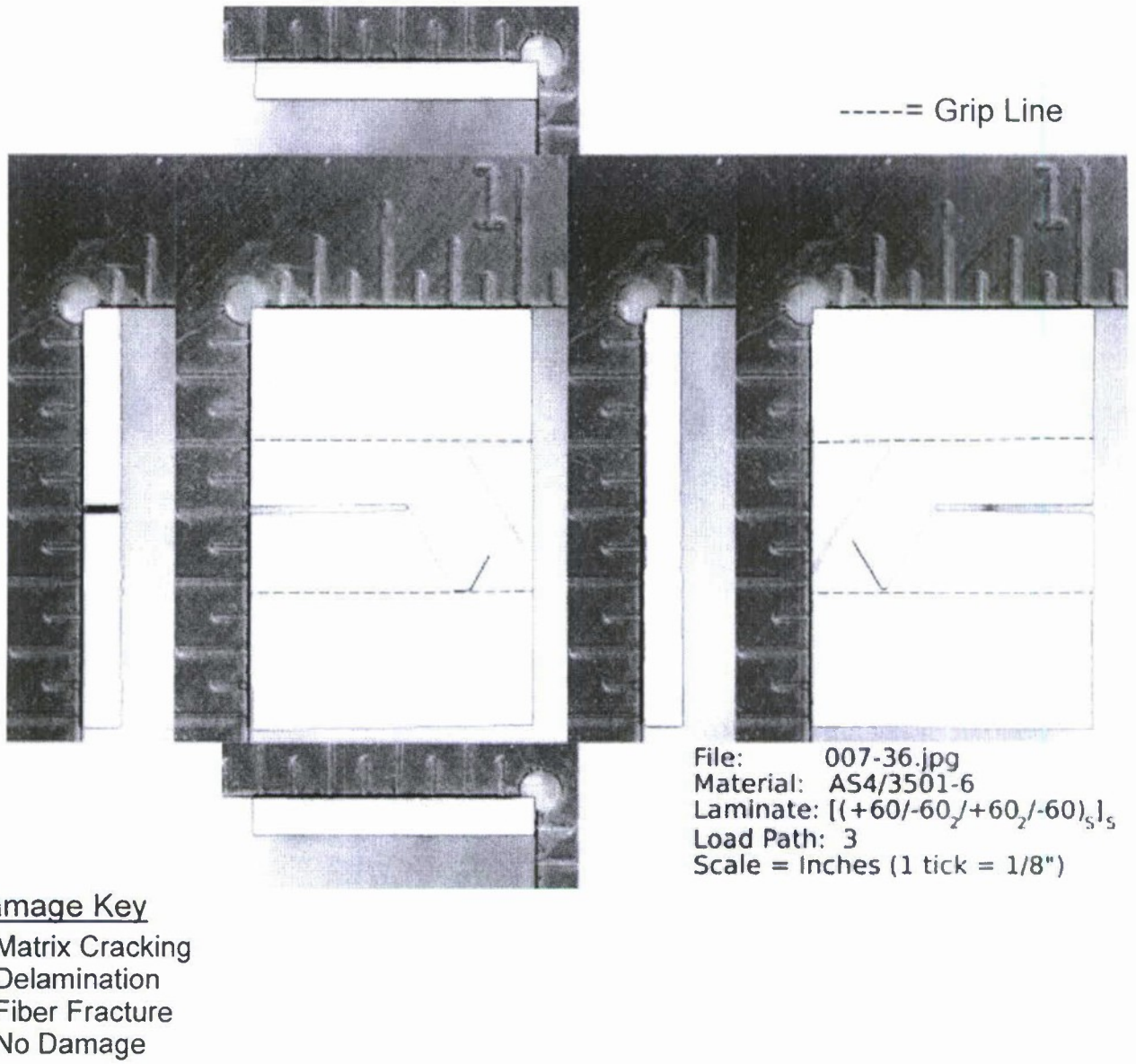

Figure 32. Damage sketch of NRL IPL specimen 007-36 indicating a boundary (lengthscale) effect present in some specimens.

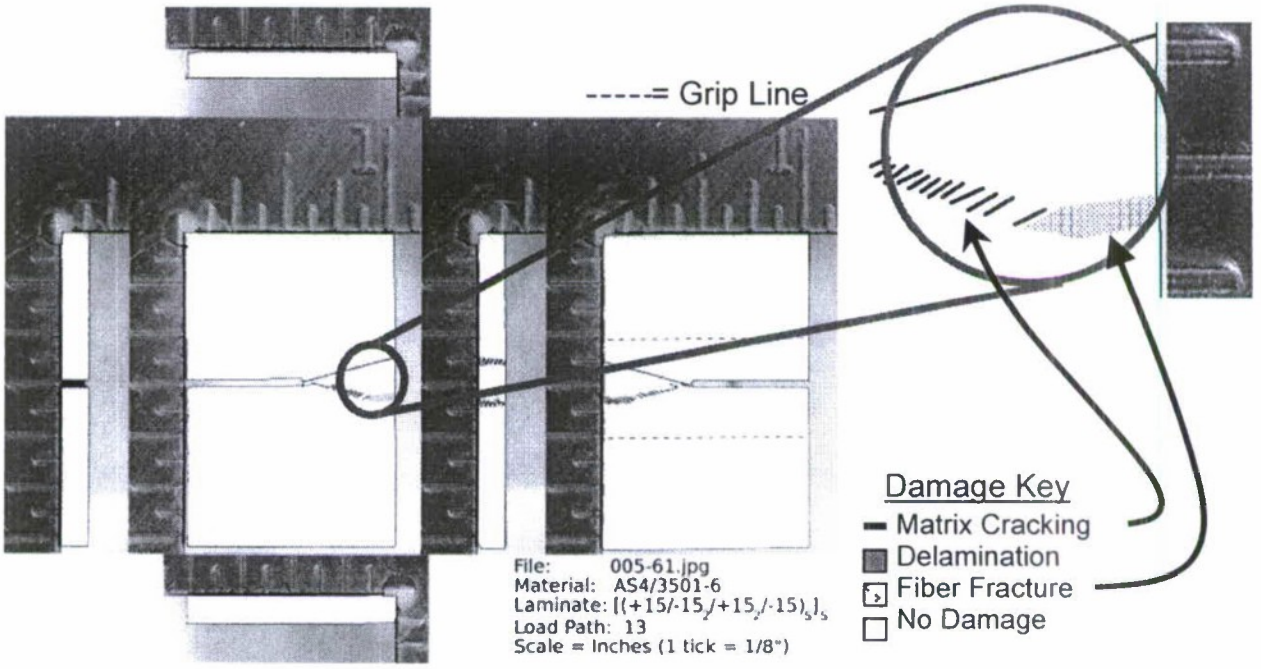

Figure 33. For the NRL IPL specimen 005-61 indicating a damage mode change along the damage progression path, *(left)* the overall damage sketch, with *(right)* the enlarged image of the particular damage.

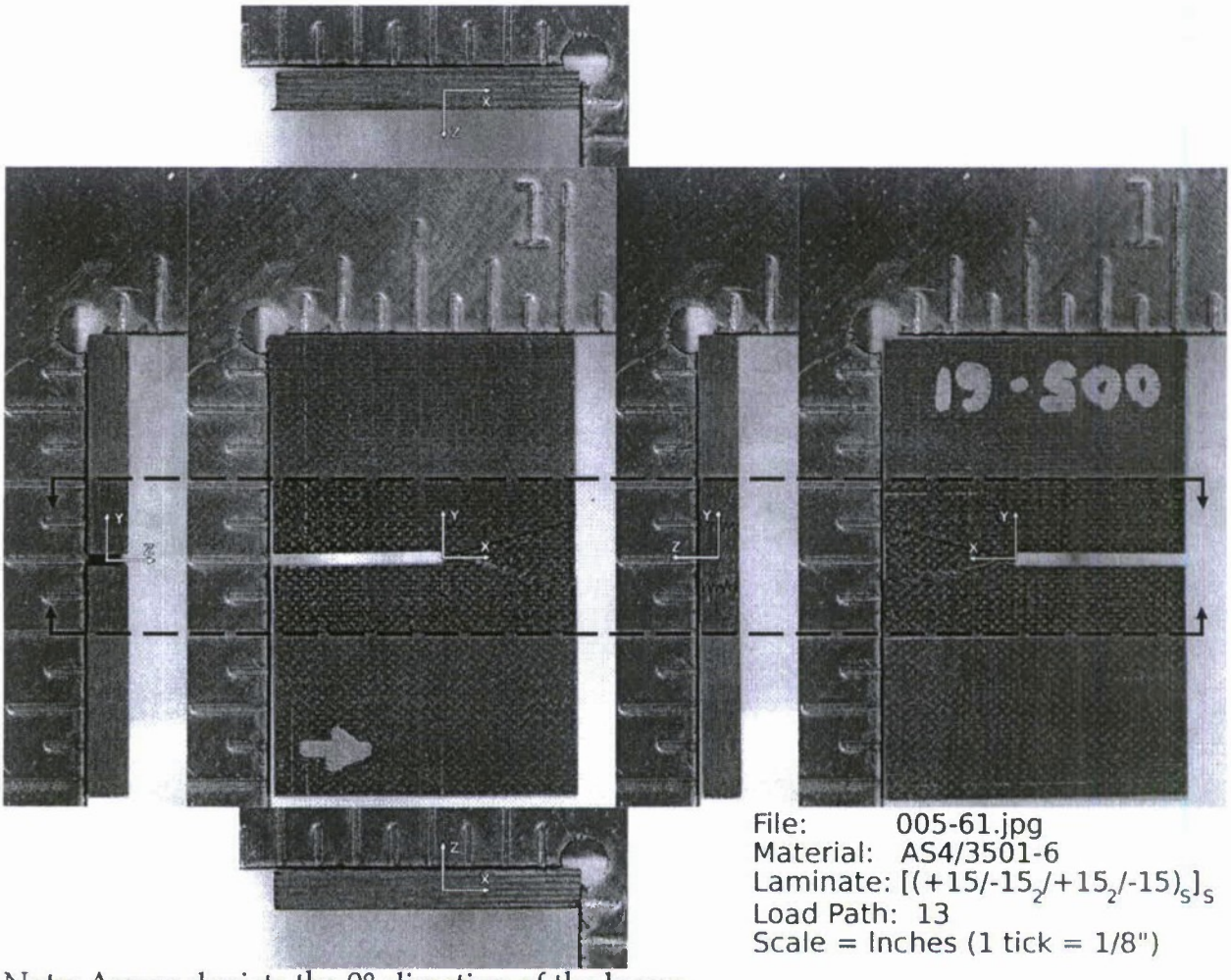

Note: Arrow depicts the 0°-direction of the layup.

Figure 34. Optical documentation photographs of a previously tested NRL IPL composite specimen made of AS4/3501-6 graphite/epoxy with a stacking sequence of $[(+15/-15_2/+15_2/-15)_S]_S$.

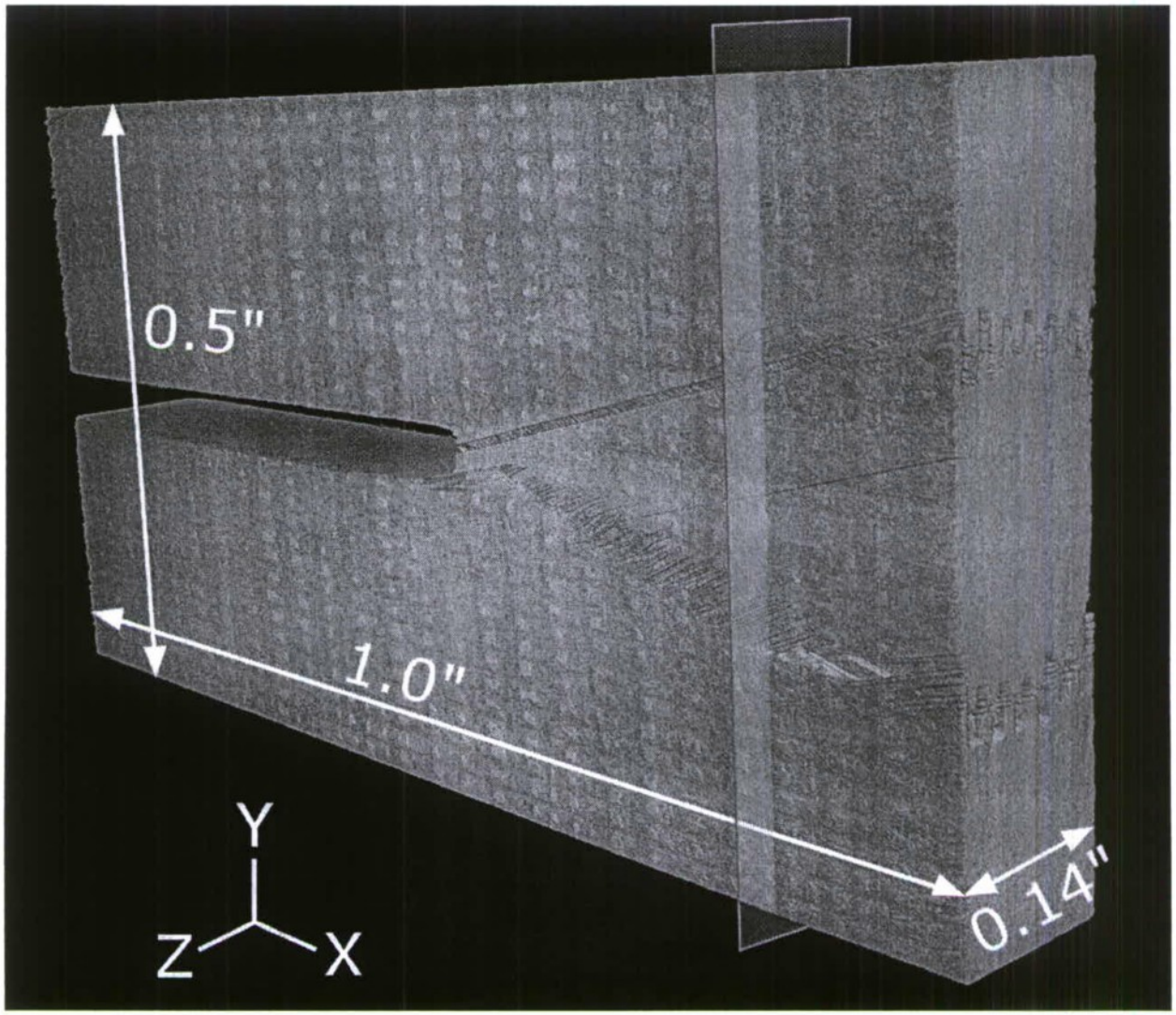

Figure 35. Virtual 3-D volume of the previously tested NRL IPL composite specimen, shown in Figure 34, with the material in the region between the dashed lines of Figure 34 virtually recreated by computer microtomography (CμT).

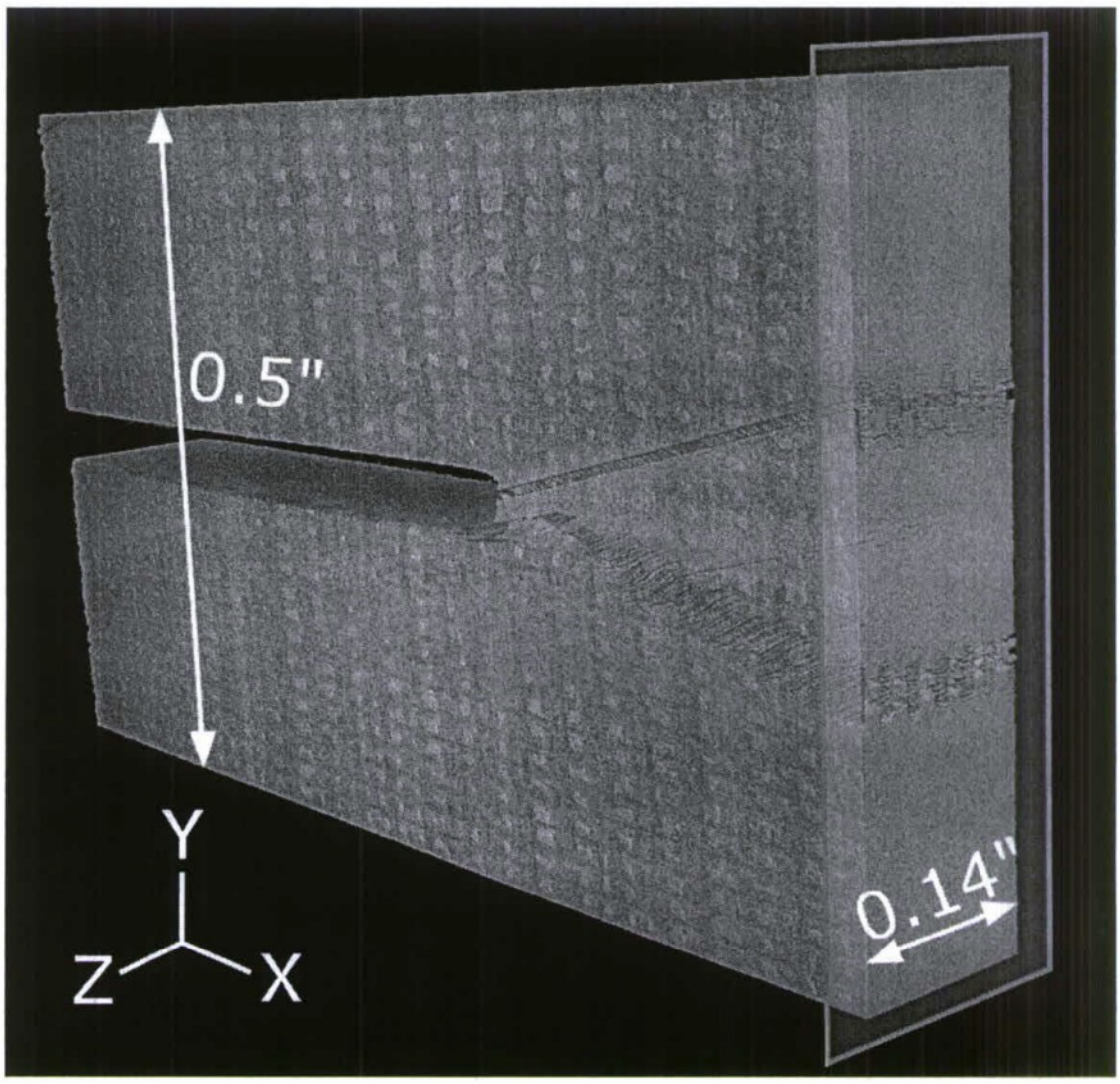

Figure 36. "Virtual cut" of the previously tested NRL IPL composite specimen, shown in Figure 34, with the end piece outlined by the shaded plane corresponding to the shaded plane intersecting the virtual 3-D volume of Figure 35.

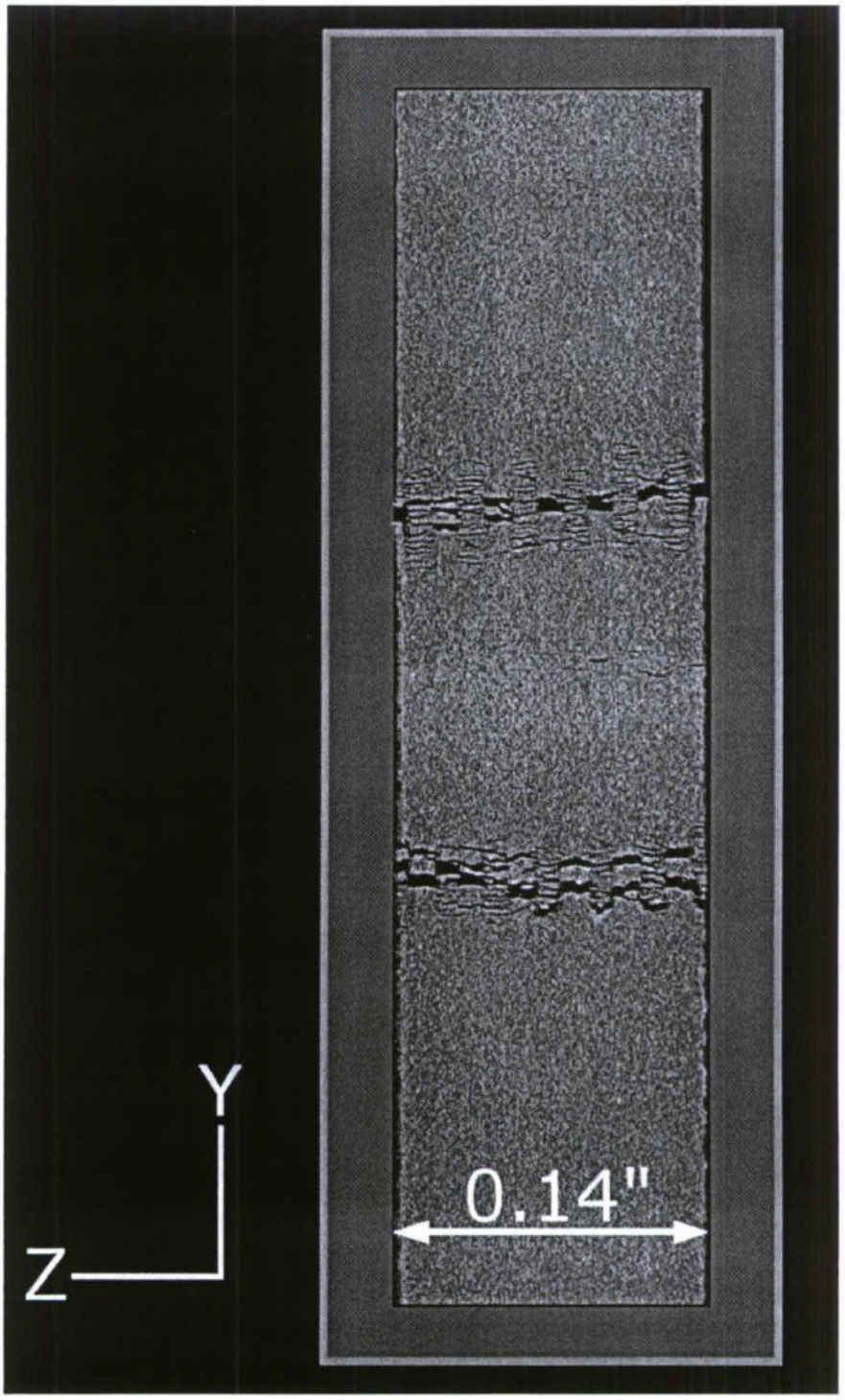

Figure 37. Planar presentation of the "virtual cut" of the previously tested NRL IPL composite specimen, shown in Figure 34, with the plane corresponding to the shaded plane intersecting the virtual 3-D volume of Figure 35.

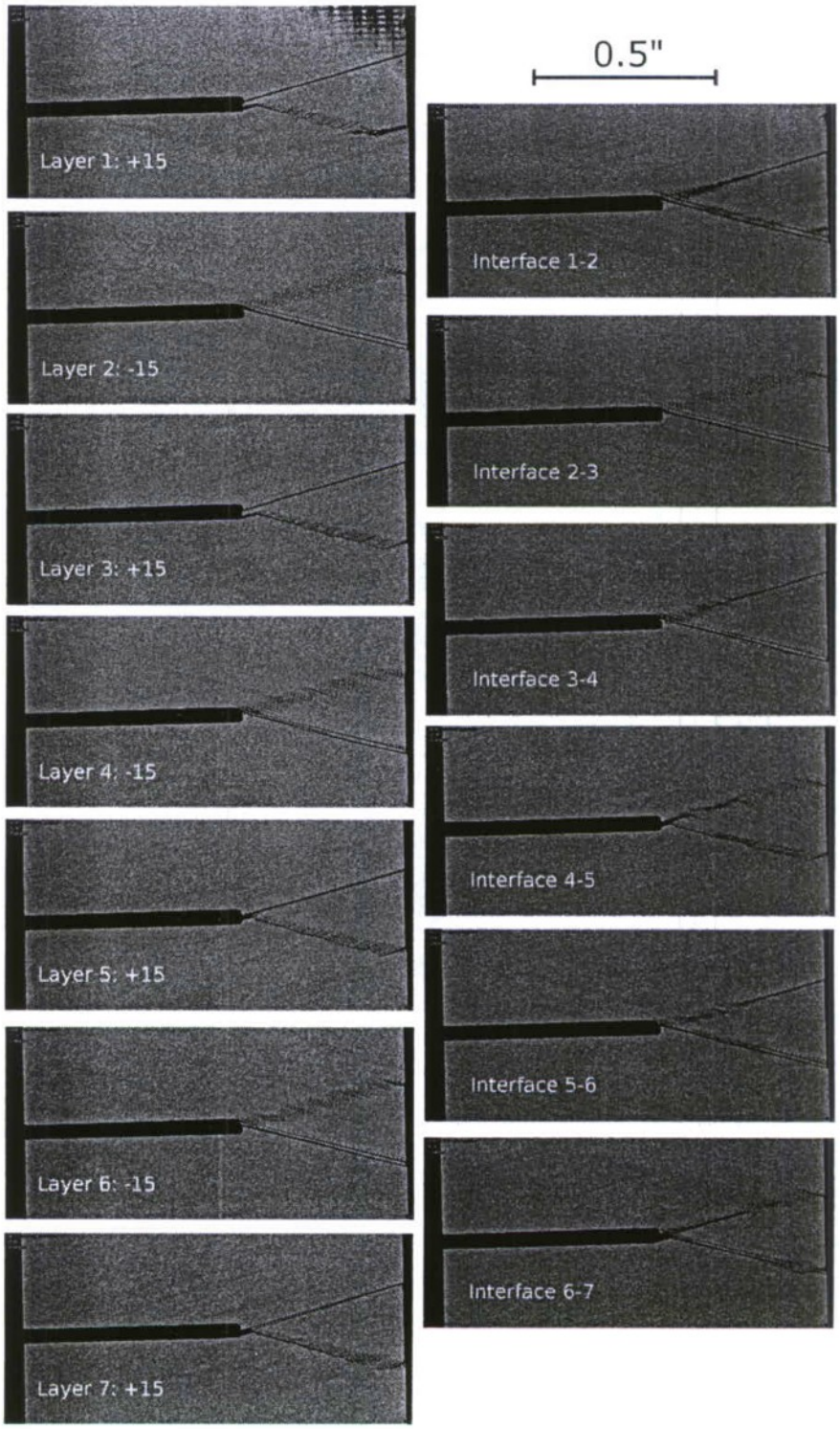

Figure 38a. Virtually sectioned views of the previously tested NRL IPL composite specimen, shown in Figure 34, with the views shown being from the 'front', with material virtually removed (sectioned) through the thickness from the front surface down. (first half)

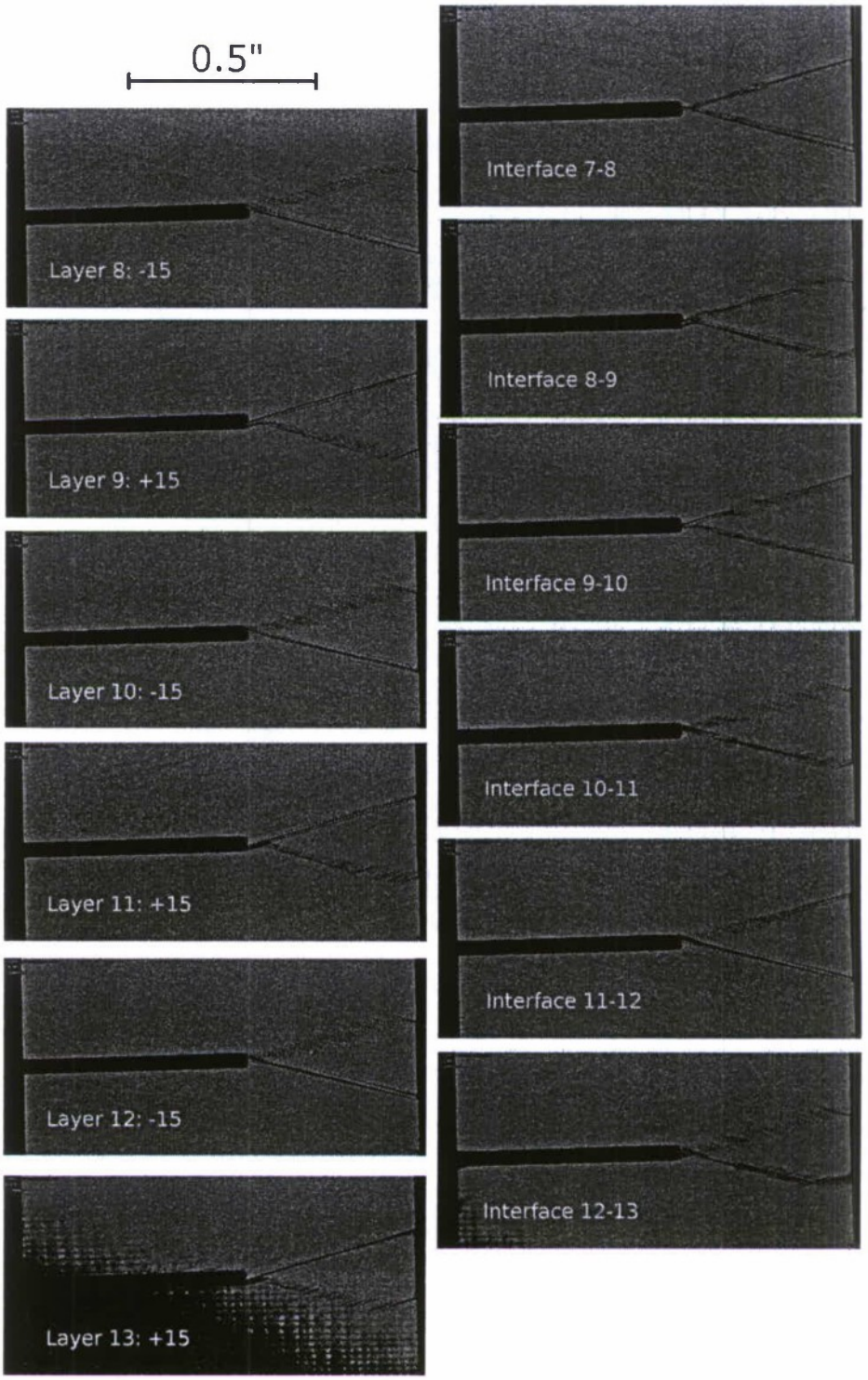

Figure 38b. Remainder (second half) of Figure 38a.

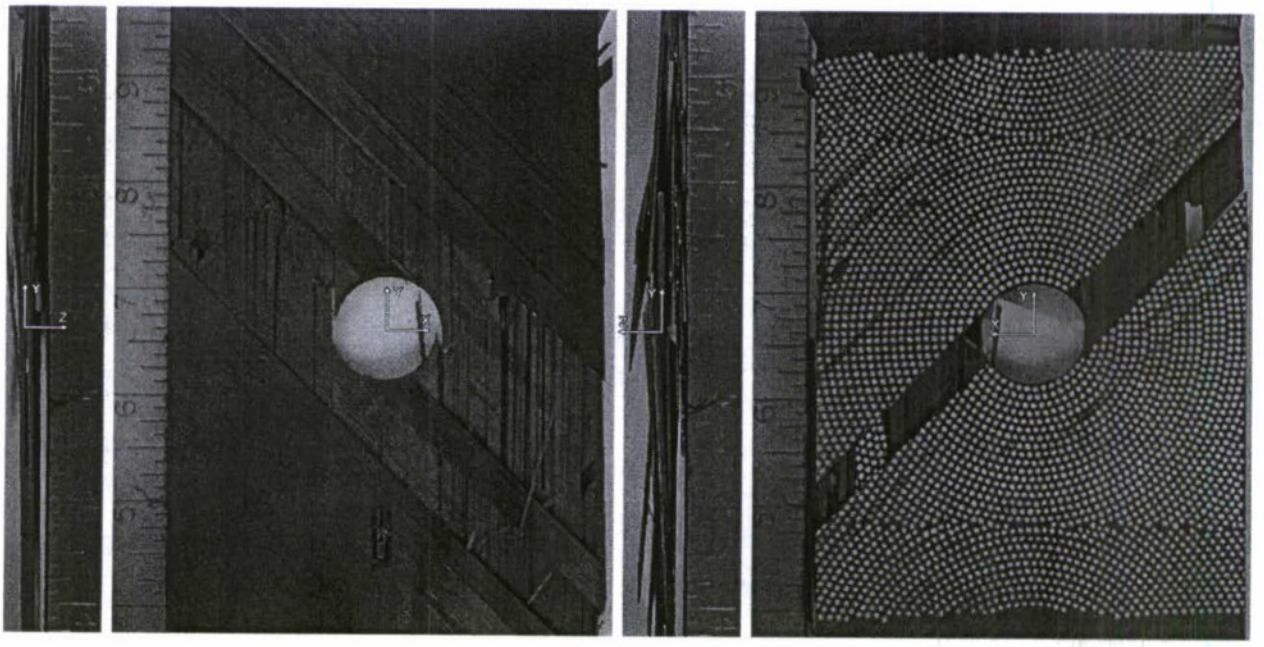

Figure 39. Optical documentation photographs of an OHT composite specimen made of AS4/3501-6 graphite/epoxy with a 1 inch hole and a stacking sequence of $[+45_4/0_4/-45_4]_S$.

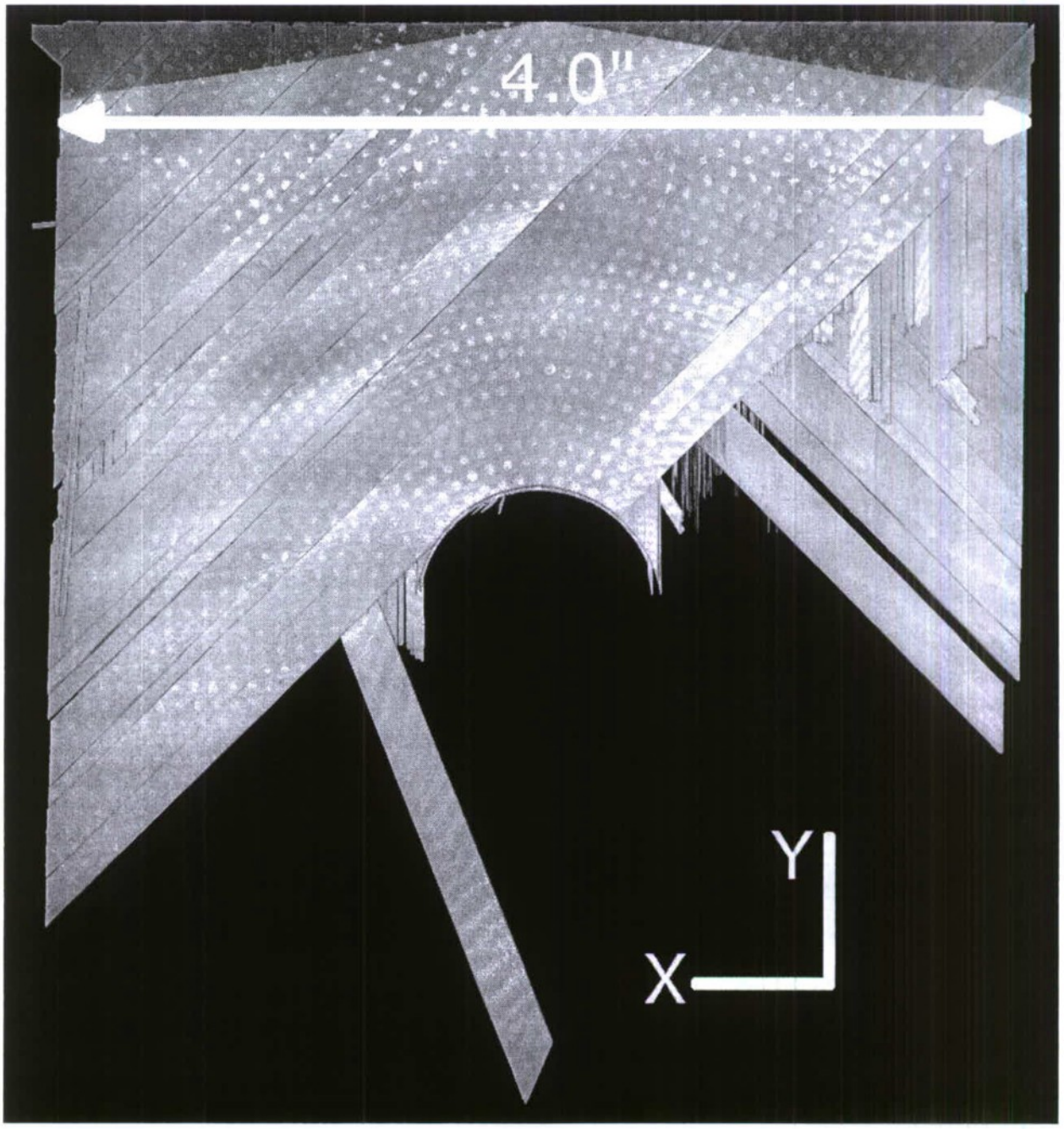

Figure 40. Virtual 3-D volume (back surface view) of the top half of a broken OHT composite test specimen, shown in Figure 39.

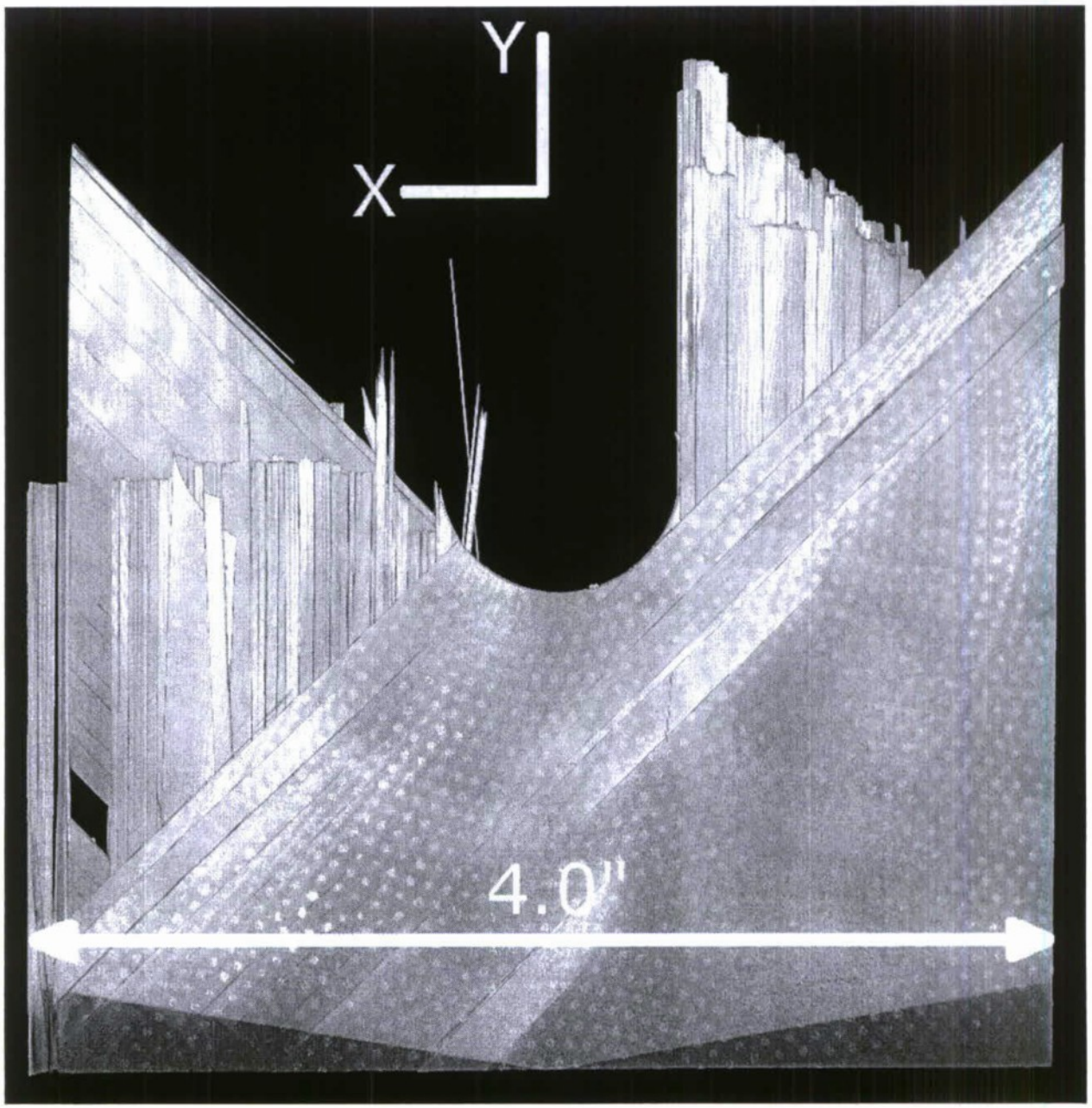

Figure 41. Virtual 3-D volume (back surface view) of the bottom half of a broken OHT composite test specimen, shown in Figure 39.

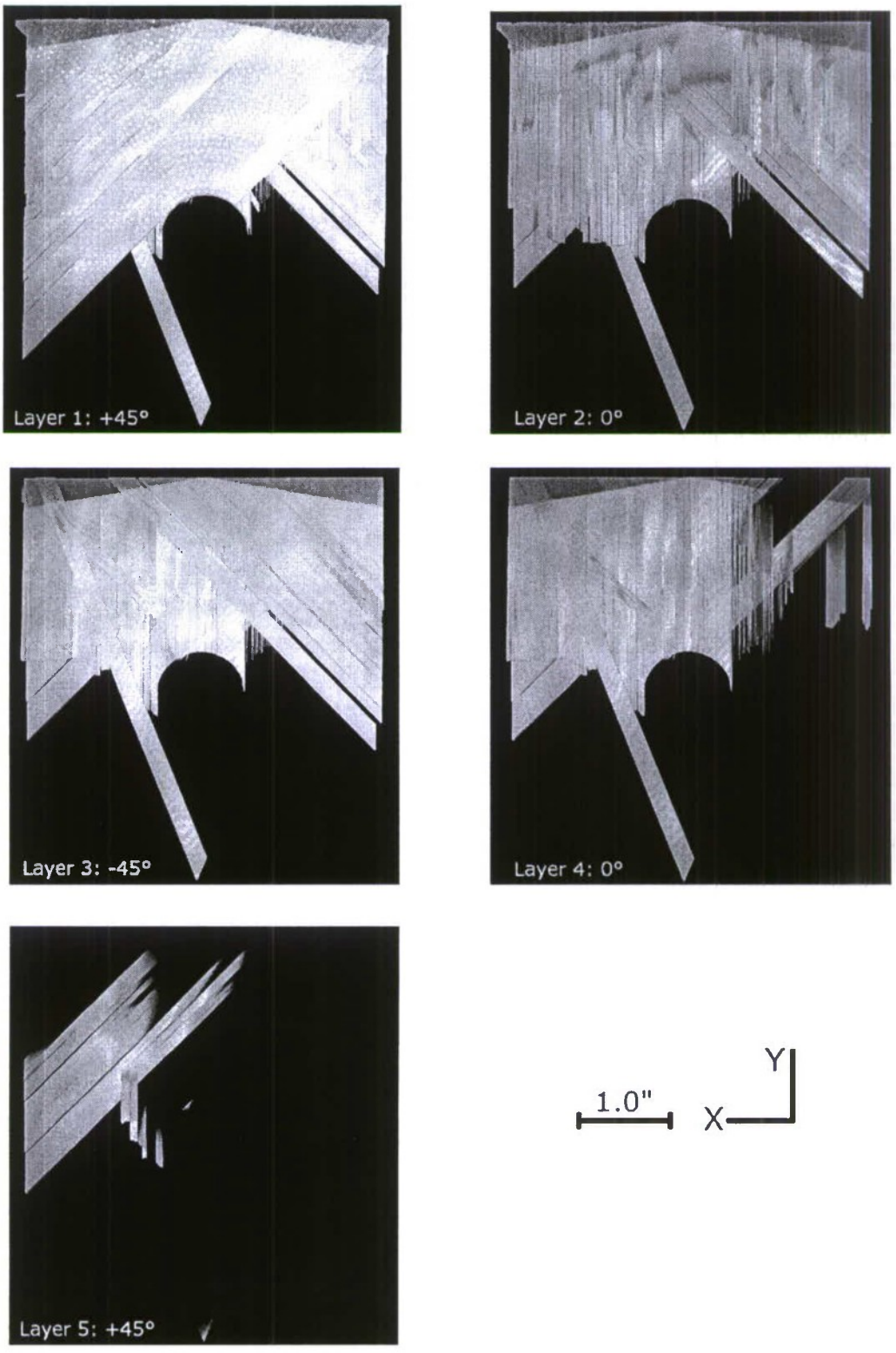

Figure 42. Virtually sectioned views of the OHT composite specimen, shown in Figure 40, with the views shown being from the 'back' , with material virtually removed (sectioned) through the thickness from the outermost surface down.

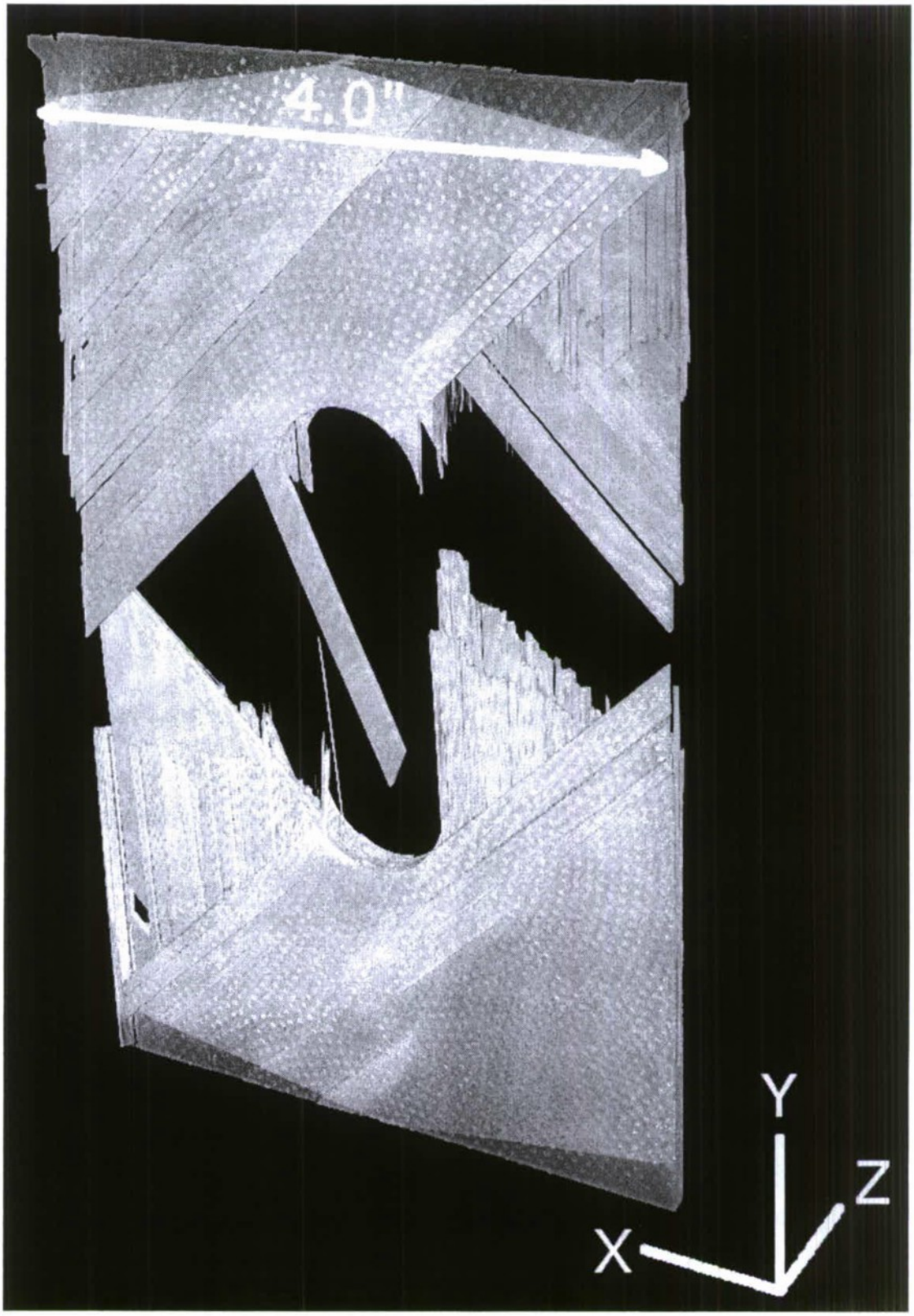

Figure 43. Three-dimensional view of the OHT specimen pieces from Figure 40 and Figure 41.